Generation and characterization of a live, bivalent vaccine against human immunodeficiency virus and Ebola virus

By

Emelissa J. Mendoza

A thesis submitted to the Faculty of Graduate Studies of

The University of Manitoba

In partial fulfillment of the requirements for the degree of

MASTER OF SCIENCE

Department of Immunology,

University of Manitoba,

Winnipeg, MB

ABSTRACT

Human immunodeficiency virus (HIV) causes acquired immunodeficiency syndrome by targeting and destroying $CD4^+$ T cells via its Envelope protein (Env), while Ebola virus (EBOV) causes a lethal hemorrhagic fever and targets antigen presenting cells (APCs) via its glycoprotein (GP). There are no licensed vaccines for either virus, posing a problem particularly in Africa, where succumbing to EBOV or HIV is a grim reality. We hypothesized that a replication-competent HIV expressing GP as a replacement for Env will redirect the virus from $CD4^+$ T cells toward antigen presenting cells and act as a live, bivalent vaccine to induce cellular and humoral immune responses against both pathogens, and confer protection against a lethal EBOV challenge in mice. Recombinant HIV-1 molecular clones containing different truncations of the GP gene to replace HIV gp120 were generated and used to rescue three GP-expressing vaccines, HIV-EBOV, HIV-EBOVΔ1, and HIV-EBOVΔ2. These demonstrated tropism for the monocyte cell line, THP-1, and decreased tropism for the $CD4^+$ T cell line, SupT1. While all vaccines induced HIV p24- and GP-specific IFN-γ-secreting T cell responses, HIV-EBOVΔ1 and HIV-EBOVΔ2 induced the most robust responses at 21 days post-vaccination (dpv), respectively. While all vaccines induced total anti-p24 and anti-GP IgG responses, HIV-EBOVΔ1 induced the most robust responses at 42 dpv. HIV-EBOVΔ1 demonstrated the highest protective efficacy against lethal EBOV challenge, followed by HIV-EBOVΔ2 and HIV-EBOV, providing 83%, 67%, and 50% survival in mice, respectively. HIV-EBOVΔ1 shows promise as a protective vaccine against EBOV, but may require further optimization and characterization regarding its mechanism of action and ability to protect against HIV.

ACKNOWLEDGEMENTS

First and foremost, I would like to thank my supervisor Dr. Gary Kobinger for giving me the opportunity to work on this unique and mentally stimulating research project, while providing me the freedom and resources to explore my own research questions. You played an important role in enhancing my independence and by constantly testing me, you strengthened my confidence and my capacity to defend my capabilities.

I would also like to thank my co-supervisor, Dr. Heidi Wood, for giving me my first research opportunity as a co-op student, despite having no prior experience. You have encouraged my growth as a researcher and remain my mentor in the scientific community. To my committee members, Dr. Xiao-Jian Yao and Dr. Blake Ball, I thank you for your constructive criticism and support, which have motivated me to expand on my critical thinking skills.

I would like to express gratitude to the members of the Special Pathogens Program for their encouragement. I would like to acknowledge Alexander Bello, Hugues Fausther Bovendo, Kevin Tierney, Derek Stein, Xiangguo Qiu, and Geoff Soule for your assistance, patience, and advice. You have strengthened both my technical skills and leadership ability.

To Mindel and the late Tom Olenick, the Manitoba Medical Service Foundation, University of Manitoba, and CIHR, I would like to express my appreciation for generously providing financial support for my research. It was an honour to receive these awards and I hope to one day be able to give back to the scientific community as you have.

Lastly, I would like to thank my friends and family. To my mother, Jocelyn Gloria, thank you for all the sacrifices you've made to bring me where I am now. To my sisters, Desiree and Arielle, thank you for taking pride in my research. To Matthew Valcourt and Raider, thank you for all of your support. I hope to make all of you proud of me one day!

TABLE OF CONTENTS

ABSTRACT ii
ACKNOWLEDGEMENTS iii
LIST OF FIGURES ix
LIST OF TABLES xi
LIST OF ABBREVIATIONS xii
CHAPTER 1: INTRODUCTION **1**
1.1. VACCINES AND IMMUNITY 1
1.1.1. History of vaccination 1
1.1.2. Basic immunology: Innate immunity 2
1.1.3. Basic immunology: Adaptive immunity 4
1.1.4. Vaccine immunology 11
1.1.5. Types of vaccines 15
1.2. HUMAN IMMUNODEFICIENCY VIRUS 21
1.2.1. Acquired immunodeficiency syndrome 21
1.2.2. Human immunodeficiency virus virology 23
1.2.3. Human immunodeficiency virus tropism and life cycle 26
1.2.4. Human immunodeficiency virus pathogenesis 28
1.2.5. Current treatments for human immunodeficiency virus and acquired immunodeficiency syndrome 30
1.2.6. Vaccine development and correlates of protection for HIV 32
1.3. EBOLA VIRUS 35
1.3.1. Ebola virus hemorrhagic fever 35
1.3.2. Ebola virus virology 37
1.3.3. Ebola virus tropism and life cycle 40
1.3.4. Ebola virus pathogenesis 42
1.3.5. Current treatments for Ebola virus hemorrhagic fever 43
1.3.6. Vaccine development and correlates of protection for EBOV 45
CHAPTER 2: STUDY RATIONALE, HYPOTHESIS, AND OBJECTIVES **49**
2.1. STUDY RATIONALE 49

2.1.1. Influence of EBOV on the HIV pandemic and the need for a dual-acting vaccine 49

2.1.2. Live HIV as a vaccine vector 50

2.1.3. Targeting antigen presenting cells to enhance vaccine-induced immune responses .. 50

2.1.4. Shifting the tropism of HIV away from CD4$^+$ T lymphocytes and towards antigen presenting cells 51

2.1.5. Modifications of the EBOV glycoprotein for incorporation into the live HIV vector . 52

2.2. HYPOTHESES 53

2.3. OBJECTIVE AND AIMS 53

2.4. SIGNIFICANCE OF RESEARCH 54

CHAPTER 3: MATERIALS AND METHODS 55

3.1. GENERATION OF MOLECULAR CLONES FOR THE RESCUE OF EBOV GP-EXPRESSING HIV RECOMBINANTS 55

3.1.1. Amplification of fragments for the construction of In-fusion inserts 55

3.1.2. Chimeric PCR assembly for the generation of the mucin-like domain-deleted EBOV GP gene 59

3.1.3. Chimeric PCR assembly for the generation of In-Fusion inserts containing EBOV GP gene truncations 59

3.1.4. Cloning of the EBOV GP gene-containing inserts into pNL4-3 62

3.1.5. Transformation of TOP 10 chemically competent cells with HIV-EBOV plasmids 64

3.1.6. Extraction of plasmids from bacterial cells 64

3.1.7. DNA sequencing of HIV-EBOV molecular clones 65

3.2. CELL CULTURE 66

3.2.1. Cell culture of human embryonic kidney 293T and HeLa TZM-bl adherent cell lines 66

3.2.2. Cell culture of SUP-T1 and THP-1 suspension cell lines 66

3.3. RESCUE OF RECOMBINANT HIV-EBOV VACCINES 67

3.3.1. Transfection of HEK 293T cells with molecular clones for the rescue of HIV-EBOV vaccine candidates 67

3.3.2. Titration of virus stocks by p24 Enzyme-Linked Immunosorbant Assay 68

3.4. CONFIRMATION OF EBOV GP EXPRESSION BY HIV-EBOV VACCINES 70

3.4.1. Western blot analysis of virus supernatants 70

3.5. ANALYSIS OF HIV-EBOV VACCINE VIRION ASSEMBLY 72

3.5.1. Transmission electron microscopy of transfected HEK 293T cells producing HIV-EBOV vaccine candidates 72

3.6. CHARACTERIZATION OF HIV-EBOV VACCINE INFECTIVITY, TROPISM, AND REPLICATION 74

3.6.1. TZM-bl luciferase infectivity assay 74

3.6.2. Evaluation of HIV-EBOV vaccine tropism in THP-1 and SupT1 cell lines 75

3.6.3. Evaluation of HIV-EBOV vaccine replication in THP-1 cells 77

3.7. EVALUATION OF IMMUNE RESPONSES INDUCED BY A HOMOLOGOUS PRIME-BOOST HIV-EBOV VACCINE REGIMEN IN MICE 77

3.7.1. BALB/c mouse model for HIV and EBOV immunogenicity 77

3.7.2. Immunization of BALB/c mice with a homologous prime-boost HIV-EBOV vaccine regimen 78

3.7.3. Harvest of whole blood, serum, and spleens from immunized BALB/c mice 79

3.7.4. Quantification of vaccine-induced IFN-γ-secreting T cell responses by Enzyme-Linked ImmunoSpot 81

3.7.5. Quantification of total anti-HIV p24 IgG and anti-EBOV GP antibodies by ELISA .. 82

3.7.6. Evaluation of neutralizing antibody responses against EBOV 84

3.8. PROTECTIVE EFFICACY OF HIV-EBOV VACCINES AGAINST LETHAL MA-EBOV CHALLENGE 85

3.8.1. Lethal EBOV challenge of mice immunized with homologous prime-boost HIV-EBOV vaccine regimen 85

3.9. STATISTICAL ANALYSIS 87

CHAPTER 4: RESULTS 88

4.1. MOLECULAR CLONES FOR THE RESCUE OF THE VACCINE CANDIDATES, HIV-EBOV, HIV-EBOVΔ1, AND HIV-EBOVΔ2 WERE SUCCESSFULLY GENERATED 88

4.2. VACCINE CANDIDATES, HIV-EBOV, HIV-EBOVΔ1, AND HIV-EBOVΔ2 WERE SUCCESSFULLY RESCUED FROM HEK 293T CELLS AND EXPRESSED EBOV GP TRUNCATIONS 95

4.3. HIV-EBOV AND HIV-EBOVΔ1 DEMONSTRATED HIV-LIKE MORPHOLOGY, WHILE HIV-EBOVΔ2 DEMONSTRATED FILAMENTOUS MORPHOLOGY 99

4.4. HIV-EBOV VACCINES DEMONSTRATED SIMILAR INFECTIVITY OF TZM-BL CELLS AT AN MOI OF 0.1 101

4.5. TROPISM AND INFECTIVITY OF RECOMBINANT HIV-EBOV VACCINES 103

4.6. HIV-EBOV VACCINES WERE ABLE TO INDUCE ANTI-HIV AND ANTI-EBOV CELL-MEDIATED IMMUNE RESPONSES IN MICE ... 105

4.6.1. All HIV-EBOV homologous prime-boost vaccine regimens generated HIV p24-specific IFN-γ-secreting T cells; those induced by HIV-EBOVΔ1 were significantly higher compared to DMEM and wild-type HIV treatment at 21 days post-immunization ... 105

4.6.2. All HIV-EBOV homologous prime-boost vaccine regimens generated EBOV GP-specific IFN-γ-secreting T cells ... 108

4.7. HIV-EBOV VACCINES INDUCED ANTI-HIV AND ANTI-EBOV HUMORAL IMMUNE RESPONSES IN MICE ... 110

4.7.1. HIV-EBOV and HIV-EBOVΔ1 homologous prime-boost vaccine regimens induced significant total anti-HIV p24 and anti-EBOV GP IgG titres in mice at 42 days post-vaccination ... 110

4.7.2 All HIV-EBOV homologous prime-boost vaccine regimens were unable to generate significant EBOV neutralizing antibody titers in mice ... 112

4.8. HIV-EBOV VACCINES WERE ABLE TO CONFER PROTECTION AGAINST A LETHAL EBOV CHALLENGE IN MICE ... 114

4.8.1. HIV-EBOVΔ1, HIV-EBOVΔ2, and HIV-EBOV demonstrated 83, 67, and 50% protective efficacy against lethal EBOV challenge in mice, respectively ... 114

4.8.2. Mice immunized with the HIV-EBOVΔ1 homologous prime-boost regimen demonstrated minimal weight loss after lethal EBOV challenge ... 116

CHAPTER 5: DISCUSSION ... 118

5.1. MOLECULAR CLONES FOR THE RESCUE OF VACCINE CANDIDATES, HIV-EBOV, HIV-EBOVΔ1, AND HIV-EBOVΔ2 ... 118

5.2. RESCUE OF THE HIV-EBOV, HIV-EBOVΔ1, AND HIV-EBOVΔ2 VACCINES 120

5.3. HIV-LIKE MORPHOLOGY OF HIV-EBOV AND HIV-EBOVΔ1, AND FILAMENTOUS MORPHOLOGY OF HIV-EBOVΔ2 ... 120

5.4. INFECTIVITY OF THE HIV-EBOV VACCINES IN TZM-BL CELLS ... 122

5.5. TROPISM AND REPLICATION OF THE HIV-EBOV VACCINES ... 123

5.5.1. Tropism of HIV-EBOV vaccines in THP-1 cells and SupT1 cells ... 123

5.5.2. Infectivity of HIV-EBOV vaccines in the monocyte cell line, THP-1 ... 126

5.5.3. Other cell lines to be considered in future vaccine tropism and replication studies 127

5.6. ANTI-HIV AND ANTI-EBOV CELL-MEDIATED IMMUNE RESPONSES INDUCED BY HIV-EBOV VACCINES IN MICE ... 127

5.6.1. HIV p24-specific IFN-γ-secreting T cell responses ... 127

5.6.2. EBOV GP-specific IFN-γ-secreting T cell responses 129

5.6.3. Other cell-mediated immune responses to be considered during future vaccine immunogenicity studies 130

5.7. ANTI-HIV AND ANTI-EBOV HUMORAL IMMUNE RESPONSES INDUCED BY HIV-EBOV VACCINES IN MICE 131

5.7.1. HIV p24-specific IgG responses 131

5.7.2. EBOV GP-specific IgG responses 132

5.8. EBOV-NEUTRALIZING ANTIBODY RESPONSE INDUCED BY HIV-EBOV VACCINES IN MICE 132

5.8.1. Other antibody-mediated immune responses to be considered during future vaccine immunogenicity studies 133

5.9. PROTECTIVE EFFICACY OF HIV-EBOV VACCINES AGAINST A LETHAL EBOV CHALLENGE IN MICE 133

5.9.1. Other mouse models to be considered during future vaccine evaluation 134

CHAPTER 6: CONCLUSIONS 137

REFERENCES 139

APPENDIX 158

LIST OF FIGURES

Figure 1.1. Effector mechanisms of cell-mediated immunity...7

Figure 1.2. Effector mechanisms of humoral immunity..10

Figure 1.3. Professional antigen presenting cells promote clonal expansion and differentiation of naïve T cells by delivering three distinct signals..14

Figure 1.4. Human immunodeficiency virus structure...25

Figure 1.5. Tropism of human immunodeficiency virus...27

Figure 1.6. Ebola virus structure...39

Figure 1.7. Tropism of Ebola virus..41

Figure 3.1. Schematic of In-Fusion HD cloning of IF-GPΔ2 into the SalI and BamHI digested pNL4-3 wild-type HIV vector...63

Figure 3.2. Experimental schedule for the evaluation of immune responses induced by a homologous prime-boost HIV-EBOV vaccine regimen..80

Figure 3.3. Experimental schedule for the evaluation of protective efficacy against lethal mouse-adapted EBOV challenge induced by a homologous prime-boost HIV-EBOV vaccine regimen...86

Figure 4.1. Schematic representation of the genomes of the recombinant human immunodeficiency viruses expressing different truncations of EBOV GP.................................89

Figure 4.2. PCR amplification of fragments to construct EBOV GP-containing inserts.............91

Figure 4.3. Chimeric PCR assemblies of MLD-deleted EBOV GP and In-Fusion inserts containing EBOV GP truncations..93

Figure 4.4. Restriction digest of pNL4-3 plasmid with SalI and BamHI restriction enzymes.....95

Figure 4.5. Western blot analysis of HIV-EBOV vaccine supernatants for the detection of EBOV GP and HIV p24..97

Figure 4.6. Transmission electron microscopy of HEK 293T cells producing HIV-EBOV vaccines...101

Figure 4.7. Infectivity of HIV-EBOV vaccines of TZM-bl cells quantified by luminescence in relative light units (RLU)...103

Figure 4.8. Tropism and replication of HIV-EBOV vaccines..105

Figure 4.9. HIV p24-specific interferon-γ T cell responses induced by homologous prime-boost HIV-EBOV vaccine regimen in mice upon stimulation with HIV p24 peptides........................108

Figure 4.10. EBOV GP-specific interferon-γ T cell responses induced by the homologous prime-boost HIV-EBOV vaccine regimen in mice upon stimulation with EBOV GP peptides...110

Figure 4.11. Total anti-HIV p24 IgG and total anti-EBOV GP IgG response induced by the homologous prime-boost HIV-EBOV vaccine regimen in mice..112

Figure 4.12. EBOV neutralizing antibody response induced by the homologous prime-boost HIV-EBOV vaccine regimen in mice..114

Figure 4.13. Protective efficacy of the homologous prime-boost HIV-EBOV vaccine regimens against lethal EBOV challenge in mice..116

Figure 4.14. Percentage of weight change experienced by mice immunized with HIV-EBOV homologous prime-boost regimens after lethal EBOV challenge...118

LIST OF TABLES

Table 3.1. Sequence of the primer pairs used for PCR amplification of fragments to construct EBOV GP-containing inserts...56

Table 3.2. Primer combinations for the PCR amplification of fragments to construct EBOV GP sequence-containing inserts...58

Table 3.3. Fragment combinations for the chimeric PCR full-length inserts containing truncations of the EBOV GP gene...61

Table 4.1. Titers of HIV-EBOV vaccine stocks obtained via Lenti-X p24 ELISA...97

LIST OF ABBREVIATIONS

ADCC - Antibody-dependent cell cytotoxicity

AIDS - Acquired immunodeficiency syndrome

APC - Antigen presenting cell

CD - Cluster of differentiation

CDC - Complement-dependent cytotoxicity

CL - Containment level

CTL - Cytotoxic T lymphocyte

DC - Dendritic cell

DC-SIGN - Dendritic cell-specific intercellular adhesion molecule-3-grabbing non-integrin

DNA - Deoxyribonucleic acid

EBOV - Ebola virus

EHF - Ebola hemorrhagic fever

ELISA - Enzyme-linked immunosorbant assay

ELISPOT - Enzyme-linked immunospot

Env - HIV Envelope protein

GP - EBOV glycoprotein

HAART - Highly active antiretroviral therapy

HESN - Highly-exposed, HIV-seronegative

HIV - Human immunodeficiency virus

HTLV-III - human T-lymphotropic virus-III

IFN - Interferon

IFU - Infectious unit

IgG - Immunoglobulin G

IL - Interleukin

LAV - Lymphadenopathy-associated virus

LD_{50} - Lethal dose 50%

LTNP - Long-term nonprogressor

mAb - Monoclonal antibody

MHC - Major histocompatibility complex

MLD - Mucin-like domain

nAb - Neutralizing antibody

NK - Natural killer

NNRTI - Non-nucleoside reverse transcriptase inhibitor

NPC1 - Niemann-Pick type C1

NRTI - Nucleoside reverse transcriptase inhibitor

PCR - Polymerase chain reaction

RNA - Ribonucleic acid

RT - Reverse transcriptase

SIV - Simian immunodeficiency virus

ssRNA - Single-stranded RNA

TCR - T cell receptor

TIM-1 - T-cell immunoglobulin and mucin domain 1

TGF - Transforming growth factor

TNF - Tumor necrosis factor

VE - Vaccine efficacy

CHAPTER 1: INTRODUCTION

1.1. VACCINES AND IMMUNITY

1.1.1. History of vaccination

Vaccines are one of the most cost-effective and efficient protective measures against infectious diseases. The intentional manipulation of the immune response to generate protective immunity against pathogens dates back to the Middle Ages, with the act of variolation in Africa, India, and China. Variolation exposed healthy individuals to air-dried smallpox pustules by inhalation or by scratching the material into the skin in order to provide immunity against smallpox (Rappuoli, Pizza, Del Giudice, & De Gregorio, 2014). In 1796, Edward Jenner observed that milkmaids who acquired lesions from cowpox infection were subsequently immune to smallpox outbreaks. Based on this observation, he administered pus from lesions obtained from a milkmaid infected with the bovine disease to confer immunity to smallpox (Stern & Markel, 2005). He subsequently termed the process “vaccination” after, *vacca*, the Latin term for cow (Riedel, 2005). Later in the 19th century, Robert Koch determined that microorganisms were the etiological agents of infectious diseases, introducing the role of viruses, bacteria, fungi, and parasites in human illness (Murphy, 2012). Subsequently, Louis Pasteur developed a rabies virus vaccine in 1885, which further expanded the application of vaccination from its association with cowpox to include other inoculations that provide protective immunity. Pasteur forged vaccine development by using dead or attenuated pathogens that mimicked the infectious agent to provide immunity to naïve individuals without causing disease (Stern & Markel, 2005). Since these early discoveries, a multitude of vaccines have been developed and contributed to the eradication of smallpox and other previously morbid diseases, such as poliomyelitis, measles, mumps, and rubella, which affected millions of lives in the 20th century

(Nabel, 2013). Recently, more advanced technologies have been developed that optimize the mimicry of microorganisms to induce immunity. The generation of vaccines lacking virulence factors of pathogenic agents was made possible by the advent of recombinant DNA technologies in the 1970s (Rappuoli et al., 2014).

1.1.2. Basic immunology: Innate immunity

The human immune system is comprised of the innate and adaptive arms of immunity, which constantly interact with one another to optimize the host's ability to fend against infections and malignancies (Clem, 2011). Both arms of the immune system are reliant on the activities of leukocytes, also known as white blood cells. The innate arm of the immune system acts as the host's first line of defense, using general, rapid, and constant mechanisms of resistance. Anatomic barriers, such as mucous membranes and intact skin, act as physical barriers, which prevent the entry of pathogens into the host. In addition, the acidic nature of the skin barrier inhibits the growth of many microbes, while mucous and cilia on mucous membranes trap and propel microorganisms from the body (Clem, 2011; Sperandio, Fischer, & Sansonetti, 2015).

Physiologic barriers are another component of innate immunity. For example, the normal body temperature range inhibits the growth of pathogens, while increased temperature that occurs during a fever can further inhibit pathogen growth. Lysozyme, an enzyme found in mucous secretions and tears, can lyse bacteria by cleaving the peptidoglycan layer of the bacterial cell wall. Interferons, produced by virally infected cells can induce an anti-viral state by binding to non-infected cells in proximity. Collectin, a surfactant protein found on mucosal surfaces, can disrupt lipid membranes to directly kill microbes or aggregating pathogens in order to promote their clearance by phagocytes (Clem, 2011).

The complement cascade is another component of the innate immune system, which can utilize three different pathways for activation of complement proteins. The classical pathway initiates complement upon the binding of IgM antibodies or specific IgG antibody subclasses to surface antigens on microorganisms. The alternate complement pathway is initiated when the C3b complement protein is deposited into the surface of microbes, while the lectin complement pathway is initiated by the binding of plasma mannose-binding lectin onto microbial surfaces. All three pathways lead to common events that trigger the formation of the membrane attack complex, which induces lysis of target cells by forming pores on the cell membrane. In addition, complement promotes opsonisation, which optimizes phagocytosis of particulate antigens. Complement is also involved in initiating a localized inflammatory response (Sarma & Ward, 2011). Complement aids in optimizing adaptive immunity by inducing cells that have engulfed microbes to provide signals for the activation of lymphocytes with antigen-specific receptors (Murphy, 2012).

Cells of the innate immune system lack antigen specificity but instead recognize molecular patterns conserved in a wide range of pathogens. Pattern recognition receptors (PRRs) found on innate cells are not specific to a specific antigen, but recognize pathogen-associated molecular patterns (PAMPs) and danger-associated molecular patterns. These include toll-like receptors (TLRs) and nucleotide-binding oligomerization domain (NOD)-like receptors, which recognize components such as nucleic acids, peptidoglycan, flagellin, and lipopolysaccharide common to many pathogens. Upon recognition of PAMPs, PRRs initiate a cascade that leads to cytokine release, complement activation, opsonization, and phagocyte activation. Granulytic cells, such as neutrophils, eosinophils, basophils, and mast cells, play key roles in innate immunity. Neutrophils are generally the first to arrive to a site of inflammation and are highly active phagocytes, while eosinophils are important in the phagocytosis and clearance of parasites. Basophils, found in blood, and mast cells, found in tissues, secrete histamine and other substances, which mediate allergic reactions (Clem, 2011). Natural killer (NK) cells directly lyse target cells by secreting perforin and granzyme, regulate immune responses by releasing cytokines, and induce apoptosis of target cells by coupling death-inducing receptors (Ma, Li, & Kuang, 2016). DCs, and mononuclear phagocytes, such as monocytes and macrophages, are involved in linking innate immunity to adaptive immunity. These cells are involved in antimicrobial and cytotoxic effects, phagocytosis, cytokine production, and antigen presentation (Clem, 2011). Cytokines are proteins that bind receptors on the same cell releasing the cytokine or distant cells. Binding of cytokines to their cognate receptors optimizes adaptive immunity by promoting the differentiation of naïve cells to effector cells of the adaptive immune system. Chemokines also promote recruitment of adaptive immune cells. Inflammatory responses generated by the innate immune system increase the flow of lymphatic fluid, which carries antigen and antigen-bearing cells to lymphoid tissues (Janeway Jr, Travers, Walport, & Shlomchik, 2001).

1.1.3. Basic immunology: Adaptive immunity

In contrast to innate immunity, adaptive immunity confers antigen-specific effector functions to mediate protection. Lymphocytes play the most significant role in adaptive immunity (Murphy, 2012). The main drawback with the adaptive arm of immunity is that responses take longer to generate in comparison with the innate immune responses. The greatest benefit of adaptive immunity is the ability to generate memory, allowing for the induction of a more rapid and effective control of a pathogen upon subsequent encounter (Clem, 2011).

Cell-mediated immunity

Cell-mediated immunity is the first arm of the adaptive immune system, which mainly functions against intracellular pathogens. T lymphocytes (T cells), the primary mediators of cell-mediated immunity, possess unique T cell receptors (TCRs) on their surface, which specifically recognize cognate antigens presented by either major histocompatibility complex (MHC)-I or MHC-II. In contrast to B lymphocytes, T lymphocytes can only bind antigens that have been processed and presented by antigen presenting cells. Upon receptor engagement with its cognate antigen, T cells proliferate and differentiate into effector cells as depicted in **Figure 1.1**. Naïve $CD8^+$ T cells differentiate into cytotoxic T lymphocytes (CTLs), while naïve $CD4^+$ T cells differentiate into T helper cells, or regulatory T cells. CTLs, which express CD8 co-receptor on their surface, recognize antigenic peptides presented by MHC-I, expressed on all nucleated cell types, excluding mature erythrocytes. CTLs directly kill cells infected with intracellular pathogens, such as viruses, or malignant cells that express their cognate antigen. Upon receptor engagement and co-stimulation, CTLs release caspases into the target cell, which induces apoptosis and activates nucleases that degrade host and foreign DNA (Murphy, 2012).

T helper cells, which express CD4 on their surface, recognize antigenic peptides presented by MHC-II, primarily expressed on professional antigen presenting cells, such as macrophages, DCs, and B cells. Upon recognition of their cognate antigens on target cells, helper T cells provide the essential signals that influence the activity and behaviour of different cell types. For example, T_H1 cells produce IFN-γ, which promotes the activation of infected macrophages to destroy engulfed intracellular pathogens. T_H2 cells produce IL-4, IL-5, and IL-13, which promotes the ability of antigen-stimulated B cells to secrete antibodies and undergo isotype class switching. In addition, T_H2 cells promote switching to IgE antibodies to mediate the clearance of extracellular multicellular parasites. T_H17 cells secrete IL-17 and IL-6, which cause fibroblasts and epithelial cells to produce chemokines that recruit neutrophils to sites of infection to mediate the destruction of extracellular pathogens. Follicular T helper (T_{FH}) cells also contribute to the antibody-mediated response by producing cytokines, such as IFN-γ, which induces class switching in B cells. Regulatory T cells (T_{reg}) produce TGF (transforming growth factor)-β and IL-10 to suppress the action of lymphocytes and prevent autoimmunity (Murphy, 2012).

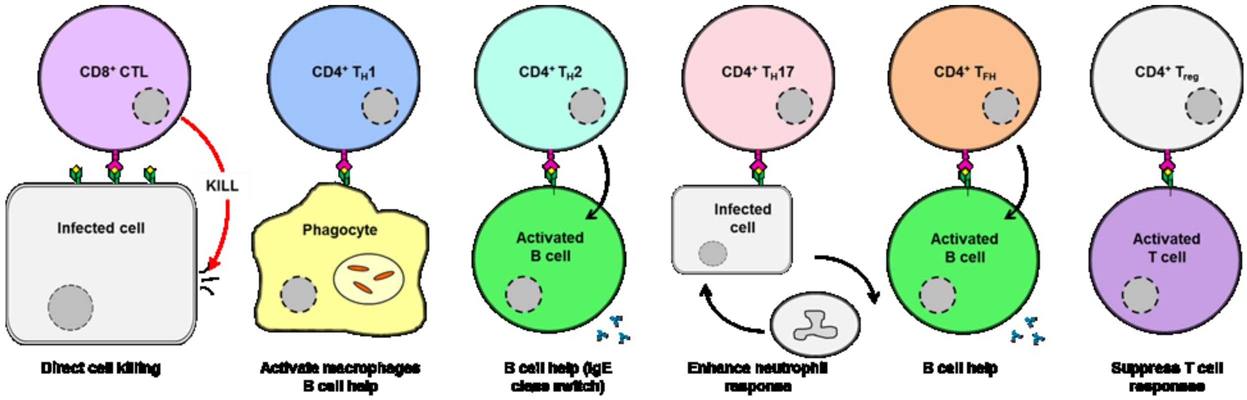

Figure 1.1. Effector mechanisms of cell-mediated immunity. $CD8^+$ cytotoxic T cells directly kill infected or malignant cells expressing their cognate antigen by secreting caspases that induce apoptosis. $CD4^+$ T_H1 cells activate infected macrophages to induce their destruction of engulfed intracellular pathogens. $CD4^+$ T_H2 cells provide signals to antigen-stimulated B cells to promote their ability secrete antibodies and undergo isotype class switching. In addition, T_H2 cells promote switching to IgE antibodies to mediate the clearance of extracellular multicellular parasites.$CD4^+$ T_H17 cells recruit neutrophils to sites of infection to mediate the destruction of extracellular pathogens. $CD4^+$ T_{FH} cells also contribute to the antibody-mediated response by inducing class switching in B cells. $CD4^+$ regulatory T cells work to suppress the action of lymphocytes in order to prevent autoimmunity. (Adapted from Murphy, 2012)

Humoral immunity

Humoral immunity, also known as antibody-mediated immunity, is the second arm of the adaptive immune system, functioning primarily against extracellular pathogens and toxins. B lymphocytes (B cells), the primary mediators of humoral immunity, possess unique B cell antigen receptors (BCRs), which are membrane bound immunoglobulins with specificity for a cognate antigen. Naïve B cells develop in the bone marrow and migrate to the lymph nodes, where they encounter antigens in native, unprocessed form. Antigens capable of activating B cells in absence of T cell help are called T-independent antigens, which include lipopolysaccaharide and bacterial polymeric flagellin. T-independent antigens generate weaker immune responses and poor memory formation in comparison to antigens provided with T cell help (Clem, 2011). Upon receptor engagement with its cognate antigen and secondary signalling by cytokines, B cells begin somatic hypermutation in which BCRs become optimized for antigen binding. These B cells proliferate and differentiate into plasma cells, which are the effector form of B cells that produce antibodies sharing the same antigen specificity as the membrane-bound BCR. Antibodies are Y-shaped molecules with two identical variable regions for unique antigen binding and a constant region, which determines the function of the antibody, as depicted in **Figure 1.2** (Murphy, 2012). In a process called neutralization, antibodies mediate protection by binding antigens on pathogens or toxins, preventing their entry into target cells. During opsonisation, antibodies mediate the engulfment and phagocytosis of pathogens to which they are bound. Antibodies can also mediate complement-dependent cell cytotoxicity by inducing the classical complement pathway to induce the membrane attack complex-mediated lysis of bacterial pathogens or infected cells. Lastly, antibodies mediate antibody-dependent cell cytotoxicity by binding infected cells expressing pathogenic antigens on their surface. This recruits natural killer cells, which bind the antibody's constant region and mediate killing of the infected cell by secreting perforin and granzymes (**Figure 1.2**)(Murphy, 2012). Early in the primary antibody response, IgM antibodies are primarily produced and class switching occurs in which the constant region of the antibodies are exchanged, allowing for production of IgG antibodies. In addition, affinity maturation contributes to the production of IgG antibodies that are better at mediating neutralization, antigen binding, and mediating opsonisation. IgG antibodies are the key antibodies in vaccination. Other antibody classes include IgA, which are found in mucous, tears, saliva, and breast milk; IgD, which are primarily bound to the surface of mature B cells; and IgE, which are involved in mediating allergic reactions (Clem, 2011).

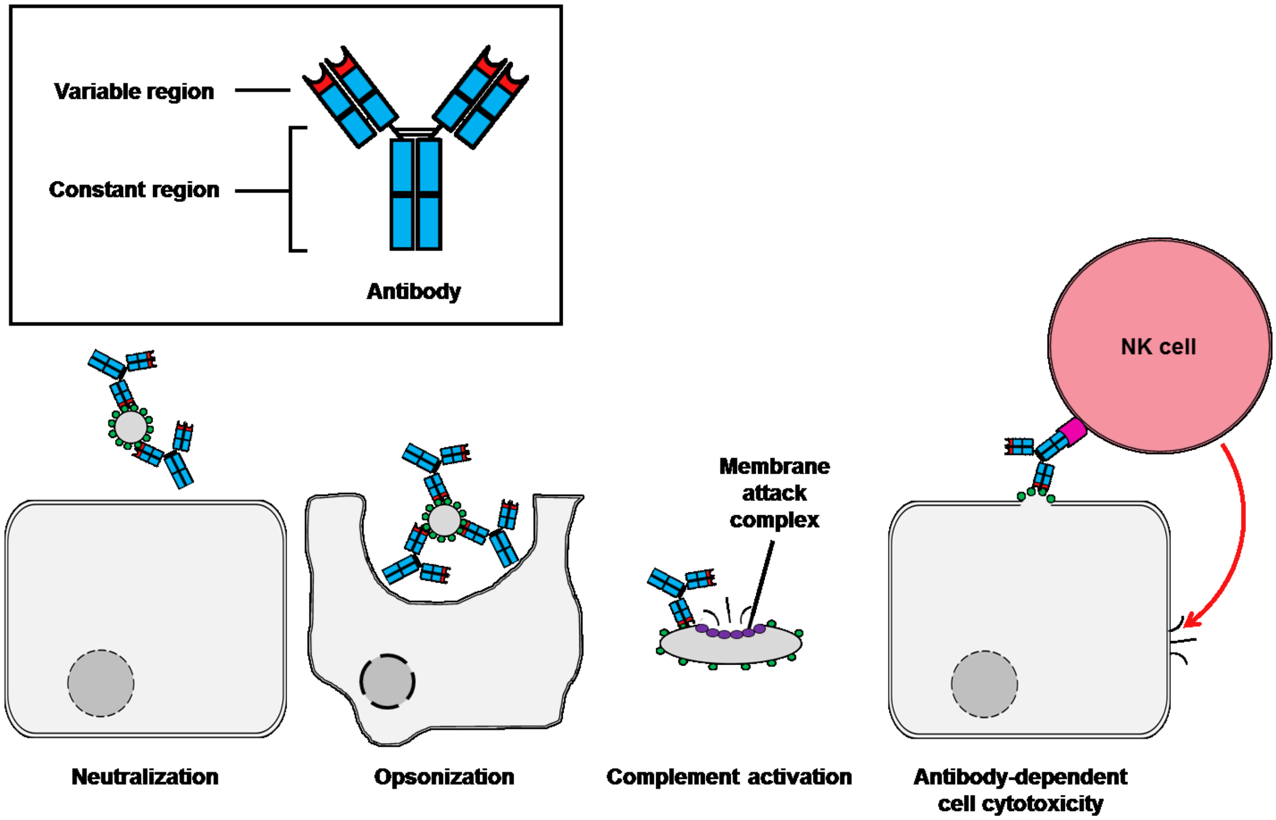

Figure 1.2. Effector mechanisms of humoral immunity. Antibodies are composed of a constant region involved in antibody function and a variable region involved binding to specific antigens. Antibodies can mediate neutralization, preventing pathogens or toxins from interacting with host cells. Antibodies can also mediate opsonisation, in which antibodies coating a pathogen promote recognition, engulfment, and digestion by phagocytes. Antibodies are also involved complement activation through the classical complement pathway, a cascade leading to the formation of the membrane attack complex on the cell surface causing lysis of a bacterium. Antibody-dependent cell cytotoxicity involves binding of antibodies to antigens expressed on the surface of an infected cell. Recognition of the antibody's constant regions by receptors on natural killer cells promotes killing of the infected cell via perforin and granzyme secretion. (Adapted from Murphy, 2012)

Immunological memory

Immunological memory, the ability of the immune system to mount a faster and more effective antigen-specific response upon subsequent exposure, is the most significant concept unique to the adaptive immune system. Since humans have a wide diversity of lymphocytes bearing unique antigen receptors, a foreign antigen may only be bound by very few lymphocytes with the appropriate receptor specificity. The few lymphocytes capable of recognizing foreign antigens undergo clonal expansion, during which, activation and proliferation occurs, yielding antigen-specific progeny that can differentiate into a sufficient amount of effector cells for pathogen clearance. Upon clearance of the invader, most effector cells undergo apoptosis. However, some cells, known as memory cells, persist after antigen elimination and are primed to provide a more rapid and effective effector response upon secondary encounter with the antigen. For example, the secondary antibody response occurs after a shorter lag period at a greater magnitude, producing antibodies with higher affinity for the antigen compared with the primary antibody response (Murphy, 2012).

1.1.4. Vaccine immunology

Successful vaccination is dependent on the development of immunological memory, which prevents infection with pathogens bearing the antigen introduced by a vaccine (Murphy, 2012). Immunological memory can be conferred by passive or active means. Passive immunization can be achieved by transferring pre-formed antibodies to a naïve individual, providing temporary protection to a particular pathogen or toxin until the antibodies are eliminated. This can occur naturally by the transfer of maternal antibodies to an infant via breast milk or artificially through the administration of convalescent plasma containing antibodies from survivors. Active immunization occurs upon exposure of a naïve individual to antigens of a pathogenic agent, which initiates innate and adaptive immunity. Unlike passive immunization, active immunization can generate long-lasting immunity. Active immunization can occur naturally through exposure and infection by a particular pathogen. For example, natural exposure to influenza virus induces the development of long-term anti-influenza immunity. Active immunization can also be induced artificially by vaccination. In contrast to natural infection, vaccination aims to generate immunity against a pathogen without inducing disease symptoms (Clem, 2011).

Role of antigen presenting cells in driving adaptive immune responses to vaccines

The main goal of vaccination is to stimulate an antigen-specific immune response and induce long-lasting immunological memory in order to provide protection upon encounter with the disease-causing pathogen. In order to achieve this, vaccine antigens need to be presented by antigen presenting cells (APCs). Antigen presentation upon infection or vaccination can occur via two pathways. Antigens that are generated endogenously are presented on MHC class I molecules by APCs to $CD8^+$ T cells. Antigens that are generated exogenously are presented on MHC class II molecules by professional APCs, including DCs, monocytes, macrophages, and B cells. Activation of naïve T cells by APCs requires at least two signals as depicted in **Figure 1.3**. The first signal involves the presentation of MHC:antigen complexes on the surface of APCs to an antigen-specific TCR of the T cell, as well as co-receptor binding to MHC. For $CD8^+$ T cells, TCRs binds MHC class I:antigen complexes on the target cell, while CD8 acts as the co-receptor that binds MHC. For $CD4^+$ T cells, TCRs bind MHC class II:antigen complexes on the target cell, while CD4 acts as the co-receptor that binds MHC. Together, these interactions mediate activation of the T cell. The second signal is the co-stimulation provided by APCs when its

CD80 or CD86 molecules bind CD28 receptors on the T cell, which leads to prolonged survival of the T cell. Since non-professional APCs lack CD80/86, they are unable to induce co-stimulation and are therefore unable to sufficiently stimulate T cell responses. In the presence of TCR engagement and the absence of co-stimulatory signals, anergy can occur, a form of T cell tolerance to the antigen. The third signal is cytokine signalling, in which cytokines produced by the APC mediate differentiation of the T cell. Thus, the cytokine environment produced by the APC influences the effector function of a T cell. For example, IL-12 and IFN-γ drive the differentiation of naïve T cells into T_H1 cells; IL-4 drives the development of T_H2 cells; TGF-β and IL-6 drive the development of T_H17 cells; IL-6 drives the development of T_{FH} cells; and TGF-β alone promotes the development of T_{reg} cells (Murphy, 2012). Recently, new vaccine strategies aim to target selected antigens directly to APC subsets in order to promote the desired immune responses, such as T_H1 vs. T_H2, necessary for protection against the particular pathogen (Gamvrellis et al., 2004).

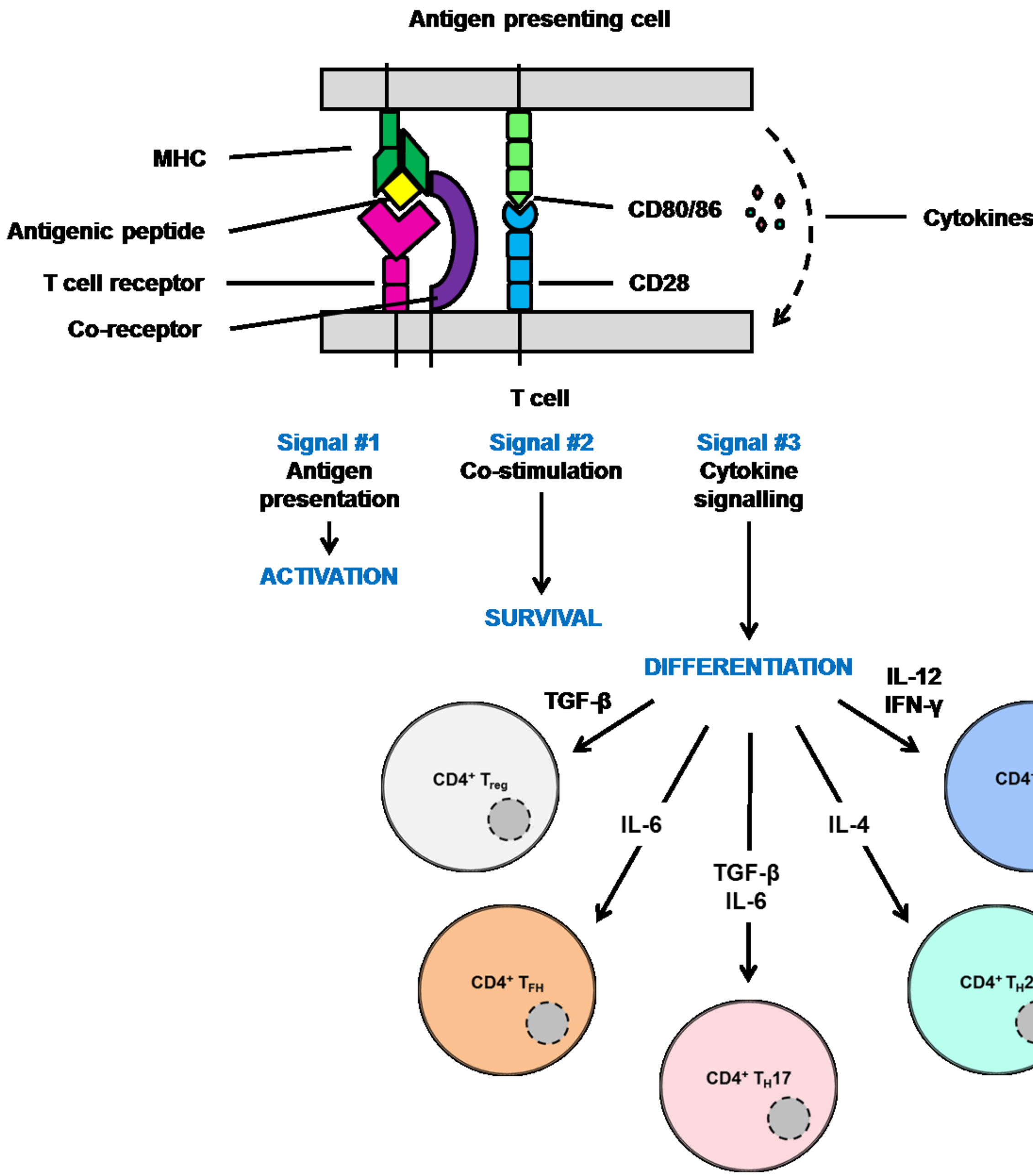

Figure 1.3. Professional antigen presenting cells promote clonal expansion and differentiation of naïve T cells by delivering three distinct signals. The first signal, antigen recognition, involves the presentation of MHC:antigen complexes on the surface of APCs to an antigen-specific TCR of the T cell. This signal also requires the binding of CD8 to MHC-I or CD4 to MHC-II for $CD8^+$ T cells and $CD4^+$ T cells, respectively. The second signal, co-stimulation, occurs by the interaction with CD80 or CD86 molecules on APCs with CD28 receptors on the T cell, leading to prolonged survival of the T cell. The third signal is cytokine signalling, in which cytokines produced by the APC mediate differentiation of the T cell into different effector subsets. (Adapted from Murphy, 2012)

1.1.5. Types of vaccines

Since the discovery of vaccination, many types of vaccines have been utilized to confer protection against infectious disease. Typically, vaccines intend to induce both arms of the adaptive immune system, as well as innate immunity. Each type of vaccine has both advantages and limitations regarding immune stimulation and safety, and thus, different vaccine types should be considered for each particular application (Clem, 2011).

Inactivated vaccines

Inactivated vaccines, also known as killed vaccines, utilize pathogenic agents that have been treated by heat, chemical, or radiation methods in order to inactivate the pathogen and eliminate its ability to cause disease (Clem, 2011). One of the first killed vaccines to be developed was for typhoid in the 19th century. Currently, polio, hepatitis A, and pertussis inactivated vaccines continue to be widely used. Upon administration, the whole killed organism is phagocytosed by immature DCs and digestion with the phagolysosome generates different antigenic fragments from the vaccine. The peptides on the activated mature DC can be presented on the surface of the cell by MHC-II, which allow antigen recognition and activation of primarily T_H2 cells. Antigens that drain along lymph channels are bound by antigen-specific B cells, which can also internalize the antigens and present them as MHC-II:peptide complexes, leading to linked recognition with T_H2 cells sharing the same antigen recognition. T_H2 cells produce IL-2, IL-4, IL-5, and IL-6, which induces activation, differentiation, and proliferation of the antigen-specific B cell. Subsequently, activated B cells undergo isotype switching from IgM to IgG and memory cell formation occurs. While primary immunization takes a minimum of 10-14 days, the secondary response to antigenic exposure occurs within 1-2 days (Baxter, 2007). An advantage of killed vaccines is safety due to their inability to cause illness or revert back to virulence. Killed vaccines are also stable and less susceptible to changes in temperature, humidity, and light, and do not require refrigeration. They can also be freeze-dried for transport. In addition, killed vaccines are unable to multiply, preventing spread to unimmunized and potentially immunocompromised individuals. Limitations of killed vaccines include their inability to generate robust immune responses since they are unable to replicate in cells. Thus, many inactivated vaccines require multiple booster immunizations to maintain long-term immunity. Lack of replication also prevents endogenous antigen processing and subsequent presentation via MHC-I molecules, limiting the CTL response generated by inactivated vaccines. In addition, since whole inactivated pathogens are used, antibodies induced by vaccination may be targeted towards antigens that are not involved in virulence. These antibodies may act antagonistically with antibodies involved in protection. Some pathogens may use this as an advantage in order to down-regulate the host's adaptive immune response (Baxter, 2007; Clem, 2011).

Subunit vaccines

Subunit vaccines are an evolution of the killed vaccine approach, using specific protein antigens instead of whole pathogen preparations. The development of an efficient subunit vaccine requires the identification of the specific antigen or antigen combination important in inducing protection against the pathogen (Baxter, 2007). Subunit vaccines are produced using DNA plasmids to induce recombinant protein expression in cell culture or foreign hosts. Virus-like particles (VLPs), which exhibit similar surface proteins as the wild-type virus but lack genetic material for replication, are an extension of subunit vaccine technology that have been used for protection against hepatitis B virus and human papilloma viruses (Ellis, 1996). Subunit vaccines comprising T-independent antigens, such as the Pneumovax vaccine against pneumococcal disease, are phagocytosed and presented by DCs and macrophages, which encounter T_H2 cells in the lymph node. However, the MHC:polysaccharide complexes are unable to induce the activation of T_H2 cells. Some non-phagocytosed polysaccharide molecules of these vaccines may encounter antigen-specific B cells in the draining lymph nodes, which can become activated without the help of T_H2 cells due to the high avidity of binding between the BCRs and the multivalent polysaccharide vaccine. However, these activated B cells are limited to IgM production due to limited isotype switching; IgM is highly efficient in activating complement, but limited in its ability to neutralize and opsonize. In addition, minimal memory cell formation is induced. In contrast, subunit vaccines comprising T-dependent antigens, such as the vaccines for hepatitis B and influenza, the presence of both MHC:protein and MHC:polysaccharide complexes on the cell surface promote migration to T cell-rich areas of the lymph node for activation of T_H2 cells upon phagocytosis by DCs. T_H2 cells can provide co-stimulation and cytokine release necessary for the production of IgG by antigen-specific plasma cells, and the promotion of memory B cell formation (Baxter, 2007). Subunit vaccines have similar advantages inactivated vaccines, in addition to the ability to induce responses specifically required for protection. The disadvantages of subunit vaccines are also similar to those of inactivated vaccines, including their limited ability in generating CTL responses and their requirement for adjuvants and multiple vaccine doses. In addition, subunit vaccines may have limited applicability to protect against diseases in which the antigens required for protection are unknown (Baxter, 2007).

Live, attenuated vaccines

Live, attenuated vaccines have demonstrated success against a multitude of human pathogens, such as smallpox, polio, and yellow fever viruses (Minor, 2015). These vaccines utilize original pathogenic agents that have been weakened by laboratory methods, including passaging the pathogen in a foreign host, which generates mutations that adapt the pathogen for enhanced virulence in the foreign host and reduced virulence in humans. For example, live, attenuated measles virus vaccines are produced by passaging the wild-type virus in chick egg fibroblasts. Another method for generating live, attenuated vaccines is to cultivate the wild-type virus in artificial growth medium at temperatures lower than that of the human body, promoting the development of a pathogen less adapted to replicate under physiological conditions. This allows the human host to eliminate the pathogen before it is able to cause infection and this method has been used to develop the cold-adapted live, attenuated influenza virus vaccine. Live, attenuated vaccines are typically administered by subcutaneous or intramuscular routes, where the vaccine can enter various cell types via receptor-mediated endocytosis. Degradation of vaccine proteins occurs within the cytosol of the cell, generating peptides that can be loaded onto MHC-I molecules displayed on the cell surface. CTLs with the appropriate antigen-specificity recognize the MHC:antigen complex, releasing cytokines that direct the infected cell to undergo apoptosis. Memory CTLs may also be formed during this process. In addition, immature DCs engulf the vaccine, initiating the same process as in killed vaccination, in which plasma cells producing IgG and memory B cells are formed (Baxter, 2007). Live, attenuated vaccines offer a multitude of advantages including the ability to induce strong cell-mediated responses, in addition to robust antibody responses and the potential to confer long-term immunity without numerous booster vaccinations. Disadvantages include the reversion back to the virulent form of the pathogen, which may limit their safety. Their use in immunocompromised individuals is also limited because even attenuated forms of the pathogen may be able to induce disease symptoms in people with weakened immune systems. In addition, live, attenuated vaccines require refrigeration to maintain stability and potency (Baxter, 2007; Clem, 2011).

Recombinant vector vaccines

Recombinant viral and bacterial vectors have been evaluated for vaccine development, including the vaccinia virus-vectored hepatitis B vaccine (Choi & Chang, 2013; Clem, 2011). Recombinant vector vaccines utilize attenuated pathogens or pathogens that do not cause severe illness in humans to express antigens that induce protection against an infectious agent. Viral vectors include recombinant retrovirus, lentivirus, vaccinia virus, adenovirus, cytomegalovirus (CMV), and Sendai virus vectors (Ura, Okuda, & Shimada, 2014). Viral-vectored vaccines mimic a natural infection, inducing adaptive immune responses similar to live, attenuated vaccines and natural infections. Attenuated recombinant bacterial vectors can also be used to express foreign antigens (Clem, 2011). Advantages of recombinant vectored vaccines are similar to those of live, attenuated vaccines such as the ability to induce robust CTL responses and antibody responses due to their ability to mimic natural infection. Additional benefits are also conferred by specific vectors. For example, retrovirus, lentivirus, and adeno-associated virus vectors can induce long-term gene expression of antigens; vaccinia virus and adenovirus vectors are highly immunogenic and have demonstrated safety in clinical trials; and CMV-vectors induce unique CTL responses. Disadvantages with recombinant vector vaccines may also be vector-specific. For example, with vaccinia virus and adenovirus vectors, pre-existing vector immunity may cause the vaccine to be cleared by the host before immunity to the antigen is generated. Risk of pathogenesis in immunocompromised individuals is a disadvantage of CMV-vectored vaccines (Ura et al., 2014). Similar to live, attenuated vaccines, recombinant vector vaccines require refrigeration in order to maintain vaccine stability and potency (Baxter, 2007).

DNA vaccines

DNA vaccines utilize plasmids encoding specific microbial antigens. Upon immunization, DNA is taken up by host cells, which utilize cellular machinery to express the antigen using a strong mammalian promoter and display membrane proteins on their cell surface which can stimulate the immune system. DNA vaccination mimics natural infection due to endogenous antigen processing and presentation of peptides by MHC-I molecules. Thus, DNA vaccines may have potential for inducing robust CTL responses in addition to strong antibody responses against the antigen. Additional advantages of DNA vaccines are their ease of production via recombinant DNA technology and their inability to cause infection and disease. DNA vaccines are also relatively inexpensive in comparison to other vaccine types. Generation of immunity against a specific antigen, enhanced stability at different temperatures, and potential for long-term immunogenicity are other advantages of DNA vaccines. Disadvantages of DNA vaccines are their limitation to protein antigens (ie. cannot be used for polysaccharide antigens), potential for inducing the development of anti-DNA antibodies, poor immunogenicity, and typical processing of bacterial and parasite proteins. Another disadvantage of DNA vaccines is the integration of foreign DNA into the host genome may promote malignancy of the host cell (Clem, 2011; Khan, 2013).

1.2. HUMAN IMMUNODEFICIENCY VIRUS

1.2.1. Acquired immunodeficiency syndrome

Human immunodeficiency virus (HIV) is the etiological agent that causes acquired immunodeficiency syndrome (AIDS), which was first documented as a fatal wasting disease associated with homosexual men and intravenous drug users in the early 1980s (Mahungu, 2011). The viruses believed to be responsible for AIDS were lymphadenopathy-associated virus (LAV) and human T-lymphotropic virus-III (HTLV-III), which were isolated from AIDS patients in France and the United States, respectively. However, these two agents were discovered to be the same virus and were renamed HIV in 1985 (Marx, 1985; Sharp & Hahn, 2011). Since then, HIV/AIDS has remained a global pandemic, with an estimated 36.9 million people living with HIV in 2014. Two million new infections and 1.6 million deaths occurred within the same year (UNAIDS, 2015).

HIV infection mainly occurs through unprotected sexual transmission involving the exchange of infectious semen or vaginal fluids. Transmission can also occur through mucocutaneous contact or direct inoculation with infected blood, which can occur via infected blood transfusions; or contaminated needles, through needle stick injury in the hospital setting or sharing of needles by intravenous drug users (Maartens, Celum, & Lewin, 2014).

The acute phase of HIV infection occurs 2-6 weeks after inoculation, during which the virus widely disseminates to lymphoid organs. 40-90% of infected individuals experience symptomatic infection, presenting as a non-specific viral syndrome involving fever, fatigue lymphadenopathy, muscle and joint pain, and weight loss. Other symptoms include maculopapular rash, oropharyngeal ulceration, and some gastrointestinal manifestations, including abdominal pain, vomiting, and diarrhea, which usually lasts for 1-2 weeks but may persist in some cases. Patients may remain asymptomatic during primary HIV infection, which may prevent early diagnosis. The acute phase of HIV infection is followed by the chronic phase of HIV infection, in which the host's immune response is able to maintain virus titres at a manageable level, known as the viral set point. However, during the chronic phase of HIV infection, $CD4^+$ T cell counts steadily decline. This phase can be asymptomatic or be punctuated by "indicator diseases" due to compromised $CD4^+$ T cell functions, such as oropharyngeal candidiasis, pelvic inflammatory disease, oral hairy leukoplakia, or herpes zoster. Weight loss, chronic diarrhea, and unexplained fever lasting for over a month may also occur. Advanced HIV infection occurs once patients' $CD4^+$ T cell count falls below 200 cells/mm^3, putting them at increased risk of acquiring opportunistic infections and malignancies. This phase manifests as HIV wasting syndrome (>10% weight loss) and encephalopathy, and many AIDS-defining conditions may arise, such as recurrent bacterial pneumonia, tuberculosis, cervical carcinoma, cryptosporidiosis, histoplasmosis, cytomegalovirus retinitis, Kaposi's sarcoma, non-Hodgkin's lymphoma, among many others (Mahungu, 2011). However, approximately 5-15% of those who become infected with HIV do not progress into AIDS and maintain high $CD4^+$ T cell counts (500 cells/µl) for over 10 years and are referred to as long-term nonprogressors (LTNPs). Within the LTNP population are viremic controllers (VCs), which maintain low but detectable HIV RNA loads (≤2000 copies/mL), and elite controllers (ECs), which maintain undetectable HIV RNA loads (<50 copies/mL) in the absence of therapy (Okulicz et al., 2009). In addition, there is a subset of highly-exposed, HIV-seronegative (HESN) individuals who remain HIV-negative despite constant exposure to HIV-positive sexual partners. These include HIV-uninfected commercial sex workers in sub-Saharan Africa, who after over five years of active prostitution, fail to become HIV-positive (Alimonti et al., 2005; Luo et al., 2012). These individuals represent a model of natural HIV immunity, believed to be affected by an individual's capacity to maintain systemic integrity by controlling inflammatory conditions at mucosal points of entry, while constraining immune activity (Poudrier, Thibodeau, & Roger, 2012).

1.2.2. Human immunodeficiency virus virology

HIV belongs to the *Lentivirus* genus within the *Retroviridae* family, distinguished by their ability to transcribe their RNA genome into DNA using a viral enzyme called reverse transcriptase (RT) (Levy, 2007b). HIV-1 and HIV-2 were introduced into the human population via zoonotic infections with simian immunodeficiency viruses from apes and sooty mangabeys, respectively (Sharp & Hahn, 2011). While both viruses are capable of causing AIDS, Group M of HIV-1 is responsible for the worldwide pandemic, while Groups N, O, and P are mainly confined to West Africa. Meanwhile, HIV-2 is less transmissible, causes slower progression into immunodeficiency, and is restricted mainly to some areas of West Africa (Maartens et al., 2014). The 9.8 kb single-stranded RNA (ssRNA) genome of HIV contains three structural genes, *gag*, *pol*, and *env*; six accessory and regulatory genes, *tat*, *rev*, *nef*, *vif*, *vpr*, and *vpu* (*vpx* in HIV-2); and long terminal repeat (LTR) sequences, flanking each RNA strand (Booth, C., Geretti, 2011). The primary transcript generated is a complete viral mRNA, which is translated into a Gag-Pol precursor. The polymerase (Pol) precursor is autocleaved by protease (PR), which subsequently yields the RNA-dependent DNA reverse transcriptase (RT) and integrase (IN) proteins. The Gag precursor is cleaved by PR into the matrix protein (MA; p17), capsid protein (CA; p24), nucleocapsid (NC; p6 and p7), as well as other viral proteins, p1, and p2. Using a different open reading frame of the full-length viral mRNA, the Env precursor, gp160, is produced and cleaved by host cellular proteases into the surface glycoprotein (gp120) and the transmembrane glycoprotein (gp41). In addition, the genome also encodes viral regulatory and accessory proteins, transactivating protein (Tat), regulator of viral protein expression (Rev), negative factor (Nef), viral infectivity factor (Vif), viral protein R (Vpr), and viral protein U (Vpu), which do not require processing by proteases (Freed, 2001; Levy, 2007b). HIV shares morphological characteristics with other lentiviruses, forming a spherical particle approximately 120 nm in diameter. Within the HIV particle is a conical core formed by p24, which encloses two copies of the NC-encased RNA genome as depicted in **Figure 1.4**. Also within the core, are the RT and IN, which associate with the genomic complex, and accessory proteins, Vif, Vpr, Nef, and p7. Env is expressed on the plasma membrane of the virus, while MA associates with the plasma membrane in the intracellular space (Engelman & Cherepanov, 2012). The fast and error-prone replication by HIV RT can introduce a new mutation every 3.4 x 10^5 base pairs, causing substantial diversity in the geographic distribution of HIV strains in circulation (Mansky & Temin, 1995). Within the pandemic HIV-1 Group M, there are 11 different subtypes including A–D, F–H, J, and K. At the individual level, a vast population of viruses, known as a quasispecies, arises in a single infected patient (Ndung'u & Weiss, 2012).

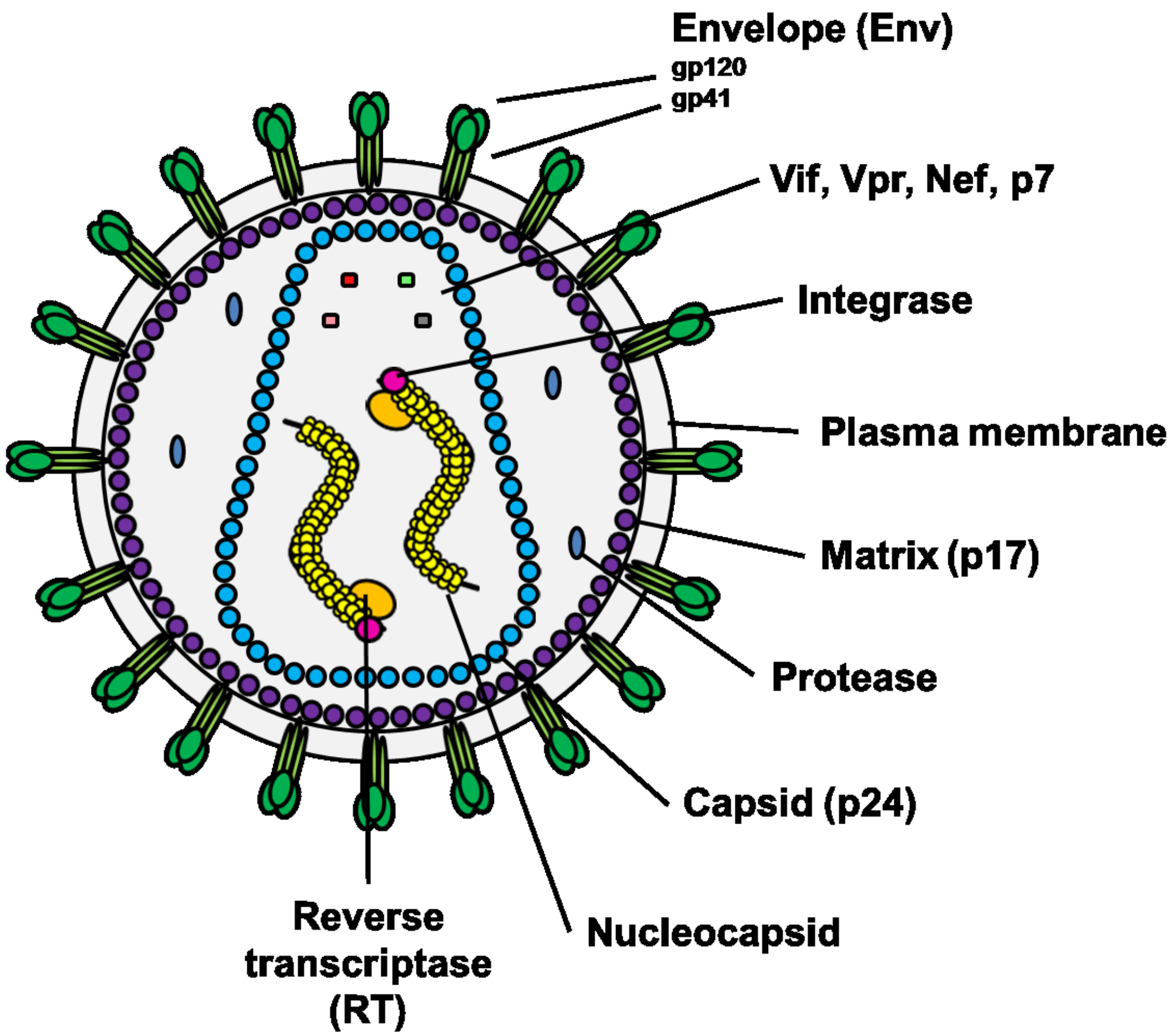

Figure 1.4. Human immunodeficiency virus structure. HIV is a spherical enveloped virus with Envelope glycoproteins embedded around its plasma membrane. Within its conical core formed by capsid proteins, are two copies of the positive-sense RNA genome encased in nucleocapsid proteins and interacts with HIV integrase and reverse transcriptase. Also within the core are the accessory proteins, Vif, Vpr, Nef, and p7. (Adapted from Engelman & Cherepanov, 2012**)**

1.2.3. Human immunodeficiency virus tropism and life cycle

Activated $CD4^+$ T cells are the main targets of HIV. The tropism of HIV for $CD4^+$ T cells is directed by the HIV Env on the surface of the virus, which are trimeric structures comprising three heterodimers of gp120 and gp41 that specifically bind to cluster-of-differentiation (CD)4 molecules on $CD4^+$ T cells as depicted in **Figure 1.5** (Permanyer, Ballana, & Esté, 2010). The gp120 receptor-binding surface unit of Env binds CD4 molecules, which results in conformational changes that expose co-receptor binding sites on gp120, allowing it to interact with and either CXCR4 or CCR5 chemokine co-receptors on target cells, for X4- and R5-tropic HIV strains respectively. Co-receptor binding leads to additional conformational changes that expose hydrophobic N-terminal heptad repeat (HR) regions within the gp41 fusogenic transmembrane subunit of Env. Insertion of this region of gp41 into the target cell membrane brings the viral and cellular membranes into close proximity, allowing for fusion of the virus into the target cell (Arts & Hazuda, 2012; Garg, Mohl, & Joshi, 2012).

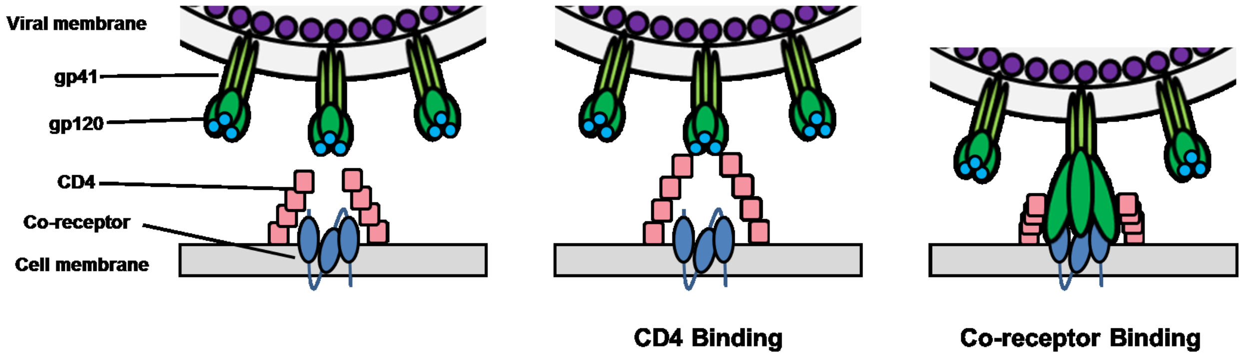

Figure 1.5. Tropism of human immunodeficiency virus. HIV tropism for CD4$^+$ T cells occurs through the specific binding of the gp120 subunit of HIV Env with CD4 molecules present on target cells. CD4 binding results in a conformational change in gp120, which allows it to interact with co-receptors CXCR4 or CCR5, for X4- and R5-tropic viruses, respectively. Co-receptor binding results in conformational changes that expose fusogenic regions of the gp41 subunit of Env, mediating entry of the virus into the host cell. **(**Adapted from Permanyer et al., 2010**)**

Upon viral entry and fusion, the viral core is delivered into the host cytoplasm, where a slow dissolution process of uncoating occurs to protect the viral RNA genome, while allowing access to deoxynucleoside triphosphates required for reverse transcription and proviral DNA synthesis. Reverse transcription of the viral genome occurs, forming the viral pre-integration complex (PIC), comprising viral and cellular components. The PIC is transported to the nucleus where integrase mediates the integration of viral DNA into the host genome. Integration of viral DNA is critical in sustaining viral DNA for subsequent expression of viral RNAs for future progeny and HIV mRNAs for the production of viral proteins. While cellular machinery initiates transcription of the proviral sequence, the HIV regulatory protein, Tat, is required for transcript elongation (Arts & Hazuda, 2012). Assembly of the HIV virion occurs on the inner plasma membrane of the host cell and is mediated by Gag polyprotein and the Gag-Pol-Pro polyprotein. The polyproteins bind and interact with the plasma membrane to form spherical particles, concentrate Env deposition at the membrane, and package the genomic RNA. Budding, which is the release of the virion from the plasma membrane, is mediated by the host endosomal sorting complexes required for transport (ESCRT) machinery. Upon release, viral maturation occurs in which HIV protease cleaves the Gag and Gag-Pro-Pol polyproteins, forming the MA, CA, NC, p6, PR, RT, and IN proteins, which rearrange to form mature and infectious particles. Mature HIV is distinguished by the presence of a distinct conical core (Sundquist & Kräusslich, 2012).

1.2.4. Human immunodeficiency virus pathogenesis

The morbidity of HIV infections is primarily caused by the infection and progressive depletion of activated $CD4^+$ T cells, which express high levels of CD4 and co-receptors CXCR4 or CCR5 (Berkowitz et al., 1998). Thus, the presence of activated $CD4^+$ T cells is crucial to HIV pathogenesis, providing the virus with more susceptible cell targets (Okoye & Picker, 2013). Upon recognition of cognate antigens and appropriate co-stimulation in the presence of particular cytokines in the microenvironment, naïve $CD4^+$ T cells differentiate into a range of effector $CD4^+$ T cells, also known as T helper cells. T helper cells play a crucial role in the adaptive arm of the immune system by producing cytokines that aid in the function of other immune cells. For example, in the presence of interleukin (IL)-12, naïve $CD4^+$ T cells are polarized towards differentiation into T_H1 cells, which primarily produce interferon (IFN)-γ and enhance cellular immunity against intracellular pathogens. The presence of IL-4 can drive differentiation of naïve $CD4^+$ T cells to T_H2 cells, which produce IL-4, IL-5, and IL-13 and enhance humoral immunity to control extracellular pathogens, such as helminthes. These are only two examples out of many roles T helper subsets play in adaptive immunity (Zhou, Chong, & Littman, 2009). During HIV infection, cytopathic effects and release of viral progeny due to direct infection ultimately leads to the destruction of $CD4^+$ T cells (Bell, 2007). In addition, HIV Env also mediates bystander apoptosis, a phenomenon in which Env expression on the surface of infected cells mediates syncytia formation, gp41-mediated hemifusion, and autophagy, inducing cell death in uninfected neighbouring $CD4^+$ T cells (Garg et al., 2012). The subsequent decline in $CD4^+$ T cells and defects in their responsiveness results in extreme immunosuppression and enhanced susceptibility to life-threatening infections and malignancies (Keating, 2012). HIV also infects monocytes and macrophages, which can express low levels of CD4, it induces secretion of growth factors, initiating a process of cell division that yields around 1000 cell clones. These clones are programmed to induce maturation of B lymphocytes and $CD8^+$ cytotoxic T lymphocytes upon exposure to the specific HIV antigen. In addition, these macrophages can interact with $CD4^+$ T cells, leading to their activation and priming their responses to antigens

(Gallo, 2012). Increased innate and adaptive immune activation is another hallmark of HIV infection. Early in HIV infection, massive depletion of activated $CD4^+$ T cells within the gastrointestinal tract (GT) occurs, failing to recover even after antiretroviral therapy. T helper 17 cells and mucosal-associated invariant T cells within the GT, which are important in anti-bacterial defence, are preferentially depleted. This, along with increased enterocyte apoptosis and enhanced GT permeability, results in increased plasma concentration of microbial products, which can lead to activation of $CD4^+$ T cells in the systemic circulation, optimal for targeting by HIV (Maartens et al., 2014).

1.2.5. Current treatments for human immunodeficiency virus and acquired immunodeficiency syndrome

Prior to 1996, limited therapeutic options were available for HIV infections and AIDS. Clinical management of HIV infection focused on treating common opportunistic infections with available drugs and managing AIDS-related diseases (Arts & Hazuda, 2012). The improvement of antiretroviral therapies (ARTs) since the mid-1990s transformed what was once a fatal illness into a manageable chronic disease, with global AIDS-related deaths decreasing from 2.3 million in 2005 to 1.6 million in 2012. As a result, however, HIV prevalence is increasing globally and HIV continues to infect about 2.3 million people annually. The current highly active antiretroviral therapy (HAART) regimen uses a combination of drugs with different mechanisms of action. The first component of a standard HAART regimen consists of two nucleoside reverse transcriptase inhibitors (NRTIs), such as lamivudine or emitricitabine combined with abacavir, zidovudine, or tenofovir (Levy, 2007a; Maartens et al., 2014). NRTIs are analogs of nucleoside substrates, which are utilized by the HIV polymerase to inhibit its function (Arts & Hazuda, 2012). The second component of HAART is a non-nucleoside reverse transcriptase inhibitor (NNRTI), such as delavirdine, efavirenz, or nevipiravine; a protease inhibitor, such as amprenavir, tipranavir, indinavir, or saquinavir; or an integrase inhibitor, such as raltegravir (Levy, 2007a; Maartens et al., 2014). NNRTIs inhibit the polymerase of HIV by binding a non-catalytic allosteric site on the protein, while protease inhibitors prevent the cleavage of the HIV gag and gag-pol polyprotein precursors, inhibiting virion maturation. Integrase inhibitors block strand transfer, preventing the integration of the HIV provirus into host DNA. Other HIV drugs include fusion inhibitors, which are peptides that mimic domains of gp41 to prevent virus entry, and co-receptor antagonists, which bind co-receptors on target cells needed for entry. These regimens can dramatically inhibit viral replication, reducing plasma viral loads to concentrations below limits of detection (<50 RNA copies/mL) and promoting reconstitution of the immune system (Arts & Hazuda, 2012). Side-effects and toxicities are common with HAART, contributing to the risk of non-adherence to the drug regimen. The most common side effects include hematological toxicities, such as bone marrow suppression, anemia, and neutropenia caused by zidovudine; psychiatric effects, such as sleep disturbance, dizziness, depression, and paranoia caused by efavirenz; renal toxicity caused by tenofovir; mitochondrial dysfunction caused by NRTIs; and peripheral neuropathy caused by didanosine and stavudine. Other common side-effects include allergic reactions, metabolic abnormalities, hepatotoxicity, and oseteopaenia (Rodger, A.J., Marshall, N., Geretti, A.M., Booth, 2011). Although HAART has dramatically improved the prognosis for HIV-infected patients, lack of availability in developing countries, inability to target latent HIV reservoirs in the host, and drug-resistance due to the high mutation rate of the virus remain obstacles for future drug development (Levy, 2007a). In addition, HAART cannot independently eliminate HIV infection, which remains an incurable illness (Arts & Hazuda, 2012). Thus, an efficacious vaccine to protect against HIV infection is crucial.

1.2.6. Vaccine development and correlates of protection for HIV

Despite the ongoing efforts invested into developing a vaccine to protect against HIV infection, a safe and effective vaccine still does not exist. One major hurdle in vaccine development is HIV's vast diversity and ability to escape a myriad of host immune responses (Excler, Tomaras, & Russell, 2013). Vaccination may also activate $CD4^+$ T cells, potentially increasing the number of cell targets for the virus (Bukh et al., 2014a). While consideration of viral proteins associated with control of virus replication is crucial to rational vaccine design, a consensus remains to be made about the ideal HIV protein for use as an HIV vaccine antigen (McDermott & Koup, 2012). Although promising results from early pre-clinical and clinical data allowed for their advancement to large-scale efficacy trials, most Phase II/III trials for HIV vaccines have failed to demonstrate vaccine efficacy, such as the VAX004 study, in which the bivalent clade B gp120 subunit vaccine demonstrated a meager vaccine efficacy (VE) of 6% (65% CI: 14-24%, p=0.59). The VAX003 study evaluated the efficacy of the subunit vaccine comprising clade B MN HIV gp120, as well as the recombinant clade A/E A244 strain gp120, which had a VE of 0.1% (95% CI: 30.8-23.8, p=0.99) (Sheets, Zhou, & Knezevic, 2016). In one case, a trial was halted early due to the apparent increase in HIV transmission risk in vaccinees as seen in the Phase IIb STEP trial, which evaluated an Adenovirus serotype 5 (Ad5)-vectored vaccine expressing HIV-1 Gag, Pol, and Nef (Sekaly, 2008). The higher HIV acquisition rates observed in those vaccinated in the STEP trial was likely due to pre-exisiting immunity to the Ad5 vector, which caused vaccination-induced mucosal memory T cell activation. This mucosal

T cell activation can potentially increase susceptibility to HIV by increasing the number of activated $CD4^+$ T cell targets (Bukh et al., 2014b). To date, the only vaccine regimen to demonstrate modest efficacy comprised a replication-defective canarypox vector (ALVAC) in combination with a recombinant gp120 protein (AIDSVAX), evaluated in 16,402 heterosexual men and women at risk of HIV-1 infection in the RV144 clinical trial in Thailand. Within the first year of vaccination, VE approached 60% in subjects, but waned to 31.2% over 3.5 years (Rerks-Ngarm et al., 2009).

Humoral correlates of protection against HIV

Many vaccine design efforts have focused on attempting to induce broadly neutralizing antibodies (nAbs), primarily targeted against HIV gp120. Most broadly nAbs inhibit entry of HIV into host cells by targeting the receptor binding site, therefore preventing engagement of gp120 with CD4, blocking the interaction of gp120 with co-receptors, or preventing the exposure of the fusogenic region within gp41 (Montefiori, 2009). HIV-specific neutralizing antibodies, including those targeting regions in gp41, have been shown to protect against HIV infection upon passive transfer in macaques and humanized mice (Malbec et al., 2013). Although these nAbs, which block HIV from entering target cells, were previously considered a crucial element in conferring anti-HIV protection, an analysis of the RV144 trial showed that none of the sera from vaccinated recipients were able to neutralize a panel of 20 HIV-1 isolates in circulation in Thailand during the course of the trial. However, almost all vaccinated participants developed binding antibodies to gp120, particularly to the V1V2 and V3 regions, differing considerably from HIV-infected patients. Vaccinees also demonstrated a higher level of gamma-immunoglobulin (IgG)3 isotype antibodies involved in mediating antibody-dependent cell cytotoxicity (ADCC). These responses deteriorated rapidly from 79% prevalence at peak immunity (week 26) to 0% at year 1, which correlated with the rapid decline in VE observed after 1 year. Thus, high levels of non-neutralizing gp120-binding antibodies that mediate ADCC may be a better correlate of protection than nAbs (Corey et al., 2015). Still, many hurdles exist regarding the induction of protective anti-HIV antibody responses by vaccination. An ideal vaccine would induce antibodies that target a wide range of rapidly mutating HIV variants with up to 35% differences in amino acid sequence and overcome glycan shielding of the HIV envelope (Klein et al., 2013).

Cell-mediated correlates of protection against HIV

Over the past 20 years, $CD8^+$ T cell-mediated immunity has become recognized as a key driver in limiting HIV infection and slowing the onset of disease (McDermott & Koup, 2012). Inducing $CD8^+$ T cell memory may be advantageous in terms of HIV vaccine design because unlike humoral immunity, which relies on the constantly evolving HIV Env antigen, $CD8^+$ T cell memory may be less susceptible to viral genetic instability by additionally recognizing epitopes from internal viral proteins that are indispensable for replication (Masopust, 2009). In both acute and chronic stages of SIV infection in rhesus macaques, SIV replication was controlled predominantly by the presence of $CD8^+$ T cells, while depletion of $CD8^+$ T cells led to increased viral replication and accelerated disease progression (Jin et al., 1999; Matano et al., 1998; Schmitz et al., 1999). The $CD8^+$ cytotoxic T cell response is considered significant in conferring long-term control of HIV in humans (Fonteneau et al., 2003; Sekaly, 2008; Streeck, Frahm, & Walker, 2009). In particular, Gag-specific $CD8^+$ T cell responses are critical in the maintenance of low viral loads during primary HIV-1 infection and are associated with delayed AIDS progression in LTNPs (Radebe et al., 2015). In large cohorts of HIV-infected adults and neonates, Gag-specific $CD8^+$ T cell responses correlate with improved clinical outcome and control of virus replication regardless of major histocompatibility complex (MHC). Control was shown to be directly related to the number of Gag-specific T-cell epitopes targeted in the protein (Masemola et al., 2004; McDermott & Koup, 2012; Nqoko et al., 2011). Although the Ad5-vectored cytotoxic T lymphocyte (CTL)-inducing vaccine in the STEP trial failed to demonstrate VE, the $CD8^+$ T cells induced by vaccination targeted epitopes within Gag, Pol, and Nef that are subject to variation, which may have allowed HIV to escape control. In addition, vaccine-induced $CD8^+$ T cells in vaccinees had reduced quality and limited effector functions, secreting mainly IFN-γ and tumor necrosis factor (TNF), but little IL-2 (Saunders, Rudicell, & Nabel, 2012).

1.3. EBOLA VIRUS

1.3.1. Ebola virus hemorrhagic fever

Ebola virus (EBOV) is the etiological agent of Ebola virus hemorrhagic fever (EHF). EBOV was discovered in 1976 when an acute illness of high fatality rapidly spread among healthcare workers in northern Zaire (now the Democratic Republic of the Congo) and southern Sudan, resulting in approximately 430 deaths. Similar in morphology, but antigenically different to the Marburg virus, the previously unknown pathogen was named Ebola virus after the river closest to Yambuku (Johnson, Lange, Webb, & Murphy, 1977). Additional EBOV outbreaks have occurred since then, primarily in the tropical regions of sub-Saharan Africa. This includes the 1995 outbreak in Kikwit, Democratic Republic of Congo that killed 245 of the 317 people infected, as well as the 2000 outbreak in Uganda that killed 224 of the 425 people infected

(Muyembe-Tamfum, Kipasa, Kiyungu, & Colebunders, 1999; Okware et al., 2002). The most recent outbreak in 2014-2015 was the largest of all, killing over 11,316 individuals out of the 28,639 infected, although these numbers are almost certainly underestimated due to the difficulties in reporting the epidemiological data (WHO, 2016).

EBOV is transmitted primarily by direct contact with blood and other bodily fluids of infected patients or animals, such as vomit, urine, semen, and sweat, by which virus can enter the host through breaks of skin or mucosal surfaces. Thus, patient care, sexual practices, consumption of infected bushmeat, or traditional burial practices can increase the risk of transmission (Meyers, Frawley, Goss, & Kang, 2015). Reuse of medical equipment such as syringes and personal protective equipment in combination with poor prevention measures and improper healthcare facilities can contribute to amplification of transmission during an outbreak, such as the 1995 EBOV outbreak in Kikwit, Democratic Republic of the Congo (Guimard et al., 1999). Although aerosol transmission can occur experimentally in non-human primates (NHPs), this mode of transmission has not been documented in humans (Olinger et al., 2005). Recently, molecular evidence demonstrated sexual transmission via infective EBOV in semen, which can persist over 179 days after the onset of disease (Mate et al., 2015).

After 2-21 days of incubation, EHF usually begins as a non-specific flu-like illness including fever, fatigue, progressive sore throat, and muscle soreness (Meyers et al., 2015). Within two days of disease onset, the virus may reach concentrations over 10^8 copies/mL in the blood, contributing to the aggressive nature of EBOV (Towner et al., 2004). Severe manifestations of EHF comprise symptoms such as abdominal pain, maculopapular rash, vomiting and diarrhea, which may contain blood from hemorrhagc and coagulation abnormalities (Heymann et al., 1980). In addition, mental confusion and encephalopathy can also occur. EBOV has a high mortality rate of 30-90% , with death resulting from multi-organ failure and hypovolemic shock usually occurring 6-16 days after initial symptom detection (Meyers et al., 2015). Those who survive EHF may shed virus in bodily fluids for up to 3 months, while experiencing fatigue, joint pain, anorexia, and memory loss (Nkoghe, Leroy, Toung-Mve, & Gonzalez, 2012; Rowe et al., 1999). Patients may experience long-term effects, such as psychosis and inflammation of the spinal cord, liver, testicles, and uvea (Feldmann, Sanchez, & Gesibert, 2013).

1.3.2. Ebola virus virology

Ebola virus (EBOV) belongs to the *Ebolavirus* genus within the *Filoviridae* family (Kuhn et al., 2010). The 19 kb non-segmented negative-sense ssRNA genome of EBOV contains short extragenic regions containing signals required for replication, transcription initiation, and genome packaging at the 3' and 5' ends. Each of the seven genes encoded by the EBOV genome is flanked by highly conserved transcription start and stop signals and separated by intergenic regions consisting of 4–7 non-conserved nucleotides in length. From 3' to 5', the EBOV genome encodes the nucleoprotein (NP), polymerase co-factor viral protein (VP)35, matrix protein VP40, glycoprotein (GP), replication-transcription protein VP30, minor matrix protein VP24, and RNA-dependent RNA polymerase (L) (Mühlberger, 2007). In addition, EBOV expresses a secreted non-structural version of EBOV GP, known as sGP. NP, VP30, and VP35 encapsidate the viral genome, forming the nucleocapsid, while VP40 acts as the major matrix protein to initiate the budding of filamentous viral particles from infected cells (N. Sullivan, Yang, & Nabel, 2003). Like other filoviruses, EBOV is an enveloped pleomorphic, and filamentous virus approximately 80 nm in diameter and varying in length up to 14,000 nm. EBOV may also appear as “6”-shaped and circular particles (Geisbert & Jahrling, 1995). Within the EBOV filament is the NP-encased RNA genome as depicted in **Figure 1.6**. L associates with the polymerase co-factor, VP35, on the genomic complex, along with VP24, and the transcription factor, VP30. Surrounding the viral genomic complex is VP40, which maintains virus morphology, and GP spikes, which are expressed on the viral membrane (Nguyen, Binder, Boianelli, Meyer-Hermann, & Hernandez-Vargas, 2015).

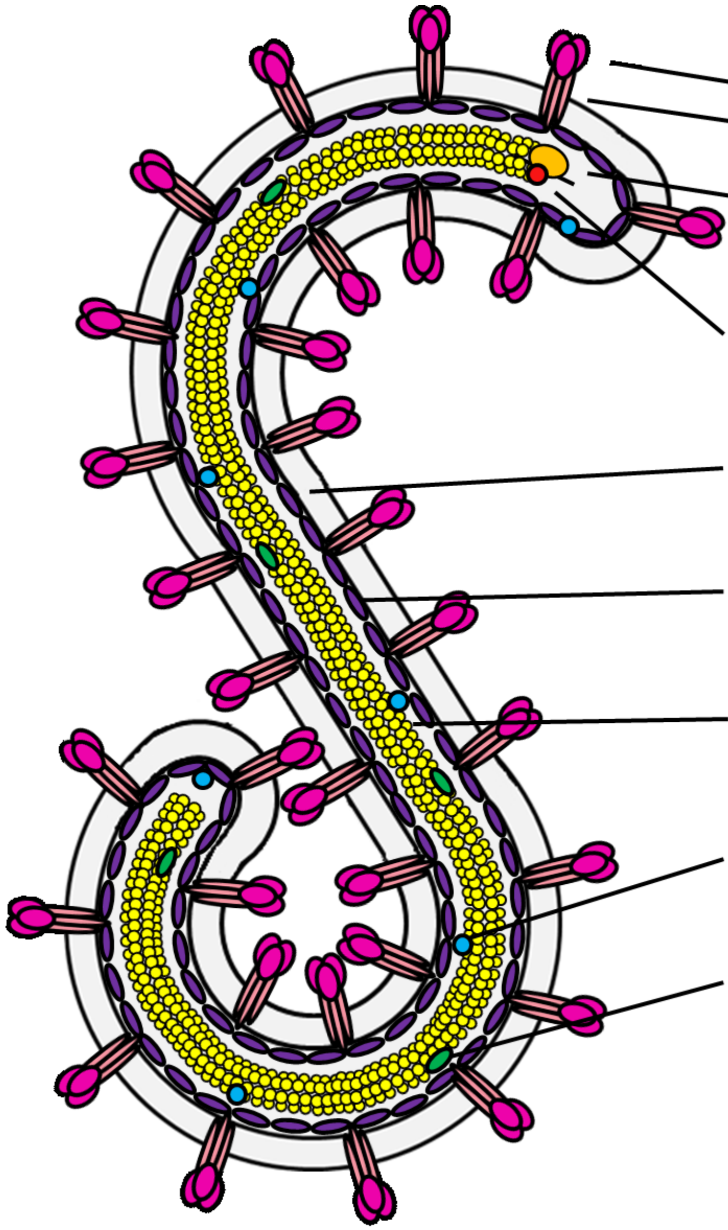

Figure 1.6. Ebola virus structure. EBOV is a filamentous enveloped virus with glycoproteins embedded around its plasma membrane. Within the virion, the negative-sense RNA genome is encased in nucleocapsid proteins and interacts with the polymerase co-factor VP35 and the RNA-dependent RNA-polymerase (L). Also within the particle are matrix proteins VP40 and transcription factors VP30. (Adapted from Nguyen et al., 2015)

1.3.3. Ebola virus tropism and life cycle

The tropism of EBOV towards monocytes, macrophages, DCs, hepatocytes, and endothelial cells is directed by EBOV GP, which are trimeric structures comprising three monomers of GP1 and GP2. In contrast to HIV, EBOV does not directly target $CD4^{+}$ T cells (Falasca et al., 2015). The GP1 subunit of EBOV GP is responsible for cellular attachment, containing putative receptor-binding regions and a heavily glycosylated region called the mucin-like domain (MLD). The GP2 subunit of EBOV GP is responsible for mediating fusion of the viral and host cell membranes, containing a hydrophobic internal fusion loop, two heptad repeats, a CX6CC disulfide bond motif, a membrane-proximal external region, as well as a transmembrane anchor (Lee & Saphire, 2009). During attachment, GP1 binds to attachment factors on target cells, such as dendritic cell-specific intercellular adhesion molecule-3-grabbing non-integrin (DC-SIGN) and T-cell immunoglobulin and mucin domain 1 (TIM-1) (**Figure 1.7**), and becomes internalized into cell endosomes by macropinocytosis. The vesicles that contain EBOV mature into lysosomes or late endosomes with a low pH that results in proteolytic processing by cellular cysteine proteases, such as cathepsins B and L, removing heavily glycosylated regions of GP1. Processing results in a conformational change in EBOV GP, which exposes the hydrophobic fusion loop within the GP2 subunit that allows it to interact with the Niemann-Pick type C1 (NPC1) receptor, which is utilized as an essential fusion receptor for virus entry (Kuroda et al., 2015; N. Sullivan et al., 2003).

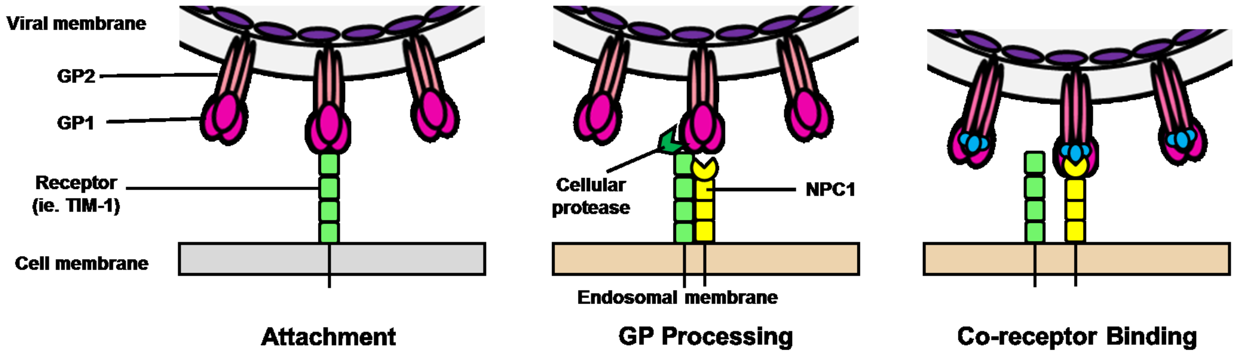

Figure 1.7. Tropism of Ebola virus. EBOV tropism for macrophages, monocytes, dendritic cells, and other targets occurs through the specific binding of the GP1 subunit of EBOV GP with receptors such as TIM-1 on the surface of target cells. Attachment results in internalization of the EBOV virion into endosomes by macropinocytosis. Within late endosomes, GP processing occurs, in which cellular cysteine proteases, such as cathepsin B, which remove heavily glycosylated regions in GP1, exposing co-receptor binding sites. Cleavage exposes fusogenic regions of the GP2 subunit of GP, mediating entry of the virus into the host cell. (Adapted from Takada, 2012)

Upon viral entry and fusion, viral proteins, NP, VP35, VP30, and L, as well as the RNA genome are delivered into the cytoplasm of the target cell. The viral polymerase complex of L and co-factor VP35 mediate the transcription of the negative-sense viral RNA, yielding mRNAs that are translated by cellular ribosomes. In addition, full-length positive-sense RNA copies of the viral genome are synthesized during replication and subsequently serve as templates for replication of genomic RNA synthesis. Assembly takes place at the plasma membrane, where GP and VP40 are embedded. The NP-encapsidated full-length viral RNA genome, along with other structural proteins interact with VP40 and GP and bud from the host cell surface (Takada, 2012).

1.3.4. Ebola virus pathogenesis

The morbidity of EBOV infections is caused by productive infection of DCs, monocytes and macrophages, allowing for transport of the virus through the lymphatic system to lymph nodes, and through the blood to the spleen and liver (Messaoudi, Amarasinghe, & Basler, 2015). Infection of macrophages and hepatocytes in the liver can result in organ damage and contribute to hemorrhagic effects of EBOV. Infection of monocytes and macrophages promotes the release of pro-inflammatory cytokines, such as TNF and IFN-γ, which can disrupt vascular endothelium architecture and other tissues, leading to endothelial leakage, rash, and hemorrhagic effects. This vascular dysfunction and loss of endothelial barrier function are considered important contributors to EBOV fatalities. Infection of macrophages and activation of neutrophils also contributes to inflammation, resulting in fever, malaise, and gastrointestinal effects later in disease progression. In contrast, infection of DCs results in aberrant DC function and lack of pro-inflammatory responses (Mohamadzadeh, Chen, & Schmaljohn, 2007). Aberrant DC maturation is mediated by EBOV VP35 and VP24 and prevents viral antigen processing and presentation, and aberrant stimulation of T cells, which inhibits their ability to initiate and optimize adequate adaptive immune responses to the virus (Ilinykh et al., 2015). In addition, VP35 and VP24 inhibit the innate immune response using distinct mechanisms. EBOV VP35 suppresses the production of IFN-β by inhibiting the RIG-I pathway in multiple ways. This includes preventing IRF-3 phosphorylation, inactivating IRF-7, and inhibiting the activation of IFN-inducible dsRNA and Dicer-dependent protein kinase R. In addition, VP24 is capable of disrupting both Type I and Type II interferon signalling by inhibiting antiviral gene transcription. VP24 inhibits the nuclear accumulation of dimerized phosphorylated STAT-1, involved in both Type I and II signal propagation cascades (Falasca et al., 2015). As viral titers increase later in EBOV infection, patients undergo a severe immunosuppression characterized by lymphopenia, deficient T cell response, and T cell apoptosis, despite being unable to infect T cells. These effects are believed to be caused by virally-induced upregulation of co-inhibitor molecules including B7-H1 on DCs and monocytes, which can interact with programmed death receptor PD1 on T and B cells. Eventually, viral burden can no longer be controlled by dysregulated adaptive and innate immune responses and fatality occurs (Mohamadzadeh et al., 2007).

1.3.5. Current treatments for Ebola virus hemorrhagic fever

Although research for the development of therapeutics has been ongoing since 1976, progress in drug development has greatly accelerated in the past 10-15 years. In particular, drug candidates for the treatment of EHF had not yet been evaluated in humans until the EBOV outbreak of 2014-2015 (WHO, 2014). Prior to the outbreak, the main method to alleviate EHF was supportive therapy, comprising intravenous Ringer’s lactate or saline to compensate for EHF fluid loss; paracetamol to treat pain and fever; midazolam, profolol, or ketamine to provide mild sedation; diazepam to inhibit vomiting; and omeprazole to relieve diarrhea (ClinicalTrials.gov, 2014a). During the outbreak, multiple drug candidates were evaluated under compassionate use provision, as well as Phase I trials to evaluate safety and immunogenicity and Phase II/III trials to evaluate drug efficacy (Mendoza, Qiu, & Kobinger, 2016). Small molecule drugs, such as amiodarone, brincidofovir, and favipiravir, were repurposed from their original indications for use in EHF patients in clinical trials (ClinicalTrials.gov, 2014a, 2014b, 2015c). However, due to the variation in rates across time and sites, statistically supported efficacy by these drugs became impossible to determine and, significant therapeutic benefit could not be concluded from the trials (Mendoza et al., 2016). Convalescent plasma from EHF survivors, and the TKM-Ebola siRNA therapeutic blocking the translation of EBOV VP24, VP35, and L, were also evaluated in clinical trials, but also failed to demonstrate significant efficacy (ClinicalTrials.gov, 2014c, 2015a; ISRCTN.com, 2015; PACTR.org, 2015). One of the most promising of the therapeutics evaluated during the recent outbreak was ZMapp, a monoclonal antibody cocktail comprising three humanized antibodies targeting EBOV GP (ClinicalTrials.gov, 2015d, 2015e; Davidson et al., 2015; Qiu et al., 2014). Of the 23 patients who received either ZMapp or ZMAb, the precursor cocktail to ZMapp, only three patients succumbed to EHF. One of these patients died after receiving only two of three scheduled doses, while the other two patients died after receiving only one dose. However, since the majority of these patients received additional treatments and intensive standard of care, the ongoing Phase II trial will be necessary to address the true clinical efficacy of ZMapp (Mendoza et al., 2016).

1.3.6. Vaccine development and correlates of protection for EBOV

Prior to the recent 2014-2015 EBOV outbreak, only two vaccines had been evaluated for safety and immunogenicity in human Phase I clinical trials (Marzi & Feldmann, 2014)**.** The first of these was the three-plasmid recombinant DNA vaccine, which encoded EBOV NP, and transmembrane-deleted EBOV and Sudan Ebola virus (SEBOV) GPs. This regimen was safe and immunogenic, but further studies demonstrated that transmembrane-deleted GP antigens are not optimal for protection and that NP was negligible for conferring protection (Martin et al., 2006; N. J. Sullivan et al., 2006). A subsequent Phase I trial was conducted to evaluate a replication-defective adenovirus 5 (rAd5)-vectored vaccine, encoding full-length EBOV GP, Ebola-rAd5. The vaccine was safe and induced EBOV-specific T-cell and antibody responses (Ledgerwood et al., 2010). This vaccine platform was abandoned due to high-pre-existing immunity against Ad5 in the human population, which may have contributed to only modest immunogenicity (Sarwar et al., 2015). However, these candidates had not been licensed for use in humans or evaluated in populations affected by EBOV (Agnandji et al., 2015; Marzi & Feldmann, 2014). During the outbreak however, multiple vaccine candidates were evaluated in human trials. In addition, the most clinically advanced vaccines were employed in Phase II/III efficacy trials in EBOV-affected regions of West Africa. The ChAd3-EBO Z vaccine is a replication-defective chimpanzee adenovirus serotype 3-vectored vaccine expressing EBOV GP that has demonstrated safety and efficacy in Phase I trials and is being evaluated in the PREVAIL I randomized control efficacy trial in Liberia (ClinicalTrials.gov, 2015b; De Santis et al., 2016; Tapia et al., 2016). The rVSV-ZEBOV vaccine is a glycoprotein-deleted vesicular stomatitis vectored-vaccine expressing EBOV GP that has also demonstrated safety and efficacy in Phase I trials and is being evaluated in the PREVAIL I trial, in addition to the Ebola ça suffit (PACTR201503001057193) ring vaccination efficacy trial in Guinea, and the STRIVE trial in Sierra Leone (ClinicalTrials.gov, 2015f; Huttner et al., 2015; Pan African Clinical Trials Registry, 2015; Regules et al., 2015). Interim results of the Ebola ça suffit trial from July 2015 demonstrated a vaccine efficacy of 100% (95% confidence interval 74.7–100.0; p=0·0036) at 6 day post-vaccination. These preliminary results suggest that protection conferred by rVSV-ZEBOV may be induced quickly (6–21 days) and potently by a single injection of vaccine. However, 43 serious adverse events were reported in trial participants. Of these, 1 participant experienced a febrile reaction at 3 dpv considered to be causally related to vaccination. The other serious adverse events were considered unrelated to vaccination and it is important to note that participants who experienced malaria or other febrile illnesses were provided treatment free of charge (Henao-Restrepo et al., 2015). Completed results of this study and of the STRIVE trial are pending, but rVSV-ZEBOV shows promise as it proceeds to licensure.

Humoral correlates of protection against EBOV

Humoral responses have been demonstrated to play a critical role conferring protection against EBOV. In particular, antibodies that target EBOV GP are associated with vaccine-induced protection. In cynomolgus macaques immunized with rVSV-ZEBOV, EBOV GP-specific IgG antibodies were shown to be critical for protection against lethal EBOV challenge (Marzi et al., 2013). Depletion of B cells, which secrete antibodies, and depletion of $CD4^+$ T cells, which provide T cell help for antibody responses, resulted in significantly reduced vaccine-induced protection in both guinea pigs and non-human primates (NHPs) upon lethal EBOV challenge. Furthermore, in both guinea pigs and NHPs, total anti-EBOV GP antibodies demonstrated the highest correlation with survival upon EBOV challenge. While these results highlighted the importance of total EBOV GP-specific IgG antibody levels as a correlate of protection against EBOV, the mechanism in which they provide immunity remains elusive (Wong et al., 2012). The ZMapp™ monoclonal antibody (mAb) cocktail for the treatment of EBOV comprises three humanized mAbs from two precursor cocktails, ZMAb and MB-003 that neutralize EBOV by binding distinct regions in EBOV GP (Pettitt et al., 2013; Qiu et al., 2011, 2012). This cocktail was demonstrated to reverse EHF symptoms in 100% of NHPs challenged with EBOV, even when treatment was administered up to 4 days post-challenge, providing further evidence of the importance of anti-EBOV GP antibodies in protection against EBOV (Qiu et al., 2014). However, serum EBOV GP-specific neutralizing antibody levels only correlated modestly with survival in guinea pigs and did not correlate with significant survival in NHPs, suggesting that alternate antibody-mediated mechanisms are involved in protection against EBOV. These could include antibody-dependent cell-mediated cytotoxicity, complement-dependent cytotoxicity, or inhibition of virus budding (Wong et al., 2012). Therefore, an EBOV vaccine should induce a robust humoral response against EBOV GP.

Cell-mediated correlates of protection against EBOV

Alternate perspectives suggest that EBOV GP-specific $CD8^+$ T cell responses may be crucial in providing protection against EBOV (N. J. Sullivan et al., 2006). Mice vaccinated with alphavirus replicon particles expressing each of the EBOV proteins, GP, NP, VP24, VP30, VP35, and VP40, and EBOV-specific $CD8^+$ T cells were isolated from immunized mice, expanded by peptide stimulation, and transferred into naïve mice. 100% of the mice receiving EBOV-specific $CD8^+$ T cells were protected upon lethal EBOV challenge (Olinger et al., 2005). Furthermore, another murine adoptive transfer study demonstrated the ability of EBOV GP-specific $CD8^+$ T cells to confer protection against EBOV challenge (Kelly Lyn Warfield & Olinger, 2011). The protective ability of EBOV GP-specific $CD8^+$ T cells was further analyzed in NHPs immunized with the Ebola-rAd5 vaccine expressing EBOV GP. In this study, NHPs that were depleted of $CD8^+$ T cells demonstrated lower levels of survival upon lethal EBOV challenge compared to those not depleted, suggesting the importance of EBOV GP-specific $CD8^+$ T cells in mediating protection against EBOV. However, the monoclonal antibody against CD3 that was used to deplete T cells demonstrated variable levels of T cell depletion, which was as low as 85% in some cases (N. J. Sullivan et al., 2011). In the study by Wong et al. (2012), NHPs that survived EBOV challenge did demonstrate increased IFN-γ-secreting cells upon *ex vivo* stimulation of splenocytes with EBOV GP peptides compared to non-surviving NHPs. However, rVSV-ZEBOV-immunized mice depleted of $CD8^+$ T cells were all protected against lethal EBOV challenge (Wong et al., 2012).

CHAPTER 2: STUDY RATIONALE, HYPOTHESIS, AND OBJECTIVES

2.1. STUDY RATIONALE

2.1.1. Influence of EBOV on the HIV pandemic and the need for a dual-acting vaccine

With over 11,316 fatalities out of 28,639 infections to date, the 2014-2015 Ebola virus (EBOV) outbreak in West Africa was the largest and deadliest EBOV epidemic in history (Butler, 2014; WHO, 2016). The outbreak was further accelerated due the absence of licensed therapeutics and vaccines (Chowell & Nishiura, 2014). Meanwhile, HIV continues to burden the population, with almost 70% of the world's HIV-positive population residing in Africa (Ogunbodede, 2004). On one hand, the EBOV outbreak in West Africa exacerbated the HIV epidemic by causing the death of primary healthcare providers in an already resource-limited setting. In addition, the outbreak shifted medical attention towards the more acute illness and away from the control measures for many chronic illnesses, such as HIV (Wainberg & Lever, 2014). The EBOV outbreak further hindered medical care-seeking due to the fear of contracting EBOV, transportation restrictions, and the overflow of patients in healthcare facilities (Ndawinz, Cissé, Diallo, Sidibé, & D'Ortenzio, 2015; Tattevin et al., 2015). Thus, the increase in HIV/AIDS deaths due to decreased adherence to treatment regimens from the EBOV outbreak was estimated to be 16.2%, 13%, and 9.1% in Guinea, Liberia, and Sierra Leone, respectively (Parpia, Ndeffo-Mbah, Wenzel, & Galvani, 2016). Thus, in the absence of a licensed vaccine for either virus, a dual-acting vaccine against both EBOV and HIV would be an ideal and cost-effective immunization strategy, especially in Africa, where succumbing to either virus is a grim reality.

2.1.2. Live HIV as a vaccine vector

Live, attenuated replication-competent vectors in vaccine design are desirable for their capacity to generate a mild infection, prolonging antigen exposure for the engagement of pathogen recognition and the adaptive arm of the immune system, thus providing longer lasting immunity (Parks, Picker, & King, 2013). Also, live vaccines can facilitate strong cell-mediated responses, as well as antibody responses, which may be advantageous for protection against both HIV and EBOV (Clem, 2011). In addition, of all vaccines tested in non-human primate (NHP) models with simian immunodeficiency virus (SIV), live attenuated SIVs remain the most efficacious vaccines in protecting against wild-type SIV. However, reversion back to wild-type and subsequent disease progression has been documented, making the use of this specific vaccine unreasonable from a safety perspective (Fukazawa et al., 2012). Therefore, a live, attenuated replication-competent HIV, lacking the ability to infect $CD4^{+}$ T cells and unable to revert and cause immunodeficiency, may be an ideal platform for vaccine candidates.

2.1.3. Targeting antigen presenting cells to enhance vaccine-induced immune responses

The induction of a robust, well-regulated innate inflammatory response is correlated with an improved outcome after EBOV infection (Osvaldo Martinez, Valmas, & Basler, 2007). Innate immune responses elicited by the experimental vaccine, VSVΔG/EBOV GP, were demonstrated to increase survival in mice when challenged with a lethal dose of mouse-adapted EBOV (Williams, Qiu, Fernando, Jones, & Alimonti, 2015). It has also been proposed that protective immunity against HIV is most likely driven by HIV vaccine candidates eliciting appropriate innate immune response profiles to optimize the priming of adaptive immunity (Excler et al., 2013). APCs, key players of the innate immune response, present viral antigens upon infection, activating naïve lymphocytes for induction of cytolytic and memory responses (Fonteneau et al., 2003). Targeting vaccine vectors to DCs and macrophages is highly desirable and vaccine vectors, such as adenovirus and vesicular stomatitis virus (VSV), that express and direct high levels of antigen to APCs have been shown to induce potent immune responses (Cao et al., 2013; Ciavarra et al., 2000). Since HIV infection and subsequent depletion of $CD4^+$ T cells results in the immunodeficiency associated with AIDS, an ideal vaccine candidate should target viral antigens to APCs for the induction of innate immunity, while sparing $CD4^+$ T cells to prevent immunosuppression.

2.1.4. Shifting the tropism of HIV away from $CD4^+$ T lymphocytes and towards antigen presenting cells

In contrast to HIV, which uses Env to target $CD4^+$ T cells (Bell, 2007; Yuan, Li, & Zhang, 2013) EBOV uses GP (Osvaldo Martinez et al., 2007; Wahl-Jensen et al., 2011) to target antigen-presenting cells, such as macrophages, monocytes, and DCs without using CD4 receptors for cell entry (Chan, Speck, Ma, & Goldsmith, 2000; Yonezawa, Cavrois, & Greene, 2005). Thus, immunization with a live-attenuated HIV lacking Env but pseudotyped with GP (HIV-EBOV) is expected to shift infection to APCs and not $CD4^+$ T cells. Such a vaccine should induce and optimize protective immune responses against both EBOV GP and HIV antigens (Pollara et al., 2005). $CD4^+$ T cells would be left unharmed and retain their capacity to coordinate adaptive immune responses, preventing AIDS. Furthermore, this novel bivalent vaccine candidate would provide a cost-effective prevention strategy in resource-limited settings.

2.1.5. Modifications of the EBOV glycoprotein for incorporation into the live HIV vector

The nascent polypeptide chain of the EBOV glycoprotein contains an N-terminal 32 amino acid signal peptide, which directs it to the endoplasmatic reticulum to be folded and modified by the addition of carbohydrates (Marzi et al., 2006). Since the sequence encoding the signal peptide of HIV Env would need to be conserved to maintain the alternate open reading frame for the expression of HIV vpu, it is possible that processing of the nascent EBOV GP polypeptide chain could instead be directed by the HIV Env-derived signal. Therefore, one modification of EBOV GP includes the removal of the additional EBOV GP-derived signal peptide.

The 150 amino acid mucin-like domain (MLD) of EBOV GP is associated with cell cytotoxicity, causing rounding of cells and detachment from the extracellular matrix. The MLD also mediates the down-regulation of β1 integrin and MHC-I on the cell surface. Since EBOV GP directs the virus to many APC subsets, it is possible that the cytotoxicity of these cells mediated by the MLD could be involved in innate immune dysregulation, subsequently hindering the formation of optimal adaptive immune responses (Francica, Matukonis, & Bates, 2009). Thus, another modification of EBOV GP for the insertion into the vaccine platform includes the deletion of the MLD. In addition, removal of the MLD region of EBOV GP has been demonstrated to have a minimal impact on EBOV neutralizing antibody induction upon immunization (Osvaldo Martinez, Tantral, Mulherkar, Chandran, & Basler, 2011).

Therefore, three variations of EBOV GP will be incorporated in place of gp120 in the HIV vector to create three different vaccine candidates – full-length EBOV GP, signal peptide-deleted EBOV GP, and MLD_deleted EBOV GP.

2.2. HYPOTHESES

The central hypotheses of this thesis are:

1. Live HIV expressing EBOV GP as a functional replacement of HIV Env, HIV-EBOV, will exhibit tropism away from $CD4^+$ T cells and towards antigen presenting cells

2. Immunization with HIV-EBOV will induce cellular and humoral immune responses associated with protection against both HIV and EBOV in a mouse model

3. Immunization with HIV-EBOV will demonstrate protective efficacy against EBOV in a mouse model

2.3. OBJECTIVE AND AIMS

In order to address the hypotheses, the primary objective of this thesis is to develop and evaluate the immunogenicity of a live, bivalent vaccine against EBOV and HIV with tropism for APCs and not $CD4^+$ T cells and evaluate its protective efficacy against EBOV infection

The objective is addressed in the following aims:

1. Rescue live HIV-1 recombinants expressing EBOV GP as a replacement for HIV Env

2. Characterize the infectivity, tropism, and replication of HIV-EBOV candidates in $CD4^+$ T cells and antigen presenting cells, such as monocytes

3. Characterize the cell-mediated and humoral responses against EBOV and HIV following immunization with HIV-EBOV vaccine candidates in mice

4. Evaluate the protective efficacy of HIV-EBOV vaccine candidates against lethal mouse-adapted EBOV challenge in mice

2.4. SIGNIFICANCE OF RESEARCH

The study of this novel bivalent vaccine approach for the simultaneous prevention of EBOV and HIV infection can generate substantial knowledge on the span of immune responses initiated upon shifting the delicate balance of HIV replication away from $CD4^+$ T cells toward APCs. Importantly, this approach may one day serve as a cost-effective, dual-acting vaccine to provide protection in the ongoing battles against EBOV and HIV.

CHAPTER 3: MATERIALS AND METHODS

3.1. GENERATION OF MOLECULAR CLONES FOR THE RESCUE OF EBOV GP-EXPRESSING HIV RECOMBINANTS

3.1.1. Amplification of fragments for the construction of In-fusion inserts

For the amplification of each fragment, the reaction set-up consisted of 34 µL nuclease-free water, 10 µL HF buffer, 1 µL dNTP, 1 µL 10 mM forward and reverse primers for each specific fragment as listed in **Table 3.1.**, 2 µL of template, and 1 µL iProof DNA polymerase. The thermal cycling conditions performed were initial denaturation at 95 °C for 1 minute, followed by 35 cycles of denaturation at 95 °C for 25 seconds, annealing at 58 °C for 25 seconds, and extension at 72 °C for 30 seconds/kb of desired amplification product. The last stage of thermal cycling was final extension at 72 °C for 5 minutes. The subsequent PCR amplifications mentioned in this report followed the same reaction set-up and thermal cycling conditions, unless otherwise specified.

Table 3.1. Sequence of the primer pairs used for PCR amplification of fragments to construct EBOV GP-containing inserts.

Primer Name	Primer Sequence (5'-3')	Template
4-3A-**SalI**-F	GAATTGGGT**GTCGAC**ATAGCAGAATAG	pNL4-3
4-3A-SalI-R	**CCTGTAACGCCCAT**TTCTGTAGCACT	pNL4-3
4-3A-SalIΔSP-R	**TCCAAGTGGGAT**TTCTGTAGCACTACA	pNL4-3
4-3B-GP-F	AGTGCTACAGAA**ATGGGCGTTACAGG**	pCAGGS-EBOV GP
4-3B-GP-R	GAACAAAGCTCCTAT**CTAAAAGACAAATTTG**	pCAGGS-EBOV GP
4-3B-GPΔSP-F	TGTAGTGCTACAGAA**ATCCCACTTGGA**	pCAGGS-EBOV GP
4-3B-GPΔM-F	GCAGTGAA**ATTGCTGGAGTCGCAG**	pCAGGS-EBOV GP
4-3B-GPΔM-R	**CCAGCAAT**TTCACTGCGAATTTTTC	pCAGGS-EBOV GP
4-3C-BamHI-F	**CAAATTTGTCTTTTAG**ATAGGAGCTTTGTTC'	pNL4-3
4-3C-**BamHI**-R	AAGTGCTAA**GGATCC**GTTCACTAATCGA	pNL4-3

All primers were designed based on the HIV-1 vector pNL4-3 (GenBank Accession: AF324493) and EBOV (Mayinga) GP gene, complete coding sequence (GenBank Accession: U23187.1). "F" stands for forward and "R" stands for reverse indicating the direction of primer extension. Underlined and bolded are the restriction enzymes conserved between the amplified fragment and the pNL4-3 vector in order to mediate cloning. In blue, are sequences of homology with the EBOV GP gene.

Purification of the DNA fragments was accomplished by gel electrophoresis on 0.9% agarose gel performed at 120 V for 45 minutes, allowing isolation of the proper fragments by molecular weight. The DNA bands were visualized using a Safe Imager™ 2.0 Blue Light Transilluminator (Invitrogen, CA, USA) and the appropriate DNA bands as described in **Table 3.2.** were excised from the gel using a scalpel. DNA was extracted following the QIAquick Gel Extraction Kit Spin Protocol (QIAGEN, ON, Canada). Gels containing DNA were melted in 3 volumes Buffer QG by incubating at 50°C for 10 minutes. One gel volume of 95% isopropanol was added to the dissolved DNA and mixed. The solution was added to a QIAquick column and centrifuged at 17,900 x g for 1 minute to bind DNA. Flow-through was discarded from the column and 750 µL Buffer PE was added to the column to wash the bound DNA. The tubes were centrifuged at 17,900 x g for 1 minute, flow-through was discarded, and the tubes were centrifuged for an additional 1 minute at 17,900 x g to remove excess Buffer PE. DNA was eluted from the column by adding 50 µL Buffer EB, allowing to incubate at room temperature for 1 minutes, and centrifuging at 17,900 x g for 3 minutes. DNA was stored at -20 °C until later use. The subsequent gel electrophoresis procedures and gel purifications mentioned in this report followed the same procedure, unless otherwise specified.

Table 3.2. Primer combinations for the PCR amplification of fragments to construct EBOV GP sequence-containing inserts.

Fragment	Primer Combination	Size of product
4-3A	4-3A-SalI-F + 4-3A-SalI-R	554
4-3AΔSP	4-3A-SalI-F + 4-3A-SalIΔSP-R	458
4-3B-GP	4-3B-GP-F + 4-3B-GP-R	2040
4-3B-GPΔSP	4-3B-GPΔSP-F + 4-3B-GP-R	1944
4-3B-GPΔM1	4-3B-GP-F + 4-3B-GPΔM-R	931
4-3B-GPΔM2	4-3B-GPΔM-F + 4-3B-GP-R	598
4-3C	4-3C-BamHI-F + 4-3C-BamHI-R	737

All primers were designed based on the HIV-1 vector pNL4-3 (GenBank Accession: AF324493) and Zaire Ebola virus Mayinga strain glycoprotein (GP) gene, complete cds (GenBank Accession: U23187.1). "F" stands for forward and "R" stands for reverse indicating the direction of primer extension.

3.1.2. Chimeric PCR assembly for the generation of the mucin-like domain-deleted EBOV GP gene

In order to generate full-length EBOV GP gene containing a deletion of the MLD, chimeric PCR assembly was performed. A reaction mix using the iProof DNA polymerase kit (BIO-RAD, CA., USA) was prepared consisting of 30 μL nuclease-free water, 10 μL HF buffer, 1 μL dNTP, 1 μL iProof DNA polymerase, as well as 2 μL 4-3B-GPΔM1 and 4-3B-GPΔM2 fragments. The first thermal cycling stage allowed these fragments to anneal to each other by their homologous ends, allowing them to act as primers for extension. The conditions of this stage were initial denaturation at 98 °C for 1 minute, followed by 5 cycles of: denaturation at 98 °C for 30s, annealing at 58 °C for 30s, and extension at 72 °C for 30s/kb of desired amplification product.

The reaction was allowed to pause at 4 °C, during which, the reaction was removed and 2 μL of 10 mM primers 4-3B-GP-F and 4-3B-GP-R were added. The second stage of the chimeric PCR procedure allowed amplification of the full-length insert using PCR thermal cycling conditions mentioned earlier. The subsequent chimeric PCR assemblies mentioned in this report followed the same reaction set-up and thermal cycling conditions, unless otherwise specified. The amplified product was visualized, excised, and extracted according to procedures mentioned earlier to yield the 4-3B-GPΔM fragment (1514 bp).

3.1.3. Chimeric PCR assembly for the generation of In-Fusion inserts containing EBOV GP gene truncations

Chimeric PCR assembly was used to generate full-length In-Fusion (IF) inserts containing EBOV GP gene truncations. To generate IF-GP, IF-GPΔ1, and IF-GPΔ2, DNA fragments were combined in the initial chimeric PCR mix as listed in **Table 3.3.** The intial thermal cycling stage was performed to allow the three fragments to anneal to each other by homologous ends. In the second stage of chimeric PCR assembly, 2 μL of 10 mM primers 4-3A-SalI-F and 4-3C-BamHI-R were added to allow extension of the full-length IF inserts. The amplified products were visualized, excised, and extracted according to procedures mentioned earlier to yield IF-GP, IF-GPΔ1, and IF-GPΔ2, which contained full-length EBOV GP, signal peptide-deleted EBOV GP, and MLD-deleted EBOV GP, respectively.

Table 3.3. Fragment combinations for the chimeric PCR full-length inserts containing truncations of the EBOV GP gene.

Insert	Fragment Combinations	Size of product
IF-GP	4-3A + 4-3B-GP + 4-3C	3294
IF-GPΔ1	4-3AΔSP + 4-3B-GPΔSP + 4-3C	3198
IF-GPΔ2	4-3A + 4-3B-GPΔM + 4-3C	2751

In-Fusion inserts were designed to contain different truncations of the EBOV GP gene flanked by HIV-derived sequences. 4-3A and 4-3AΔSP fragments flanked the 5' ends of the EBOV GP gene, while the 4-3C fragment flanked the 3' end of the gene. The 4-3B-GP, 4-3-GPΔSP, and 4-3-GPΔM fragments contained the full-length, signal sequence-deleted and mucin domain sequence-deleted EBOV GP sequence, repectively.

3.1.4. Cloning of the EBOV GP gene-containing inserts into pNL4-3

In order to remove the sequence for HIV gp120, the pNL4-3 plasmid was double digested in a reaction containing 39 μL nuclease-free water, 5 μL NE Buffer 3, 1 μL 100x Bovine Serum Albumin (BSA), 1 μL SalI Restriction Enzyme, and 1 μL BamHI Restriction enzyme (New England Biolabs, MA, USA). The digestion was allowed to incubate at 37 °C for one hour followed by inactivation at 65 °C for 20 minutes. The digestion product was electrophoresed and the band at 12,245 bp was gel purified as described previously. IF-GP, IF-GPΔ1, and IF-GPΔ2 were cloned into the digested pNL4-3 vector following the protocol for In-Fusion HD cloning (Clontech, CA, USA) to yield plasmids, pNL4-3ZGP, pNL4-3ZGPΔ1, and pNL4-3ZGPΔ2, respectively, as depicted in **Figure 3.1**. The reaction set up consisted of 2 μL insert, 4 μL digested vector (pNL4-3), 2 μL nuclease-free water, and 2 μL In-Fusion HD Enzyme Mix. The reaction was incubated at 50 °C for 15 minutes, cooled on ice for 10 minutes, and the clones were immediately transformed into chemically competent cells.

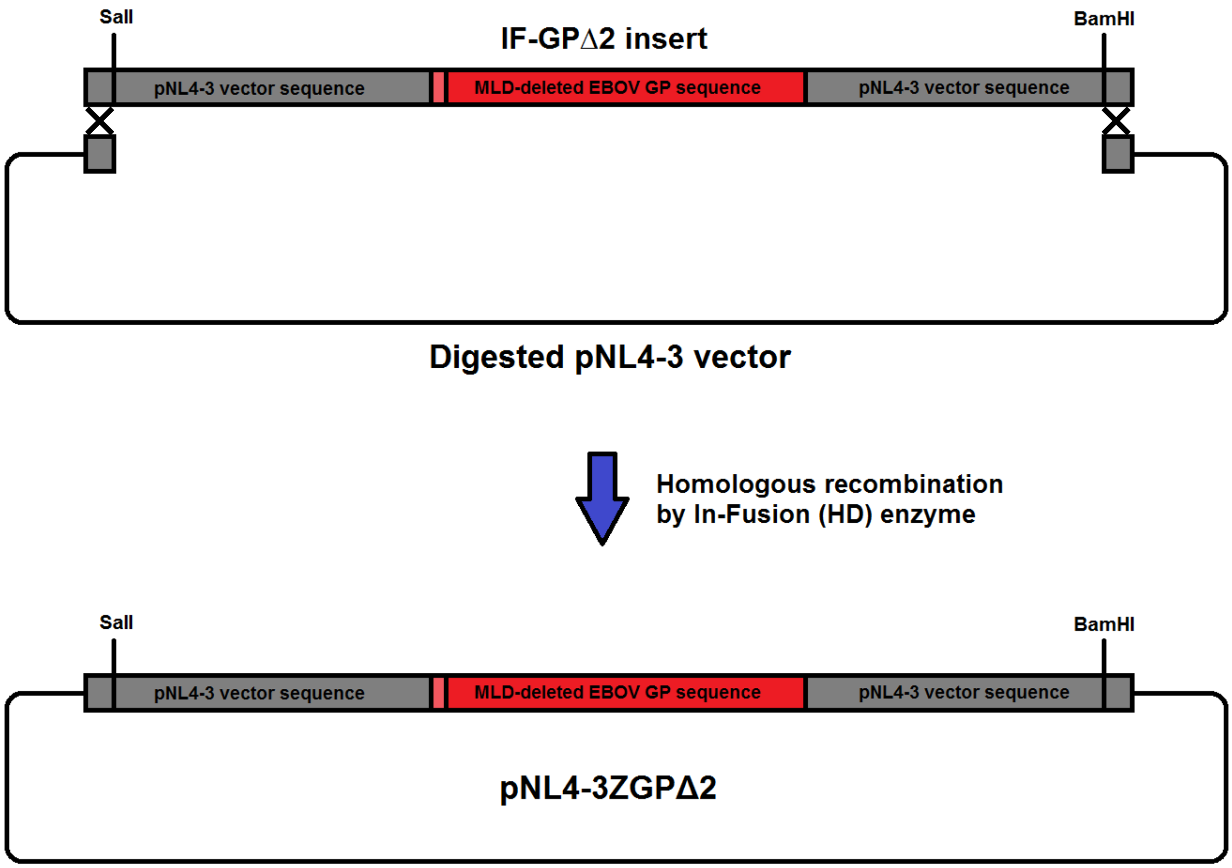

Figure 3.1. Schematic of In-Fusion HD cloning of IF-GPΔ2 into the SalI and BamHI digested pNL4-3 wild-type HIV vector. The IF inserts containing different truncations of the EBOV GP sequence contained 14 base pairs of homology with the digested pNL4-3 vector, allowing for homologous recombination by the In-Fusion HD enzyme.

3.1.5. Transformation of TOP 10 chemically competent cells with HIV-EBOV plasmids

For each clone, one vial of TOP 10 chemically competent *E. coli* was thawed on ice and transformed with 2 μL of cloning product. The cloning product was allowed to adhere to the surface of the bacteria by incubating ice for 30 minutes. The reaction was heat shocked at 42 °C for 30 seconds to allow DNA to enter bacterial cells, and the reaction was placed back on ice where 250 μL S.O.C. medium was added. The cells were shaken horizontally for 1 hour at 37 °C. 50 μL of the transformation reaction was diluted with 50 μL S.O.C. medium. For selection of transformed colonies, 100 μL of the diluted reaction was plated onto one Luria-Bertani (LB)-lennox plate supplemented with 100 μg ampicillin/mL, and the remaining liquid was plated onto another. The transformed cells containing plasmids encoding ampicillin-resistance were allowed to incubate at 37 °C overnight.

3.1.6. Extraction of plasmids from bacterial cells

Colonies were selected from transformation plates using an inoculation loop and added to flasks containing 250 mL LB-lennox broth supplemented with 100 μg ampicillin/mL. The bacterial cultures were allowed to incubate at 37 °C overnight. Glycerol stocks were prepared by adding 800 μL of the bacterial culture to 500 μL glycerol aliquots. Glycerol stocks were stored at -80 °C and were used to prepare future overnight bacterial cultures.

To isolate DNA plasmids from bacteria, the protocol for QIAfilter Plasmid Maxi Kit (QIAGEN, ON, Canada) was followed. Bacterial cultures were added to three 50 mL Falcon tubes and centrifuged at 7,000 x g at 4 °C for 20 minutes. Supernatant was discarded into buckets containing bleach. The cell pellets obtained for each construct were pooled together and suspended in 10 mL Buffer P1. To lyse the bacterial cells, 10 mL Buffer P2 was added and allowed to incubate at room temperature for 5 minutes. To neutralize the reaction, 10 mL of cold Buffer P3 was added and the lysate was allowed to incubate on ice for 10 minutes. The tubes were centrifuged at 7,000 x g for 20 minutes to pellet the cell debris. The supernatant containing the DNA was added to QIAfilters equilibrated with 15 mL Buffer QBT to allow DNA to bind to the column. The DNA was washed twice by adding 30 mL Buffer QC and allowing it to flow through the column. To elute the DNA, 15 mL Buffer QF was added to the column and the flow-through was added to a clean 50 mL Nalgene Oak Ridge Round-bottom tube (Thermo Fisher Scientific, MA, USA). To precipitate the DNA, 10 mL of 100% isopropanol was added and mixed well. To pellet the DNA, tubes were centrifuged at 13,000 x g at 4 °C for 30 minutes. Supernatant was discarded and the pellet was washed by adding 30 mL 70% ethanol. The tubes were centrifuged at 13,000 x g at 4 °C for 30 minutes, supernatant was discarded, and the pellet was allowed to dry at room temperature. The dried DNA pellet was resuspended in 750 µL of Buffer EB. Plasmid preparations were stored at -20 °C until further use.

3.1.7. DNA sequencing of HIV-EBOV molecular clones

To confirm the integrity of the constructs, the extracted plasmids were sequenced by the DNA Core Facility at the National Microbiology Laboratory (MB, Canada) using primers spaced approximately every 750 bp of the pNL4-3 backbone and EBOV GP sequence **(Appendix Table 1)**. DNASTAR Lasergene Molecular Biology Software (DNASTAR, WI, USA) was used to analyze assembled sequencing data, using pNL4-3ZGP, pNL4-3ZGPΔ1, and pNL4-3ZGPΔ2 sequences as templates.

3.2. CELL CULTURE

3.2.1. Cell culture of human embryonic kidney 293T and HeLa TZM-bl adherent cell lines

cDMEM-10 media was used to culture human embryonic kidney (HEK) 293T cells, as well as human cervical carcinoma (HeLa) TZM-bl cells (ATCC: PTA-5659), and was composed of Dulbecco's modified essential medium (DMEM) supplemented with 10% heat-inactivated fetal bovine serum (FBS), ~1.68 mM L-glutamine, ~0.62 μg/mL sodium bicarbonate, and ~16.8 μg/mL penicillin-streptomycin. cDMEM-5 was used as a diluent for virus stocks and was prepared the same way, except using 5% FBS instead of 10%.

To maintain these adherent cell lines, media from cells at 90-100% confluence in a T75 flask was discarded. The monolayers were washed with 10 mL PBS and cells were trypsinized by adding 4 mL 0.05% trypsin to cell layer and incubating at 37 °C and 5% CO_2. HEK 293T cells are easily trypsinized and released from the surface of the flasks by 1 minute, while TZM-bL cells are more adherent and require incubation for at least 3 minutes. After trypsinization, 16 mL cDMEM was added to the cells and mixed thoroughly to inactivate the trypsin. Cell lines were maintained by adding 1 mL of the cell suspension to a new flask containing cDMEM-10 and passaging every 4-5 days.

3.2.2. Cell culture of SUP-T1 and THP-1 suspension cell lines

cRPMI-10 media was used to culture the T-lymphoblast SUP-T1 [VB] (ATCC® CRL-1942TM) and the monocytic THP-1 (ATCC® TIB-202TM) cell lines and was composed of RPMI-1640 supplemented with 10% heat-inactivated fetal bovine serum (FBS), ~1.68 mM L-glutamine, ~0.62 μg/mL sodium bicarbonate, and ~16.8 μg/mL penicillin-streptomycin.

To maintain these suspension cell lines, the media containing cells within a T75 flask was aseptically transferred to a 50 mL Falcon tube and centrifuged at 125 x g at room temperature for 5 minutes. Supernatant was discarded and the cell pellet was resuspended to achieve a concentration of 2-4 x 10^5 cells/mL. Cultures were allowed to incubate horizontally at 37 °C and 5% CO_2. This process was repeated when cultures reached a concentration of approximately 8x10^5 cell/mL, which occurred about 4-5 days after seeding, without allowing the concentration to exceed 1 x 10^6 cells/mL.

3.3. RESCUE OF RECOMBINANT HIV-EBOV VACCINES

3.3.1. Transfection of HEK 293T cells with molecular clones for the rescue of HIV-EBOV vaccine candidates

All procedures involving live HIV-EBOV candidates, as well as wild type HIV, were performed in containment level 3 (CL-3) or higher. To generate each virus stock, two 15 cm culture dishes were seeded with 6.67 x 10^6 HEK 293T cells (Passage 10-15) the day before transfection and allowed to incubate at 37 °C overnight. The following day, media from each dish containing cells at 80-90% confluence was discarded and replaced with 20 mL cDMEM-5. For each virus, two transfection reactions were prepared by adding 110 µL room-temperature Opti-MEM reduced serum media (GIBCO, CA, USA; 31985062) to two 1.5 mL Eppendorf tubes. Without touching the polystyrene tube, 45 µL of FuGENE 6 Transfection Reagent (Promega, WI, USA; E2691) was injected directly into the media. The reagents were mixed well and allowed to incubate at room temperature for five minutes. After incubation, 5 µg of pNL4-3, pNL4-3ZGP, pNL4-3ZGPΔ1, pNL4-3ZGPΔ2, or pNL4-3dEnv-GFP DNA plasmid was added to the transfection reagent to rescue HIV wt, HIV-EBOV, HIV-EBOVΔ1, HIV-EBOVΔ2, or NL4-

3dEnv-GFP, respectively. A mock transfection reaction was prepared by adding 20 μL of water to the transfection reagent. After mixing, the transfection reactions were allowed to incubate at room temperature for 30 minutes. Each lipid nanoparticle-DNA complex mixture was added to designated dishes containing HEK 293T cells in a drop-wise fashion. The plates were immediately transferred to a containment level (CL)-3 laboratory and allowed to incubate at 37 °C for 72 hours.

After 72 hours, the dishes containing cells transfected with pNL4-3dEnv-GFP were visualized under an ultraviolet microscope to detect GFP expression as an indicator for successful transfection procedure. For each virus, supernatant from transfected cells were collected into 50 mL Falcon tubes and centrifuged at 1,200 x g for 5 minutes to remove extra cell debris. The supernatant was passed through a 0.45-micron filter and brought to a total volume of 40 mL by addition of cDMEM-5. 1 mL aliquots were prepared and stored at -80 °C.

3.3.2. Titration of virus stocks by p24 Enzyme-Linked Immunosorbant Assay

To obtain titers for each virus stock, a vial of each stock was gamma irradiated with 2.5 mRad for use in CL-2 laboratories. After gamma irradiation, the titres of the stocks were calculated by following the protocol for Lenti-X™ p24 Rapid Titer Kit (Clontech, CA, USA; 632200). For each stock, a 1 in 300 dilution was prepared diluting virus stocks in cDMEM-5 and mixing well. The components of the kit were equilibrated to room temperature and a p24 positive control stock solution was prepared by diluting 20 μL of the p24 Control (10 ng/mL) into 980 μL fresh cDMEM-5 for a 1:50 dilution (200 pg/mL stock solution). The standard curve was prepared by dispensing 500 μL cDMEM-5 into 4 tubes labelled 100 pg/mL, 50 pg/mL, 25 pg/mL, and 12.5 pg/mL. Two-fold serial dilutions were prepared by adding 500 μL of the working stock to the 100 pg/mL tube and mixing well. Pipet tips were replaced and 500 µL of the new solution was added into the next tube. This procedure was repeated for the subsequent dilutions. cDMEM-5 was used as the negative control sample. Coated strips were fitted into the holding frame and 20 µL Lysis Buffer was added to each well. 200 µL of diluted virus stock or control was added to designated wells in duplicate. The plate was covered, surface decontaminated and allowed to incubate at 37 °C for 1 hour (+/- 5 minutes) to allow HIV p24 in virus supernatant to bind to the wells. Contents of the wells were discarded and wells were washed by filling to the brim with 1X Wash Buffer dispensed from a squeeze bottle. Wash buffer was discarded and washes were repeated five times. The plate was inverted and tapped firmly on absorbent paper towels to dry. 100 µL biotin-conjugated anti-HIV p24 detector antibody was added to each well. The plates were allowed to incubate at 37 °C for 1 hour (+/- 5 minutes). Contents of wells were discarded and the plate was washed 5 times. 100 µL streptavidin-HRP conjugate was added to each well. The plate was allowed to incubate at 37 °C for 30 minutes. Contents were discarded and 100 µL Substrate Solution was immediately added to wells using a multi-channel pipettor. The plates were covered with foil to protect from light exposure and allowed to incubate at room temperature for 20 minutes. The reaction was stopped by adding 100 µL Stop Solution to each well using a multi-channel pipettor, causing the blue solution to turn a yellow colour. The bottom of the plate was dried and any bubbles were eliminated by poking with a 10 µL pipet tip. The absorbance value of each well was read at 450 nm immediately.

Assay validation was performed by ensuring that the absorbance of the negative control was ≤0.10 and that the 100 pg/mL standard was ≥0.60. The average absorbance of each sample was obtained and the standard curve was generated by plotting the concentration of each HIV p24 standard as a function of Average Absorbance. Using Microsoft Excel, a graph was plotted and a line of best fit was generated. The equation for the line of best fit was **$\text{Concentration}_{\text{Sample}}$ (pg/mL) = 117.8 x Average $\text{Absorbance}_{\text{Sample}}$** for the ELISA for the titration of HIV, HIV-EBOV, HIV-EBOVΔ1, and NL4-3dEnv-GFP. The equation for the line of best fit was **$\text{Concentration}_{\text{Sample}}$ (pg/mL) = 126.6 x Average $\text{Absorbance}_{\text{Sample}}$** for the ELISA for the titration of HIV-EBOVΔ2. The Average Absorbance for each diluted sample was entered into to these equations to obtain the concentration of HIV p24 in each diluted sample. To obtain the HIV p24 concentrations for each virus stock, the sample concentrations were multiplied by 300 and 5 to account for the fact that each sample was diluted 1:300 and that 200 µL was used for each well, as shown in **Equation 3.1.**

Equation 3.1. $\text{HIV p24 concentration}_{\text{Stock}}\ (\text{pg/mL}) = \text{Concentration}_{\text{Sample}}(300)(5)$

The titers of vaccine stocks in infectious units (IFU) per mL were obtained using **Equation 3.2.**

Equation 3.2. $\text{Infectious unit titer}_{\text{Stock}} = \text{HIV p24 concentration}_{\text{Stock}}\ (0.001\ \text{ng/pg})(1.25 \times 10^{7}\ \text{lentivirus particles/ng})(0.001\ \text{IFU/lentivirus particle})$

3.4. CONFIRMATION OF EBOV GP EXPRESSION BY HIV-EBOV VACCINES

3.4.1. Western blot analysis of virus supernatants

Western blot (WB) Loading Buffer was prepared by adding 50 µL 2-Mercaptoethanol to 950 µL sodium dodecyl sulphate (SDS). Gamma-irradiated virus stocks were diluted three-fold in WB Loading Buffer. Samples were mixed and heated at 95 °C for 15 minutes to denature the proteins. To separate proteins based on size, 30 μL of sample, along with 3 μL MagicMark XP Western Protein Standard (Life Technologies, CA, USA; LC5603), was loaded into the wells of two 10-well Any kD™ Mini-PROTEAN® TGX™ Gel (BIO-RAD, CA, USA; 456-9033) and samples were electrophoresed in 1X tris-glycine SDS buffer at 140V for 50 minutes. Gels containing separated proteins were removed from the cassettes and transferred to an iBlot® Transfer Stack, nitrocellulose (Invitrogen, CA, USA; IB3010-32). Proteins were transferred from the gels to the nitrocellulose membranes by selecting the P2 transfer setting for 5 minutes. The nitrocellulose blots incubated in Blocking Buffer, which consisted of 5% skim milk diluted in PBS. Membranes were blocked on a rocking platform (speed setting 3) at room temperature for 2 hours and Blocking Buffer was removed. To detect EBOV GP, membranes were incubated with purified mouse monoclonal anti-EBOV GP, ZGP42/3.7, graciously provided by Takada and associates (Tokyo, Japan). The anti-EBOV GP antibody was diluted 1:10,000 in Dilution Buffer, which consisted of 2% skim milk diluted in PBS containing 0.05% Tween-20 (PBS-T) and was used in subsequent assays. To detect HIV p24, mouse anti-HIV p24 was diluted 1:4,000 in Dilution Buffer and added to the other nitrocellulose blot. Antigen detection was allowed to occur on a rocking platform (speed setting 3) at 4 °C overnight. The following day, the blots were washed twice with PBS-T on a rocking platform at high speed for 5 minutes. To detect the mouse monoclonal antibodies bound to antigen, goat anti-mouse horseradish peroxidase (HRP)-conjugate was diluted 1:5,000 and added to both blots. Blots were allowed to incubate with secondary antibody on a rocking platform (speed setting 3) at room temperature for 2 hours. The blots were washed twice with PBS-T on a rocking platform at high speed for 5 minutes. Amersham ECL Prime Western Blotting Detection Reagent (GE Healthcare, Little Chalfont, UK; RPN2232) was equilibrated to room temperature and prepared by adding 2 mL Solution A to 2 mL Solution B. Excess PBS-T was removed from blots by tapping gently on filter paper and blots were coated with ECL solution. The solution was allowed to incubate on the blots at room temperature for 5 minutes. ECL solution was removed and blots were transferred to a Hypercassette. In a dark room, Amersham Hyperfilm ECL (GE Healthcare, Little Chalfont, UK; 28906838) was exposed to light enzymatically produced from luminol by HRP on the nitrocellulose blots for 1 minute. To visualize the bands corresponding to EBOV GP and HIV p24, films were developed in an x-ray film processor immediately.

3.5. ANALYSIS OF HIV-EBOV VACCINE VIRION ASSEMBLY

3.5.1. Transmission electron microscopy of transfected HEK 293T cells producing HIV-EBOV vaccine candidates

To examine the morphology of the HIV-EBOV vaccines, 15 cm culture dishes were seeded with 6.67 x 10^6 HEK 293T cells (Passage 10-15) the day before transfection and allowed to incubate at 37 °C overnight. The following day, media from each dish containing cells at 80-90% confluence was discarded and replaced with 20 mL cDMEM-5. For each virus, one transfection reactions were prepared by adding 110 µL room-temperature Opti-MEM reduced serum media (GIBCO, CA, USA; 31985062) to two 1.5 mL Eppendorf tubes. Without touching the polystyrene tube, 45 µL of FuGENE 6 Transfection Reagent (Promega, WI, USA; E2691) was injected directly into the media. The reagents were mixed well and allowed to incubate at room temperature for five minutes. After incubation, 5 µg of pNL4-3, pNL4-3ZGP, pNL4-3ZGPΔ1, pNL4-3ZGPΔ2, or pNL4-3-ΔEnv-GFP DNA plasmid was added to the transfection reagent to rescue HIV wt, HIV-EBOV, HIV-EBOVΔ1, HIV-EBOVΔ2, or NL4-3ΔEnv-GFP, respectively. After mixing, the transfection reaction was allowed to incubate at room temperature for 30 minutes. Each lipid nanoparticle-DNA complex mixture was added to designated dishes containing HEK 293T cells in a drop-wise fashion. The plates were immediately transferred to a CL-3 laboratory and allowed to incubate at 37 °C for 48-72 hours.

Electron microscopy (EM) Buffer was prepared by dissolving 17.5 grams of sucrose in 250 mL 0.2M Sorenson's Phosphate Buffer (pH 7.2). Conventional electron microscopy fixative was prepared in a fume hood by combining 40 mL EM Buffer, 10 mL 16% paraformaldehyde, 8 mL 25% glutaraldehyde, and 22 mL distilled water for a final concentration of 2.5% glutaraldehyde, 2% paraformaldehyde, and 0.1M Sorenson's Buffer solution. After incubation, supernatant was discarded from transfection plates and 4 mL of EM Fixative was added to each plate. Transfected cells were allowed to fix at room temperature for 30 minutes. Fixed cells were added to 50 mL Falcon tubes and centrifuged at 1,200 x g for 5 minutes. Supernatant was removed and cell pellet was resuspended in 1 mL fresh EM Fixative. Cells were additionally fixed at 4 °C for over 2 hours.

A loose pellet was obtained by centrifuging cells at 1,200 x g for 30 minutes. In a LYNX II Automated Tissue Processor, the pellet was washed with 0.1M Sorenson's Buffer at 4 °C for 20 minutes. The pellet was treated with 1% osmium tetroxide at room temperature for 1 hour. The pellet was washed with distilled water at room temperature for 15 minutes. To dehydrate the pellet, cells were treated with 50% ethanol for 15 minutes, followed by 70% ethanol for 15 minutes, 95% ethanol for 15 minutes, 100% ethanol for 10 minutes, and propylene oxide for 10 minutes at room temperature. Infiltration was accomplished by treating pellet with a 1:1 Propylene oxide-resin solution for 4 hours, followed by 1:3 propylene oxide-resin solution for 4 hours, 100% resin solution for 4 hours (without accelerator), and 100% resin solution for 24 hours (with accelerator) at room temperature. Samples were embedded in BEEM capsules containing the accelerator, DMP-30. To harden, the samples were placed in an oven at 68C for a minimum of 24 hours. After curing, the blocks were allowed to cool to room temperature and were cut into 120 nm sections using a Leica Ultracut UCT, double stained with Uranyl Acetate and Lead Citrate. The specimen grids were examined in a Philips CM 120 transmission electron microscope operated at an accelerating voltage of 80kV, and at instrument magnification of 3,000-15,000x. Digital images of the specimens were acquired by an AMT XR-611-M CCD camera (AMT, Woburn, MA).

3.6. CHARACTERIZATION OF HIV-EBOV VACCINE INFECTIVITY, TROPISM, AND REPLICATION

3.6.1. TZM-bl luciferase infectivity assay

TZM-bl HeLa cells were used to quantify infectivity of HIV-EBOV vaccines. This is a CXCR4-positive cell line that expresses CD4 and CCR5. TZM-bl HeLa cells contain an integrated reporter gene for firefly luciferase under the control of an HIV long-terminal repeat sequence. Expression of luciferase is induced in trans by viral Tat protein soon upon infection with HIV (Montefiori, 2009). TZM-bl cells were seeded in four 96-well plates and allowed to incubate at 37 °C overnight. Media was discarded the next day and replaced with 100 µL of cDMEM-5. On each plate, cells were infected with each virus at 0.1, 1, or 10 MOI. Plates were allowed to incubate at 37 °C overnight. At 1, 2, 3, and 4 days post-infection (dpi), the supernatant was removed from the cells and harvested to evaluate replication in TZM-bl cells as described in **Section 3.6.2**. For the TZM-bl infectivity assay, cells were lysed by adding 100 µL of Glo Lysis Buffer (Promega, WI, USA; E2661) equilibrated to room temperature. Lysis was allowed to occur at room temperature for 10 minutes. After incubation, cells lysate was mixed well and transferred into labelled tubes. 100 µL of lysate was added to wells of an Immulon Flat-bottom Microlite 1+ plate (Thermo Fisher Scientific, MA, USA; 7571). 100 µL of Bright-Glo™ Luciferase Assay Buffer (Promega, WI, USA; E2620) was added to each well and mixed using a multi-channel pipettor. Luciferase expression of the TZM-bl cells, as an indicator of HIV infection, was quantified by reading luminescence using a Gen5 Microplate Reader and Imager Software (BioTek, VT, USA). The relative light units (RLU) obtained for each virus was standardized by subtraction of the relative light units of the mock-infected cells at that time point as described in **Equation 3.3.**

Equation 3.3. Standardized RLU = $RLU_{SampleDayx} - RLU_{MockDayx}$

3.6.2. Evaluation of HIV-EBOV vaccine tropism in THP-1 and SupT1 cell lines

To evaluate the tropism of the HIV-EBOV vaccines for the $CD4^+$ T cell line, SUP-T1, and monocytic cell line, THP-1, 5×10^5 cells were seeded in the wells of a 24-well plate by adding 500 µL of a 1×10^6 cell/mL cell suspension to each well. 5×10^7 IFU HIV-EBOV vaccines and wild-type HIV was added to each well to infect cells at an MOI of 10. Plates were allowed to incubate at 37 °C. After 2 dpi, cells were harvested into 1.5 mL tubes and centrifuged at 1,200 x g for 5 minutes. The supernatants were discarded and cell pellets were used for flow cytometric analysis. For each reaction, Viability Stain was prepared by combining 0.5 µL Live/Dead Aqua, 5 µL TruStain FcX, and 44.5 µL PBS. The Surface Stain was composed of mouse anti-human CD4-BV650 (clone SK3; BD, NJ, USA), mouse anti-human CD11c-BV605 (clone B-ly6; BD, NJ, USA), and mouse anti-human CD83-PE (clone HB15e; BD, NJ, USA), each diluted at 1:25. The cell pellets were washed by adding 1 mL PBS to each tube and centrifuging at 250 x g at 4

°C for 5 minutes. Supernatant was removed, cell pellets were resuspended in 50 µL Ghost Dye™ Violet 510 Viability Stain (Tonbo Biosciences, CA, USA), and allowed to incubate at room temperature in the dark for 30 minutes. Cells were washed by adding 1 mL PBS and centrifuging at 300 x g for 10 minutes. Supernatant was discarded and cells were fixed by adding 100 µL of BD Cytofix/Cytoperm™ (BD, NJ, USA; 554722) for every 5 x 10^5 cells. Cells were briefly centrifuged to ensure all cells come into contact with fixative and allowed to incubate at room temperature for 30 minutes. Cells were centrifuged at 300 x g for 10 minutes to remove supernatant. For transfer out of CL-3, cells were fixed a second time by adding 100 µL of BD Cytofix/Cytoperm™ for every 5 x 10^5 cells, incubated at room temperature for 30 minutes, and transferred into new tubes. Cells were permeabilized twice by adding 1 mL of 1X BD Perm/Wash™ (BD, NJ, USA; 554723), centrifuging at 500 x g at 4 °C for 10 minutes, and discarding the supernatant. In order to determine whether the cells were infected by the HIV-EBOV vaccines, intracellular staining for HIV p24 was accomplished by resuspending cells in 100 uL Intracellular Stain containing HIV1 p24 Antibody, FITC conjugate (Clone D45F; Thermo Scientific) at a dilution of 1:20. Cells were incubated at room temperature for 30 minutes in the dark. Cells were washed twice by adding 1 mL of 1X BD Perm/Wash™, centrifuging at 500 x g for 10 minutes, and discarding the supernatant. The cells were resuspended in 300 µL 1% formaldehyde in PBS and analyzed by flow cytometry or stored at 4 °C for later analysis.

Flow cytometry was performed using a BD LSR II™ cytometer set up with a pressure of 20 psi and an 100 µM nozzle. Rainbow fluorescent particles (BD Biosciences, CA, USA) were used to calibrate the instrument and over 10^5 cells were analyzed. Flow Cytometry Standard

(FCS) files obtained from data acquisition were analyzed using FlowJo software 8.7.1. (Treestar, OR, USA).

3.6.3. Evaluation of HIV-EBOV vaccine replication in THP-1 cells

To analyze replication of HIV-EBOV vaccines in the monocytic cell line, THP-1, 5 x 10^5 cells were seeded in wells of four 24-well plates by adding 500 μL of a 1 x 10^6 cell/mL cell suspension to each well. HIV-EBOV vaccines and wild-type HIV were diluted to a concentration of 5 x 10^4 IFU/mL, and 1 mL was added to each well to infect at an MOI of 0.1. Plates were allowed to incubate at 37 °C. At 1, 2, 3, and 4 days post-infection (dpi), cells and supernatant were harvested into 1.5 mL tubes and centrifuged at 1,200 x g for 5 minutes. Supernatants were added to labelled tubes and gamma irradiated for use in CL-2. At the 3 dpi time point, the remaining cell pellet was used to evaluate vaccine tropism as described in **Section 3.6.3**. In order to quantify virus replication, the titres of the gamma irradiated samples were obtained using the p24 ELISA as described in **Section 3.3.2**.

3.7. EVALUATION OF IMMUNE RESPONSES INDUCED BY A HOMOLOGOUS PRIME-BOOST HIV-EBOV VACCINE REGIMEN IN MICE

3.7.1. BALB/c mouse model for HIV and EBOV immunogenicity

Specific pathogen-free female BALB/c mice 4-6 weeks of age were used study to evaluate the T cell and antibody responses induced by the HIV-EBOV vaccines, as well as their protective efficacy against mouse-adapted EBOV. Six mice were housed per filtered cage using sanitized chips as bedding and nesting material. They were maintained at room temperature within a containment level 4 (CL-4) laboratory and were provided free access to food and water throughout all experiments. Mice were allowed to acclimatize to their environment for seven days prior to any manipulation.

3.7.2. Immunization of BALB/c mice with a homologous prime-boost HIV-EBOV vaccine regimen

The prime-boost regimen comprised a prime vaccination of 5×10^5 IFU of HIV-EBOV, HIV-EBOVΔ1, or HIV-EBOVΔ2 in a volume of 200 µL administered to BALB/c mice (n=12) intraperitoneally using a 28 gauge needle, followed by a boost vaccination of the same vaccine and dose after 21 days. In order to prove that anti-EBOV immune responses generated by the HIV-EBOV vaccines were not due to the HIV backbone and that anti-HIV immune responses from vaccination differ from the HIV-specific responses induced by wild-type HIV infection, control mice were inoculated with 5×10^5 IFU wild type NL4-3 intraperitoneally on Day 0 and Day 21. In addition, this control was used to show that protective efficacy of the HIV-EBOV vaccines against MA-EBOV challenge is a result of vaccine-specific immune responses and not responses elicited by wild-type HIV infection. Mice injected with 200 µL cDMEM-5 on Day 0 and Day 21 were used as mock-infected controls to prove that EBOV-specific and HIV-specific immune responses induced by vaccination are a result of the vaccine and not the media in which the vaccine is suspended. In addition, the mock control was used to show that vaccination with HIV-EBOV vaccines is more beneficial in terms of anti-EBOV and anti-HIV immunogenicity and protective efficacy against MA-EBOV than receiving no vaccination at all.

3.7.3. Harvest of whole blood, serum, and spleens from immunized BALB/c mice

At 10, 21, 31, and 42 days after prime vaccination, three mice per each intervention were terminally bled via cardiac puncture to harvest whole blood and spleens were surgically removed following the schedule as depicted in **Figure 3.2**. Approximately 100 uL of whole blood was added to labelled tubes. The remaining ~500 uL was added to BD Microtainer® Serum Separator Tubes™ (BD, NJ, USA; 365956) and allowed to clot for 30 minutes. The tubes were centrifuged at 13,000 x g for 1.5 minutes. Supernatant containing sera was removed from the pellet of red blood cells. Serum samples were heat-inactivated by incubation at 56°C for 45 minutes for use in EBOV neutralization assays performed in CL-4. Samples were then gamma-irradiated in order to transfer samples from CL-4 to CL-2.

Each spleen harvested from the mice was placed in a 0.45 micron cell strainer in a 60 mm petri dish containing 5 mL of cRPMI-10 supplemented with 1% sodium pyruvate (cRPMI-E). Spleens were mechanically disrupted using a plunger from a 3 mL syringe to obtain splenocytes. The splenonocyte suspension was filtered through the cell strainer into a 50 mL Falcon tube and centrifuged at 485 x g at room temperature for 7 minutes. The cell pellet was resuspended in 10 mL cRPMI-E. Red blood cells in the splenocyte suspension were lysed by treatment with ACK Lysis Buffer (Lonza, Basel, Switzerland) for 5 minutes. The cells were enumerated and diluted to a final concentration of 5 x 10^6 cells/mL using cRPMI-E for use in ELISPOT.

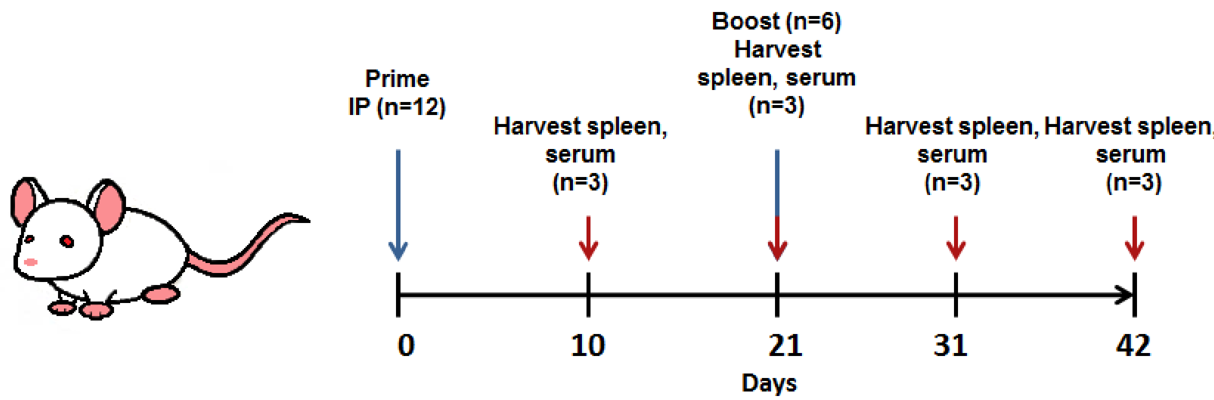

Figure 3.2. Experimental schedule for the evaluation of immune responses induced by a homologous prime-boost HIV-EBOV vaccine regimen. BALB/c mice (n=12) were immunized with 5 x 10^5 IFU HIV-EBOV, HIV-EBOVΔ1, HIV-EBOVΔ2, or wild-type HIV intraperitoneally at Day 0 and Day 21, while negative control mice were administered DMEM. On Day 10, 21, 31, and 42, three mice were sacrificed per group and used for the evaluation of vaccine-induced immune responses.

3.7.4. Quantification of vaccine-induced IFN-γ-secreting T cell responses by Enzyme-Linked ImmunoSpot

To quantify the EBOV GP- and HIV p24-specific IFN-γ-secreting T cell responses induced by vaccination in BALB/c mice, an Enzyme-Linked ImmunoSpot (ELISPOT) assay was performed using the splenocyte suspensions isolated from immunized and control mice. On the day before splenocyte harvest, 0.45 micron MultiScreen-IP Filter Plates (EMD Millipore, MA, USA; S2EM004M99) were coated with anti-mouse IFN-γ capture antibody by adding 100 µL of antibody diluted to a concentration of 1 in 200. Plates were covered and allowed to incubate at 4 °C overnight. After overnight incubation, the capture antibody was aspirated, plates were washed with PBS, and blocked by adding 100 µL of cRPMI-E to each well. Plates were allowed to block at room temperature for two hours.

To quantify the anti-EBOV GP T cell response, three EBOV GP peptide pools were prepared by diluting EBOV GP peptide pools #1, 2, or 3 in cRPMI-E to a concentration of 4 µg/mL. Each EBOV peptide pools consisted of 11 15mers, which spanned the entire length of the EBOV-GP gene and contained overlapping segments which were 9 amino acids in length. To quantify the anti-HIV p24 T cell response, an HIV p24 peptide pool was prepared by diluting PepMix™ HIV (GAG) Ultra (JPT, Berlin, Germany; PM-HIV-Gag) in cRPMI-E to a concentration of 1 µg/mL. For the positive control, ionomycin and PMA were diluted in cRPMI-E to a concentration of 1 µg/mL and 10 ng/mL, respectively. cRPMI-E was used as the negative control. For each mouse sample, 5 x 10^5 cells were added to six wells in duplicate and 100 µL of each peptide pool or control was added to designated wells in duplicate. Stimulation of the cells by peptides or controls was allowed to occur by incubating plates at 37 °C overnight.

The next day, cell suspensions were aspirated from plates and wells were washed twice with deionized water, allowing wells to soak 3-5 minutes each time. The wells were subsequently washed three times with Wash Buffer I, comprising PBS supplemented with 10% FBS. 100 μL of biotinylated mouse anti-IFN-γ diluted to 1:250 was added to each well to bind IFN-γ secreted by cells and plates were allowed to incubate at room temperature for 2 hours. The detection antibody solution was discarded and plates were washed three times by adding 200 μL Wash Buffer I to each well, allowing the plates to soak for 1-2 minutes between washes. 100 μL of streptavidin-HRP enzyme conjugate diluted 1:100 was added to each well and plates were allowed to incubate at room temperature for 1 hour. Enzyme conjugate was discarded and plates were washed four times by adding 200 μL of Wash Buffer I to each well, allowing the plates to soak 1-2 minutes between washes. The plates were washed twice with Wash Buffer II which was composed of 1X PBS. 100 μL of final substrate solution of an AEC Substrate Set (BD Biosciences, CA, USA; 551951) was added to each well and plates were monitored closely for spot development for 15 minutes to avoid overdevelopment and high background. The plates were washed with deionized water three times in order to stop the development process. Plates were dried at room temperature in the dark overnight, and fixed twice overnight with formalin solution in order to transfer plates from CL-4 into CL-2. Plates were read and spots were counted using an automated ELISPOT reader (Cellular Technology Ltd., OH, USA), while adjusting for the presence of additional or false spots.

3.7.5. Quantification of total anti-HIV p24 IgG and anti-EBOV GP antibodies by ELISA

To quantify serum anti-EBOV GP IgG titers of immunized mice, 96-well, half area, flat-bottom, high-binding microplates (Corning, NY, USA; #3690) were coated with 30 μL of transmembrane domain-deleted EBOV GP (IBT Bioservices, MD, USA; 0501-016) diluted at a concentration of 1.25 μg/mL. To quantify serum anti-HIV p24 IgG titers, microplates were coated with 30 μL of HIV-1 gag (p24) antigen (Virogen, MA, USA; 00111-V) at a concentration of 1 μg/mL. Plates were covered with plastic lids and allowed to incubate at 4 °C overnight.

The following day, the antigen solution was discarded and wells were washed six times by adding 150 μL PBS-T to each well and aspirating. Wells were blocked by adding 100 μL of Blocking Buffer (5% skim milk) to each well and incubating for 1 hour at 37 °C. Blocking Buffer was discarded and 30 μL of Dilution Buffer (5% skim milk with 0.05% tween) was added to wells in Rows B to H of each plate. Serum samples from immunized mice were diluted 1 in 300 and 60 μL of diluted serum was added to designated wells of Row A of the microplate in duplicate. The serum was diluted 2-fold by adding 30 μL of serum from Row A to the following row using a multi-channel pipettor and changing tips for every dilution. Plates were allowed to incubate at 37 °C for two hours to allow serum IgGs to bind their respective antigen bound to the ELISA plate. Plates were washed six times with PBS-T and dried onto absorbent towels. To detect serum IgG antibodies, 30 μL of goat anti-mouse IgG HRP-conjugated antibody (Cedarlane, ON, CA) diluted 1 in 1500 was added to each well of the microplate. The plates were allowed to incubate at 37 °C for 1 hour. Plates were washed six times with PBS-T and dried on absorbent towels. To visualize the presence of antigen-specific IgG in each sample, 50 μL of TMB Chromogen Solution (Thermo Fisher Scientific, MA, USA; 00-2023) equilibrated to room temperature was added to each of the wells of the microplate. Plates were allowed to incubate at 37 °C for 30 minutes. Plates were read at 405 nm using a plate reader. Positive binding results were characterized by being greater than three standard deviations when subtracting the positive control from the negative control serum.

3.7.6. Evaluation of neutralizing antibody responses against EBOV

To quantify the amount of EBOV-neutralizing antibodies induced in mice upon immunization, an EBOV-EGFP neutralization assay was performed in CL-4 using heat-inactivated serum from immunized and control mice. The previous day, 4 x 10^5 Vero E6 cells were seeded in each well of a 96-well flat-bottom plate and incubated at 37 °C overnight.

In CL-4 the following day, 50 µL of cDMEM-2 was added to wells in Rows B to H of a flat-bottom 96-well plate. Serum samples from immunized and control mice were diluted 1 in 4 by adding 50 µL of serum to 150 µL cDMEM-10 and 100 µL of diluted serum was added to designated wells of Row A of the microplate in duplicate. The serum was diluted 2-fold by adding 50 µL of serum from Row A to the following row using a multi-channel pipettor and changing tips for every dilution. 50 µL containing 100 plaque-forming units (PFU) of EBOV-EGFP, a recombinant EBOV expressing enhanced green fluorescent protein (EGFP), was added to each well of the plates. Neutralization of EBOV-GFP was allowed to occur by incubating at 37 °C for 90 minutes. Media was discarded from 96-well plates containing Vero E6 cells at 70-80% confluence and serum-virus mixtures were added to the cells. Positive controls were prepared by adding virus without serum to three columns of cells in duplicate. Negative controls were prepared by adding cDMEM-2 to three columns of cells in duplicate. Any non-neutralized virus was allowed to infect cells for 1 hour at 37 °C. After incubation, virus was removed and 100 µL cDMEM-10 was added to each well. Plates were allowed to incubate at 37 °C for 48 hours. Plates were fixed in formalin and cells infected with EBOV-GFP were counted in each well. Samples showing >50% reduction in the number of fluorescent cells compared to controls were considered positive for neutralizing antibodies.

3.8. PROTECTIVE EFFICACY OF HIV-EBOV VACCINES AGAINST LETHAL MA-EBOV CHALLENGE

3.8.1. Lethal EBOV challenge of mice immunized with homologous prime-boost HIV-EBOV vaccine regimen

BALB/c mice (n=6) received the homologous prime-boost regimen using HIV-EBOV, HIV-EBOVΔ1, HIV-EBOVΔ2, HIV, or DMEM as described above. At 42 dpv, mice were challenged with 1000 lethal dose 50% (LD_{50}) of MA-EBOV via intraperitoneal injection. Following challenge, the animals were weighed every day for 17 days, then subsequently weighed at 21 and 28 days post-challenge as depicted in **Figure 3.3**. The animals were constantly monitored for survival disease progression using an approved clinical scoring sheet to perform euthanasia at humane endpoints. Animals that survived past 28 days post-challenge were sacrificed. All procedures were performed according to the guidelines outlined by the Institutional Animal Care Committee at the National Microbiology Laboratory (NML) of the Public Health Agency of Canada (PHAC), which adhere to the guidelines of the Canadian Council on Animal Care. All infectious work was performed in the CL-4 facility at the NML, PHAC.

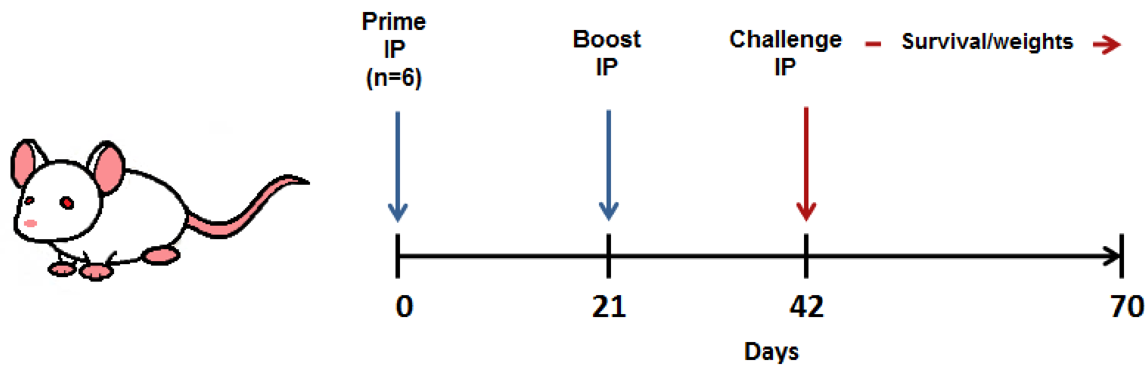

Figure 3.3. Experimental schedule for the evaluation of protective efficacy against lethal mouse-adapted EBOV challenge induced by a homologous prime-boost HIV-EBOV vaccine regimen. BALB/c mice (n=12) were immunized with 5 x 10^5 IFU HIV-EBOV, HIV-EBOVΔ1, HIV-EBOVΔ2, or wild-type HIV intraperitoneally at Day 0 and Day 21, while negative control mice were administered DMEM. Mice were challenged intraperitoneally with a lethal dose of 1000 LD_{50} mouse-adapted EBOV and monitored for survival and weights until Day 70.

3.9. STATISTICAL ANALYSIS

Results were plotted and analyzed using one-way analysis-of-variance (ANOVA) with Bonferroni correction in GraphPad Prism Software (GraphPad, CA, USA). A log-rank Mantel-Cox Test was used for survival analyses. Comparisons were made between each intervention and the DMEM controls, unless otherwise stated. P values of less than 0.05 were considered as statistically significant.

CHAPTER 4: RESULTS

4.1. MOLECULAR CLONES FOR THE RESCUE OF THE VACCINE CANDIDATES, HIV-EBOV, HIV-EBOVΔ1, AND HIV-EBOVΔ2 WERE SUCCESSFULLY GENERATED

The HIV-1 vector, pNL4-3 (GenBank Accession: AF324493), is a DNA molecular clone used for the rescue of CXCR4 (R4)-tropic laboratory HIV, NL4-3, which was chosen as the vaccine platform in this study (Berkowitz et al., 1998; Srivastava, Fernandez-Larsson, Zinkus, & Robinson, 1991). The gp120 sequence eliminated in the vaccine constructs is encoded by nucleotides (nt) 6317-7757 within the pNL4-3 vector. The sequence encoding the signal peptide of Env polypeptide (nt position 6221-6316) was conserved in order to direct EBOV GP to the endoplasmic reticulum upon translation (Li et al., 1996). The other component of HIV Env, gp41, was also conserved because it contains sequences encoding HIV rev and tat on different open reading frames. The inserts encoding EBOV GP for the replacement of gp120 were amplified from a previously developed mammalian expression plasmid containing the complete coding sequence for EBOV GP (Mayinga variant) (GenBank Accession: U23187.1). This plasmid was designated pCAGGS-EBOV GP.

Three molecular clones were designed for the rescue of the vaccine candidates, HIV-EBOV, HIV-EBOVΔ1, and HIV-EBOVΔ2, with genomes based off of the HIV wild type sequence as depicted in **Figure 4.1.** The genome for HIV-EBOV contains the full-length sequence (nt position 1-2031) encoding EBOV GP, including the sequences encoding the EBOV GP signal peptide (nt position 1-96) and mucin-like domain (MLD) (nt position 913-1455), as a replacement of HIV gp120. The signal peptide and the MLD of the EBOV GP-encoding sequence were deleted in the genomes of HIV-EBOVΔ1 and HIV-EBOVΔ2, respectively.

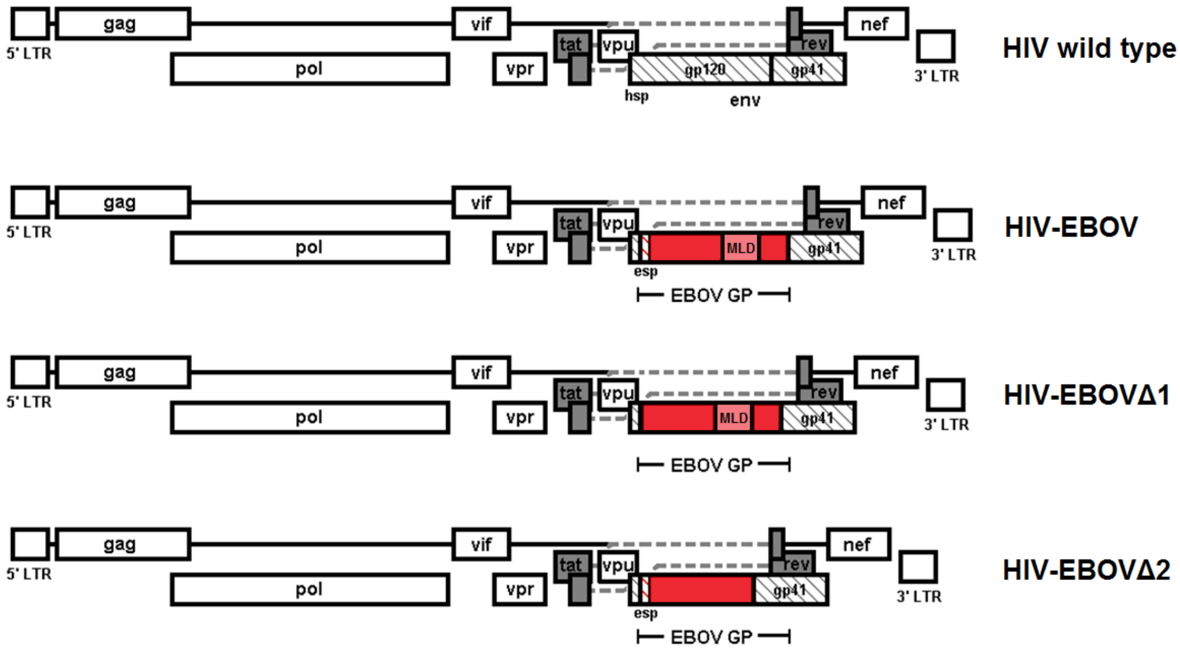

Figure 4.1. Schematic representation of the genomes of the recombinant human immunodeficiency viruses expressing different truncations of EBOV GP. As a replacement for the HIV gp120 sequence, HIV-EBOV contains the full-length EBOV GP sequence, including its signal sequence (esp) and mucin-like domain sequence (MLD). HIV-EBOVΔ1 contains an esp-deleted EBOV GP sequence and HIV-EBOVΔ2 contains an MLD-deleted EBOV GP sequence in place of HIV gp120. In all recombinant viruses, the HIV envelope-derived signal sequence (hsp) was conserved.

To generate the three different molecular clones for the rescue of HIV recombinants expressing different truncations of the EBOV GP sequence, the DNA fragments 4-3A (554 bp), 4-3AΔSP (458 bp), and 4-3C (737 bp) were successfully amplified from the pNL4-3 vector as depicted in **Figure 4.2**. These HIV-derived DNA fragments were designed to flank the EBOV GP sequence. In addition, 4-3B-GP (2040 bp), 4-3B-GPΔSP (1944 bp), 4-3B-GPΔM1 (931 bp), 4-3B-GPΔM1ΔSP (835 bp), 4-3B-GPΔM2 (598 bp) were successfully amplified from the pCAGGS-ZGP plasmid (**Figure 4.2**. These EBOV-derived fragments were designed to generate different truncations of the EBOV GP DNA sequence, namely the full-length, signal sequence-deleted, and MLD sequence-deleted EBOV GP coding sequence. The HIV-derived sequences were combined with the EBOV-derived sequences to assemble inserts for In-Fusion cloning of the different EBOV GP sequences into the pNL4-3 vector in place of HIV gp120.

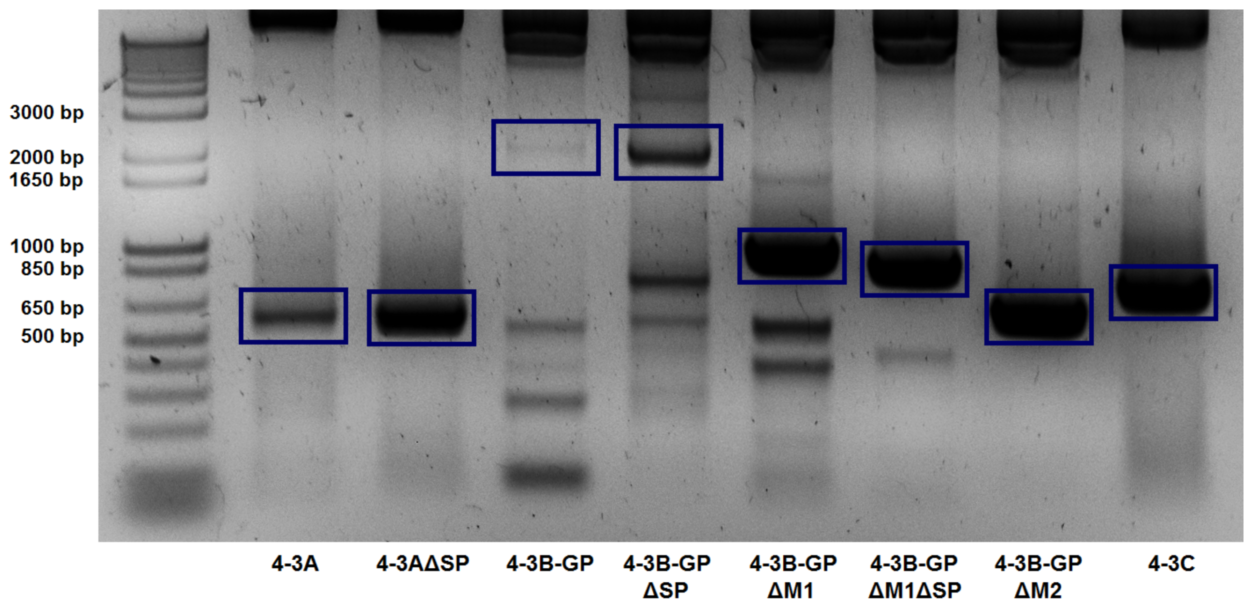

Figure 4.2. PCR amplification of fragments to construct EBOV GP-containing inserts. PCR products were resolved in a 0.9% agarose gel stained with SYBR safe DNA gel stain by electrophoresis at 120V for 45 minutes. DNA bands for 4-3A (554 bp), 4-3AΔSP (458 bp), 4-3B-GP (2040 bp), 4-3B-GPΔSP (1944 bp), 4-3B-GPΔM1 (931 bp), 4-3B-GPΔM1ΔSP (835 bp), 4-3B-GPΔM2 (598 bp), and 4-3C (737 bp) were excised, extracted, and used to generate inserts for In-Fusion cloning.

To generate the MLD sequence-deleted EBOV GP gene, 4-3B-GPΔM, was successfully generated by chimeric PCR assembly of 4-3B-GPΔM1 and 4-3-GPΔM2 as depicted in **Figure 4.3A**. The full-length In-Fusion insert, IF-GP (3294 bp) was generated by chimeric PCR assembly of the fragments 4-3A, 4-3B-GP, and 4-3C; IF-GPΔ1 (3198 bp) was generated by chimeric PCR assembly of the fragments 4-3AΔSP, 4-3B-GPΔSP, and 4-3C, shown in **Figure 4.3B**. IF-GP and IF-GPΔ1 inserts contained the full-length and signal sequence-deleted EBOV GP gene, respectively. The In-Fusion insert, IF-GPΔ2 (2751 bp), was generated from the chimeric PCR assembly of the fragments 4-3A, 4-3B-GPΔM, and 4-3C (**Figure 4.3C)**. IF-GPΔ2 contained the MLD sequence-deleted EBOV GP gene. These inserts were used for the In-Fusion cloning of the EBOV GP gene into the pNL4-3 vector, to generate the molecular clones, pNL4-3ZGP, pNL4-3ZGPd1, and pNL4-3ZGPd2, respectively.

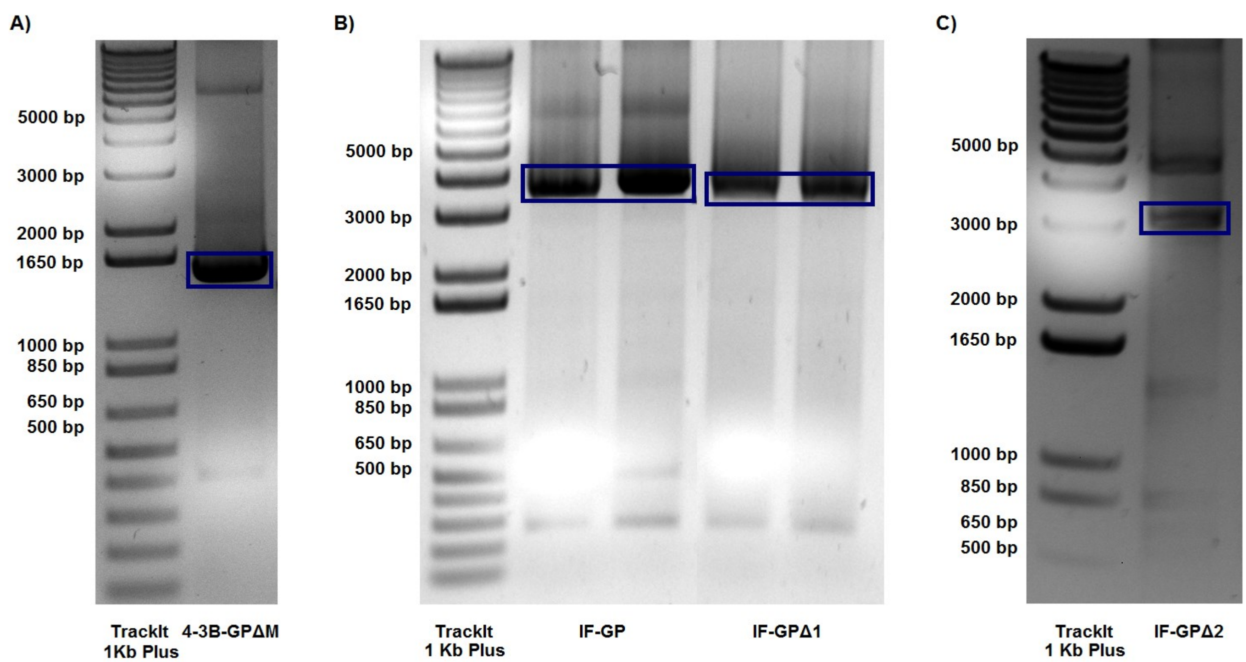

Figure 4.3. Chimeric PCR assemblies of MLD-deleted EBOV GP and In-Fusion inserts containing EBOV GP truncations. Chimeric PCR products were resolved in a 0.9% agarose gel stained with SYBR safe DNA gel stain by electrophoresis at 120V for 45 minutes. The band for 4-3B-GPΔM (1514 bp) was excised, extracted, and used to generate the IF-GPΔ2 insert (A). Bands for IF-GP (3294 bp) and IF-GPΔ1 (3198 bp) (B), as well as IF-GPΔ2 (2751 bp) (C) were excised, extracted for cloning into pNL4-3 to generate the molecular clones, pNL4-3ZGP, pNL4-3ZGPd1, and pNL4-3ZGPd2, respectively.

To permit the insertion of the In-Fusion inserts containing the EBOV GP coding sequence into the HIV genome as a replacement for the HIV gp120 sequence, the pNL4-3 vector was digested with SalI and BamHI as depicted in **Figure 4.4**. Restriction digestion eliminated the sequence encoding gp120. The DNA fragment eliminated by restriction digestion also contained other HIV vector sequences that were re-introduced into the genome upon cloning of the In-Fusion inserts. The 5' and 3' ends of the digested pNL4-3 fragment (12,245 bp) contained 15 bp of sequence homology with the In-Fusion inserts, IF-GP, IF-GPΔ1, and IF-GPΔ2 to allow for homologous recombination of the vector and insert by the In-Fusion (HD) enzyme.

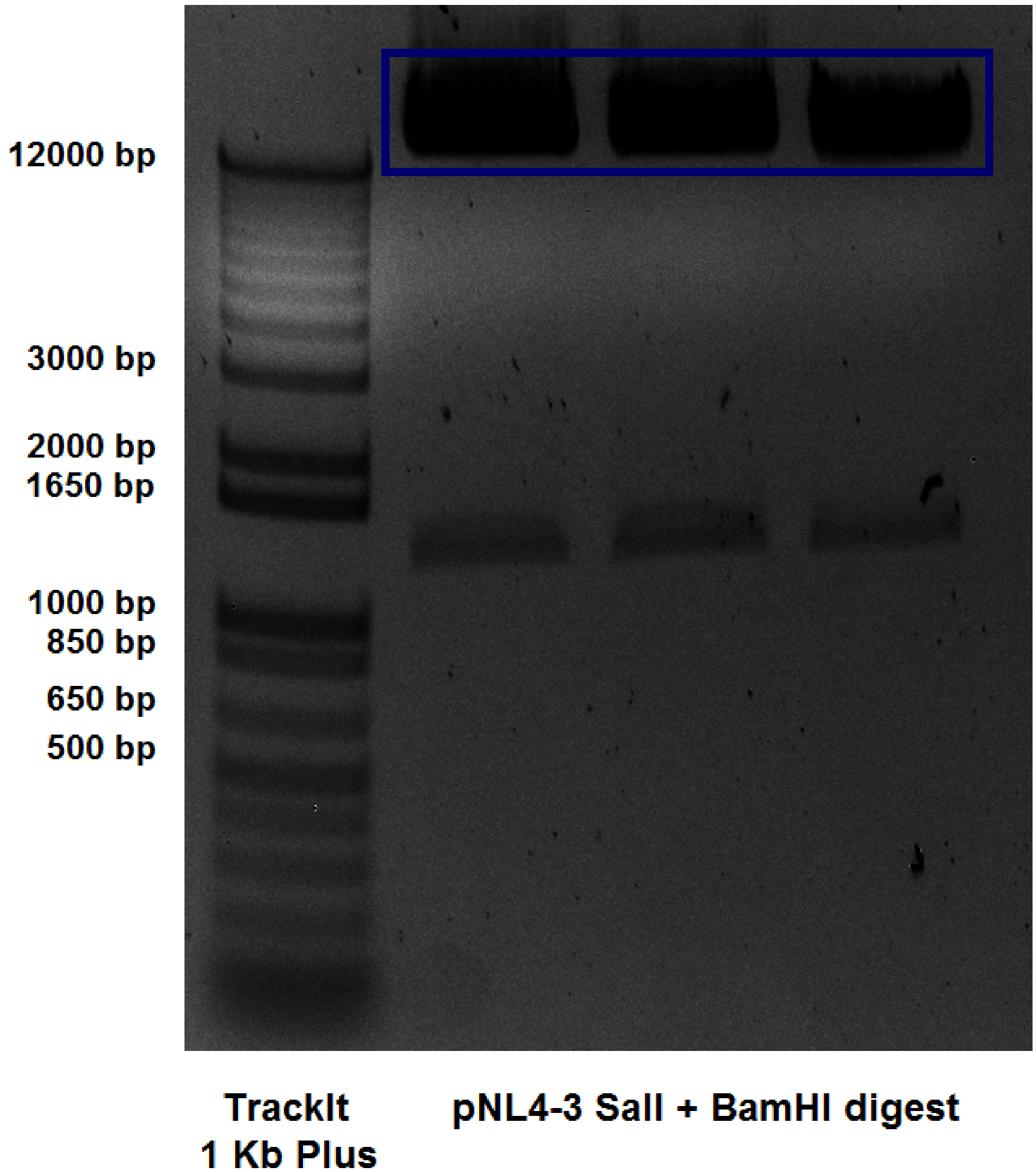

Figure 4.4. Restriction digest of pNL4-3 plasmid with SalI and BamHI restriction enzymes. The HIV-1 molecular clone was digested with SalI and BamHI restriction enzymes for 1 hour at 37 C. After restriction digestion, the HIV gp120-deleted sequence (12,245 bp) was excised, extracted, and used as the vector to introduce inserts containing the EBOV GP sequence.

IF-GP, IF-GPΔ1, and IF-GPΔ2 inserts were successfully cloned into the digested pNL4-3 vector for the generation of the molecular clones containing the full-length, signal sequence-deleted, and MLD sequence-deleted EBOV GP gene as a replacement for the HIV gp120 sequence, respectively. These molecular clones were designated pNL4-3ZGP, pNL4-3ZGPΔ1, and pNL4-3ZGPΔ2, respectively. DNA sequencing provided by the DNA Core Facility at the National Microbiology Laboratory (Winnipeg, MB, Canada) confirmed the appropriate insertion of the EBOV GP sequence and vector integrity of all of the molecular clones.

4.2. VACCINE CANDIDATES, HIV-EBOV, HIV-EBOVΔ1, AND HIV-EBOVΔ2 WERE SUCCESSFULLY RESCUED FROM HEK 293T CELLS AND EXPRESSED EBOV GP TRUNCATIONS

In order to rescue the recombinant HIV-EBOV vaccines, HEK 239T cells were transfected with the molecular clones, pNL4-3ZGP, pNL4-3ZGPΔ1, and pNL4-3ZGPΔ2. After 72 hours, the supernatants from the transfected HEK 293T cells were used as the vaccine stocks of HIV-EBOV, HIV-EBOVΔ1, and HIV-EBOVΔ2, respectively. The titers of the vaccine stocks, as well as wild-type HIV and the GFP-expressing NL4-3ΔEnv-GFP virus, were calculated by HIV p24 ELISA and are listed in **Table 4.1.**

Table 4.1. Titers of HIV-EBOV vaccine stocks obtained via Lenti-X p24 ELISA.

Virus stock	HIV p24 Concentration (pg/mL)	Lentivirus particles per mL	Infectious units per mL
HIV-EBOV	6.77×10^4	8.46×10^8	8.46×10^6
HIV-EBOVΔ1	7.58×10^4	9.47×10^8	9.47×10^6
HIV-EBOVΔ2	3.02×10^4	3.78×10^8	3.78×10^6
Wild-type HIV	6.26×10^4	7.82×10^8	7.82×10^6
NL4-3ΔEnv-GFP	7.63×10^4	9.54×10^8	9.54×10^6

Supernatants harvested 72 hours after transfection of HEK 293T cells with pNL4-3ZGP, pNL4-3ZGPΔ1, and pNL4-3ZGPΔ2 were used as vaccine stocks for HIV-EBOV, HIV-EBOVΔ1, and HIV-EBOVΔ2, respectively. Wild-type HIV and NL4-3ΔEnv-GFP stocks were similarly produced from HEK 293T cells transfected with pNL4-3 and pNL4-3ΔEnv-GFP.

To confirm the expression of full-length, signal peptide-deleted, and MLD-deleted EBOV GP by the HIV-EBOV, HIV-EBOVΔ1, and HIV-EBOVΔ2 vaccines, respectively, western blot analysis of the vaccine stocks, which comprised supernatant from transfected HEK 293T cells, was performed. As depicted in **Figure 4.5 (Top panel)**, EBOV GP was observed at around 167 kDa for HIV-EBOV and HIV-EBOVΔ1, which expressed full-length and signal peptide-deleted EBOV GP, respectively. EBOV GP was observed at approximately 123 kDa for HIV-EBOVΔ2, which expressed the MLD-deleted EBOV GP. In addition, HIV p24 for was observed at approximately 24 kDa for all HIV-EBOV vaccines, as well as wild-type HIV (**Figure 4.5, bottom panel**).

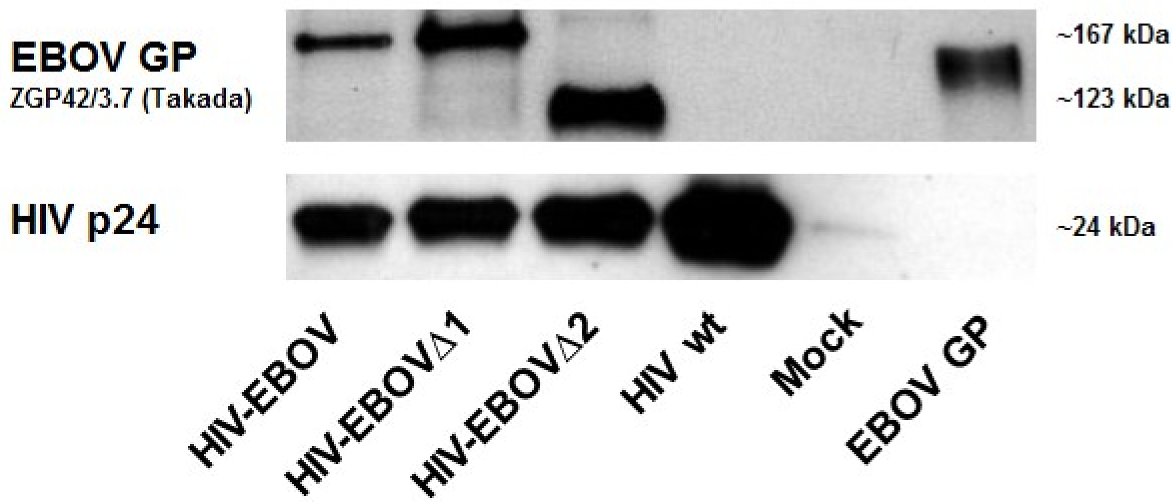

Figure 4.5. Western blot analysis of HIV-EBOV vaccine supernatants for the detection of EBOV GP and HIV p24. Supernatants from transfected HEK 293T cells were harvested to yield HIV-EBOV vaccine stocks, HIV wt, mock, and EBOV GP and resolved by 10% SDS-PAGE. After transfer to a nitrocellulose membrane, purified monoclonal antibody ZGP42/3.7 was used to detect EBOV GP, showing a ~ 167 kDa band for HIV-EBOV, HIV-EBOVΔ1, and EBOV GP control, and a ~123 kDa band for HIV-EBOVΔ2 (top panel). A mouse anti-HIV p24 antibody was used to detect HIV p24, showing 24 kDa bands for HIV-EBOV vaccines and the HIV wt control (bottom panel). Goat-anti mouse HRP-conjugated antibody was used as the secondary antibody for visualization.

4.3. HIV-EBOV AND HIV-EBOVΔ1 DEMONSTRATED HIV-LIKE MORPHOLOGY, WHILE HIV-EBOVΔ2 DEMONSTRATED FILAMENTOUS MORPHOLOGY

In order to confirm that virion particles were produced using the HIV-EBOV molecular clones, visualization of HEK 293T cells producing HIV-EBOV vaccine particles 48 hours post-transfection as successfully accomplished by electron microscopy, with representative images depicted in **Figure 4.6**. HEK 293T cells producing wild-type HIV demonstrated very little virus production at 48 hours post-transfection, but a few particles approximately 100 nm in diameter (**Figure 4.6A**). HEK 293T cells producing the full-length HIV-EBOV vaccine also demonstrated minimal particle production, with very few virions in early stages of budding (**Figure 4.6B**). HEK 293T cells producing HIV-EBOVΔ1 demonstrated the most virion production, with multiple ~100 nm particles at different stages of budding (**Figure 4.6C**). Both HIV-EBOV and HIV-EBOVΔ1 demonstrated spherical morphology similar to wild-type HIV. In contrast, the HIV-EBOVΔ2 particles produced by HEK 293T cells at 48 hours post-transfection demonstrated aberrant filamentous morphology as depicted in **Figure 4.6D**. These particles were approximately 150 nm in width, with lengths varying from 200 nm to 1 μm (**Figure 4.6D**).

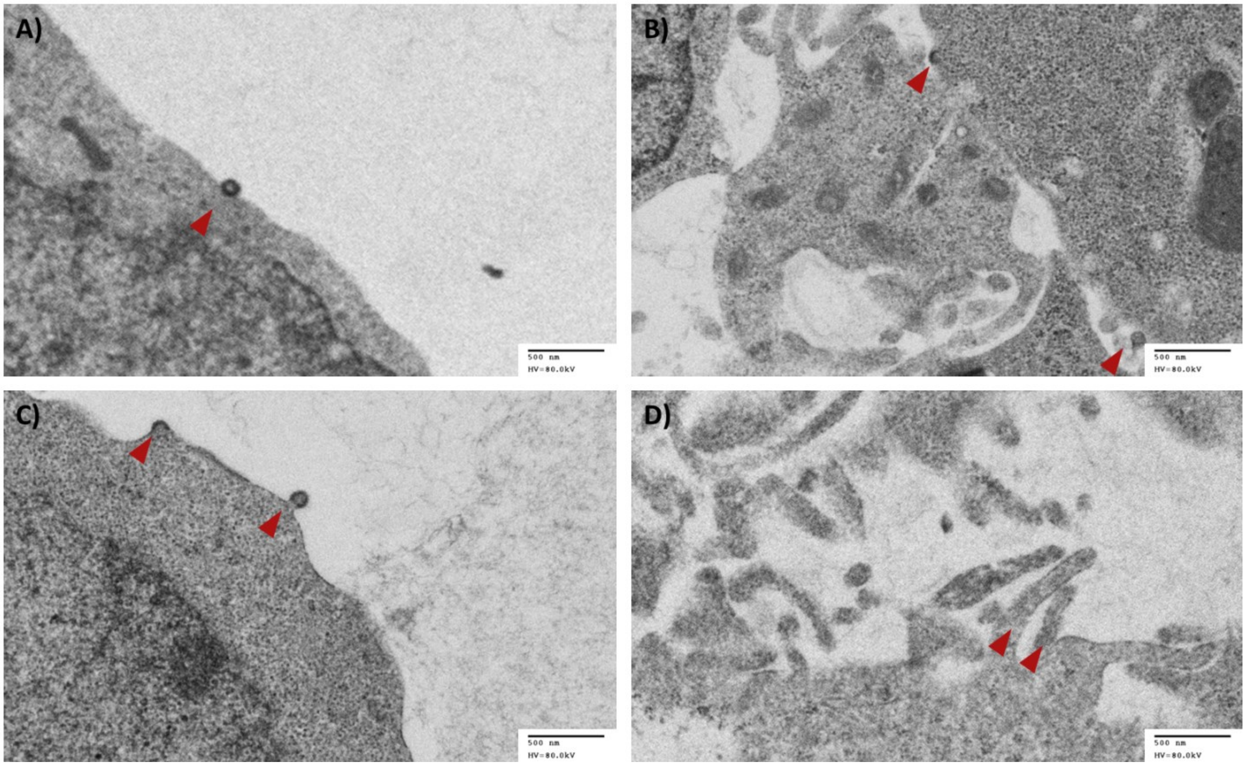

Figure 4.6. Transmission electron microscopy of HEK293T cells producing HIV-EBOV vaccines. To examine the morphology of HIV (A), HIV-EBOV (B), HIV-EBOVΔ1 (C), and HIV-EBOVΔ2 (D), HEK 293T cells were transfected with molecular clones and harvested 48 hours post-transfection. Cells producing viruses were fixed, processed, and cut into 120 nm sections, which were stained with uranyl acetate and lead citrate. Samples were examined in a Philips CM 120 transmission electron microscope operated at an accelerating voltage of 80kV and images were acquired by an AMT XR-611-M CCD camera.

4.4. HIV-EBOV VACCINES DEMONSTRATED SIMILAR INFECTIVITY OF TZM-BL CELLS AT AN MOI OF 0.1

In order to quantify the infectivity of the HIV-EBOV vaccines, the CXCR4-positive TZM-bl HeLa cell line expressing CD4 and CCR5 was infected and harvested to quantify luciferase expression. TZM-bl HeLa cells contain an integrated reporter gene for firefly luciferase under the control of an HIV long-terminal repeat sequence (Montefiori, 2009). Thus, the presence of HIV Tat upon entry into the cell line induces the expression of luciferase, which can be used to quantify infection (Wei et al., 2002). At an MOI of 0.1, HIV-EBOV vaccines demonstrated similar infectivity of TZM-bl cells, quantified by luciferase expression depicted in **Figure 4.7A**. Peak levels of luciferase activity induced in TZM-bl cells occurred at 48 hours for wild-type HIV, but 72 hours for HIV-EBOV, HIV-EBOVΔ1, and HIV-EBOVΔ2 (**Figure 4.7A**). At an MOI of 1, HIV-EBOV and HIV-EBOVΔ1 induced significantly higher levels of luciferase expression in TZM-bl cells compared to wild-type HIV and HIV-EBOVΔ2. Peak luciferase expression was observed at 72 and 96 hours post-infection for HIV-EBOV and HIV-EBOVΔ1, respectively. Meanwhile, luciferase expression induced by wild-type HIV, HIV-EBOVΔ2, and NL4-3ΔEnv-GFP diminished after 24 hours (**Figure 4.7B**). Similarly, at an MOI of 10, HIV-EBOV and HIV-EBOVΔ1 induced significantly higher levels of luciferase expression in TZM-bl cells compared to wild-type HIV and HIV-EBOVΔ2. Peak luciferase expression was observed at 96 and 72 hours post-infection for HIV-EBOV and HIV-EBOVΔ1, respectively. Meanwhile, luciferase expression induced by wild-type HIV, HIV-EBOVΔ2, and NL4-3ΔEnv-GFP was similar to background levels at all time points (**Figure 4.7C**). The NL4-3ΔEnv-GFP virus, which was used as a no glycoprotein control, was unable to infect TZM-bl cells at all MOIs (**Figure 4.7**).

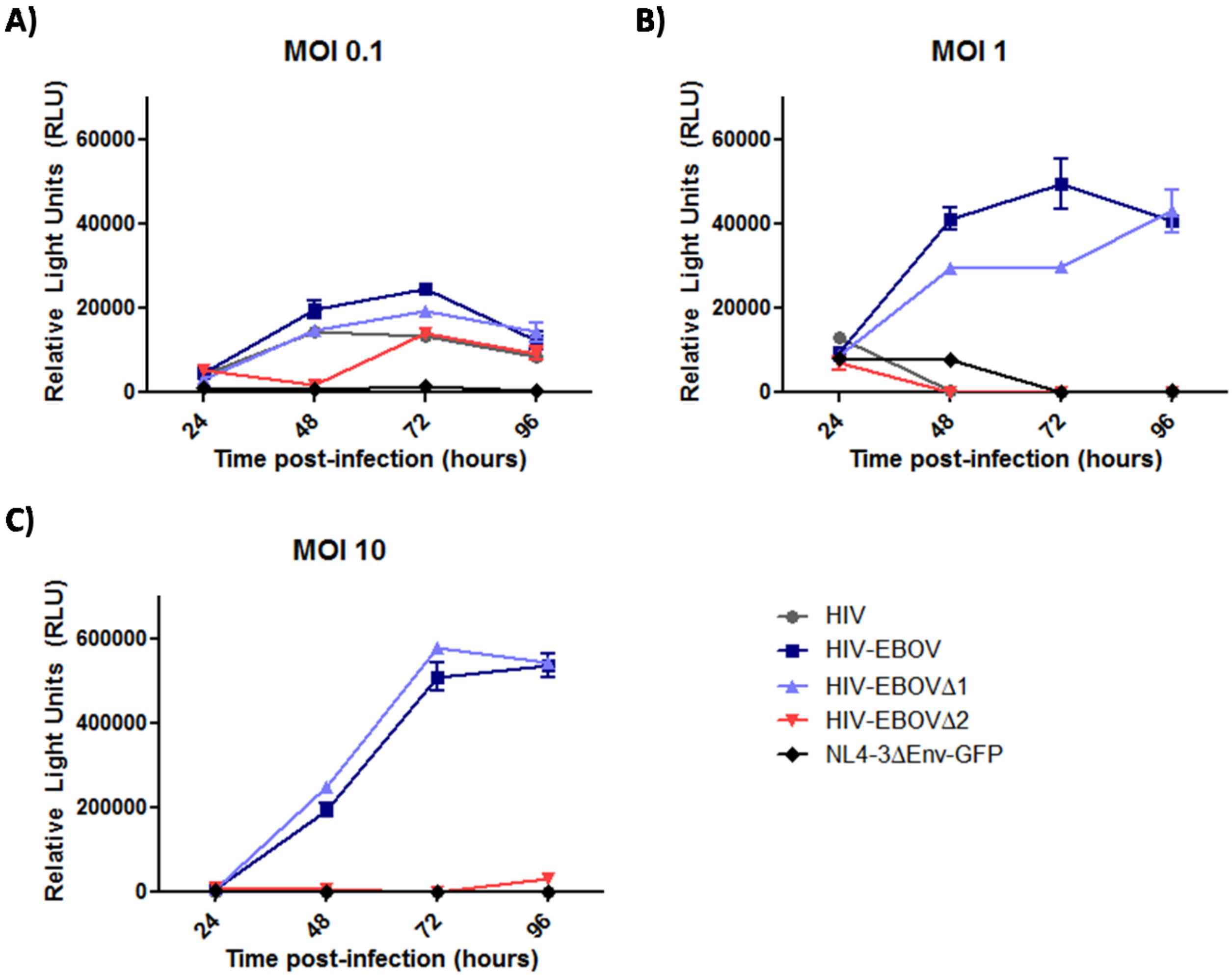

Figure 4.7. Infectivity of HIV-EBOV vaccines of TZM-bl cells quantified by luminescence in relative light units (RLU). To analyze the infectivity of the HIV-EBOV vaccine candidates, supernatants from vaccine rescue were used to infect TZM-bl cells at an MOI of 0.1 (A), 1 (B), and 10 (C). Luciferase expression induced by HIV Tat at 24, 48, 72, and 96 hours post-infection was measured using 5 x 10^4 cells per reading and standardized using readings from mock-infected cells. NL4-3ΔEnvGFP was used as a non-infectious negative control.

4.5. TROPISM AND INFECTIVITY OF RECOMBINANT HIV-EBOV VACCINES

In order to determine the tropism of the HIV-EBOV vaccines for monocytes and lack of tropism for $CD4^+$ T cells, the monocytic cell line, THP-1, and the $CD4^+$ T cell line, SupT1, were infected at an MOI of 10, harvested 2 days post-infection, and analyzed by flow cytometry. The proportion of live, infected cells was analyzed by quantifying the number of cells negative for Ghost Dye™ viability stain and positive for intracellular HIV p24. As depicted in **Figure 4.8A**, the proportion of live, infected THP-1 cells was 1.14, 0.627, 1.53, and 0.673% for HIV, HIV-EBOV, HIV-EBOVΔ1, and HIV-EBOVΔ2, respectively. The proportion of live, infected SupT1 cells was 0.912, 0.023, 0.380, and 0.205% for HIV, HIV-EBOV, HIV-EBOVΔ1, and HIV-EBOVΔ2, respectively. The proportion of Ghost Dye™ negative and FITC positive cells were 0.033 and 0.055% for THP-1 and SupT1 cells, respectively.

Replication of the HIV-EBOV vaccines in THP-1 cells was analyzed by infecting cells at an MOI of 0.1 and quantifying virus concentration of supernatants harvested from 1-4 dpi by p24 ELISA. As depicted in **Figure 4.8B**, all vaccines demonstrated replication in THP-1 cells. HIV-EBOVΔ1 demonstrated the highest amount of replication with a peak virus concentration of 82626.74 ±1140.86 IFU/mL at 3 dpi. Similarly, HIV-EBOV and HIV-EBOVΔ2, as well as wild-type HIV demonstrated peak virus concentrations of 72669.32 ± 146.03, 36640.98 ± 68.45, and 29681.74 ± 9.13 IFU/mL at 3 dpi, respectively.

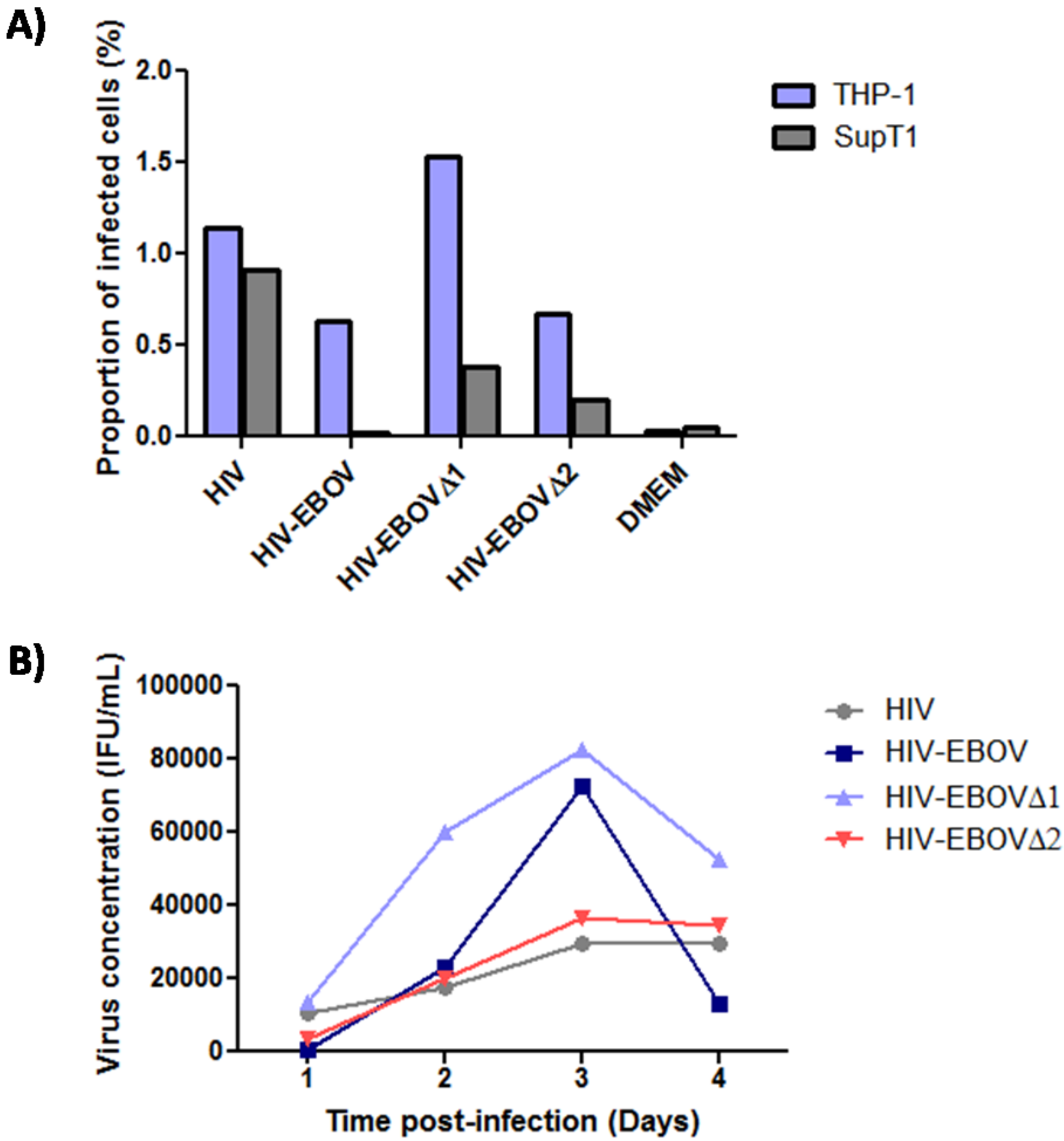

Figure 4.8. Tropism and replication of HIV-EBOV vaccines. Tropism of the HIV-EBOV vaccines for the monocytic cell line, THP-1, and the CD4$^+$ T cell line, SupT1, was analyzed by infecting cells at an MOI of 10 and quantifying the proportion of live, HIV p24-containing cells by flow cytometry at 2 dpi (A). Replication of the HIV-EBOV vaccines in THP-1 cells was analyzed by infecting cells at an MOI of 0.1 and quantifying HIV p24 concentrations from supernatants harvested from 1-4 dpi (B).

4.6. HIV-EBOV VACCINES WERE ABLE TO INDUCE ANTI-HIV AND ANTI-EBOV CELL-MEDIATED IMMUNE RESPONSES IN MICE

4-6 week old BALB/c mice (Charles River, Wilmington, MA) were used for this study since they are genetically capable of generating HIV-specific cytotoxic T cell responses associated with HIV protection in humans (Mahdavi et al., 2009). Although mice have been shown to be unable to support HIV replication due to failure at many stages in the viral cycle, immune responses against HIV-1 can be detected in mice following antigenic stimulation with protein or replication incompetent virus-based HIV vaccines (Berzofsky et al., 1988; Boberg et al., 2008; Bruce et al., 1999; Poon, Hsu, Gudeman, Chen, & Grovit-Ferbas, 2005). In addition, their use in modelling EBOV infection using mouse-adapted EBOV has been studied extensively, thus making them a highly suitable animal model to study the efficacy of vaccines against EBOV infection (Bray, Davis, Geisbert, Schmaljohn, & Huggins, 1998).

4.6.1. All HIV-EBOV homologous prime-boost vaccine regimens generated HIV p24-specific IFN-γ-secreting T cells; those induced by HIV-EBOVΔ1 were significantly higher compared to DMEM and wild-type HIV treatment at 21 days post-immunization

IFN-γ ELISPOT analysis of splenocytes harvested from immunized mice was performed in order to quantify the HIV-specific cell-mediated immune responses induced by the homologous prime-boost HIV-EBOV vaccine regimen. T cells primed by vaccination demonstrated IFN-γ secretion upon *ex vivo* stimulation with HIV p24 peptides as depicted in **Figure 4.9**. At 10 days post-immunization, 20.7 ± 12.0 and 5.3 ± 4.8 SFU/million cells were induced upon HIV p24 peptide stimulation in wild-type HIV treated mice. HIV-EBOVΔ1 followed by HIV-EBOV demonstrated the highest number of IFN-γ secreting cells (264.6 ± 49.9 and 175.7 ± 99.3 SFU/million cells, respectively), although not at a significant level compared to those induced by wild-type HIV. HIV-EBOVΔ2 induced 11.7 ± 11.7 SFU/million cells. At 21 days post-immunization, 169.3 ± 89.5 and 83.0 ± 52.9 SFU/million cells were induced upon HIV p24 peptide stimulation in wild-type HIV and DMEM-treated mice, respectively. Mice immunized with HIV-EBOVΔ1 demonstrated 698.7 ± 256.7 SFU/million cells, significantly higher ($p<0.01$) number of IFN-γ secreting cells compared to DMEM-treated mice. Further analysis also showed a significantly higher ($p <0.05$) number of IFN-γ cells compared to mice treated with wild-type HIV. HIV-EBOV and HIV-EBOVΔ2 induced more IFN-γ secreting cells (439.3 ± 190.1 and 220.0 ± 42.3 SFU/million cells, respectively) compared to DMEM. However, these were values were not significant. At 31 days post-immunization, 28.3 ± 10.9 and 11.000 ± 5.7 SFU/million cells were induced upon HIV p24 peptide stimulation in wild-type HIV and DMEM-treated mice, respectively. Mice immunized with HIV-EBOV demonstrated the highest number of IFN-γ-secreting cells, with 434.0 ± 326.6 SFU/million cells. HIV-EBOVΔ1 and HIV-EBOVΔ2 induced 382.0 ± 88.0 and 117.0 ± 57.5 SFU/million cells, respectively. None of the IFN-γ-secreting cell counts induced by HIV-EBOV vaccines were significantly higher when compared to those induced by DMEM at this time point.

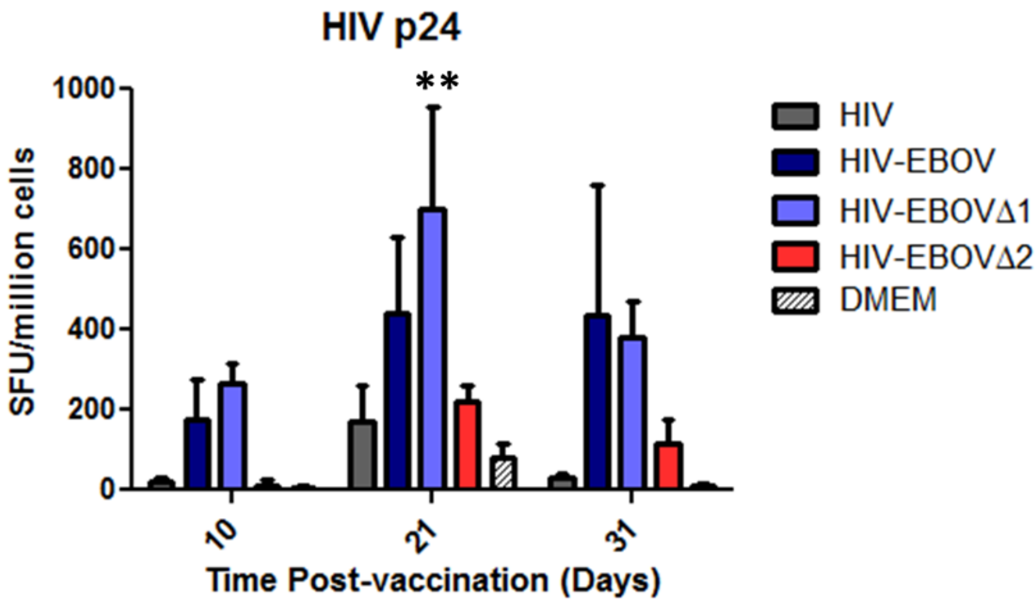

Figure 4.9. HIV p24-specific interferon-γ T cell responses induced by homologous prime-boost HIV-EBOV vaccine regimen in mice upon stimulation with HIV p24 peptides. BALB/c mice were prime immunized and boosted intraperitoneally with HIV-EBOV vaccines, HIV, or DMEM at day 0 and day 21, respectively. At days 10, 21, and 31 post-vaccination, 3 mice per group were sacrificed and ELISPOTs were performed on splenocytes stimulated with HIV p24 peptide pools in order to quantify spot-forming units (SFU) indicating IFN-γ secretion by T cells.

4.6.2. All HIV-EBOV homologous prime-boost vaccine regimens generated EBOV GP-specific IFN-γ-secreting T cells

IFN-γ ELISPOT analysis of splenocytes harvested from immunized mice was performed in order to quantify the EBOV-specific cell-mediated immune responses induced by the homologous prime-boost HIV-EBOV vaccine regimen. T cells primed by vaccination demonstrated IFN-γ secretion upon *ex vivo* stimulation with EBOV GP peptides as depicted in **Figure 4.10**. At 10 days post-immunization, 25.3 ± 12.3 and 7.3 ± 7.3 SFU/million cells were induced upon EBOV GP peptide stimulation in wild-type HIV and DMEM-treated mice, respectively. HIV-EBOV, HIV-EBOVΔ1, and HIV-EBOVΔ2 induced 175.7 ± 99.3, 264.7 ± 49.9, and 11.7 ± 11.7 SFU/million cells, respectively. However, none of these values were significantly higher than the IFN-γ secreting cell counts induced by DMEM or wild-type HIV. At 21 days post-immunization, 144.7 ± 3.2 and 32.3 ± 32.3 SFU/million cells were induced upon EBOV GP peptide stimulation in wild-type HIV and DMEM-treated mice, respectively. HIV-EBOVΔ1 and HIV-EBOVΔ2 induced 141.7 ± 111.2, and 205.0 ± 95.9 SFU/million cells, respectively. However, none of these values were significantly higher than the IFN-γ secreting cell counts induced by DMEM or wild-type HIV. Upon standardization with negative control wells, no IFN-γ-secreting T cells were observed for HIV-EBOV immunized mice at day 21 post-immunization. At 31 days post-immunization, 11.7 ± 7.6 and 32.7 ± 23.8 SFU/million cells were induced upon EBOV GP peptide stimulation in wild-type HIV and DMEM-treated mice, respectively. HIV-EBOV, HIV-EBOVΔ1, and HIV-EBOVΔ2 induced 30.3 ± 16. 3, 155.0 ± 61.7, and 130.3 ± 72.4 SFU/million cells, respectively. However, none of these values were significantly higher than the IFN-γ secreting cell counts induced by DMEM or wild-type HIV.

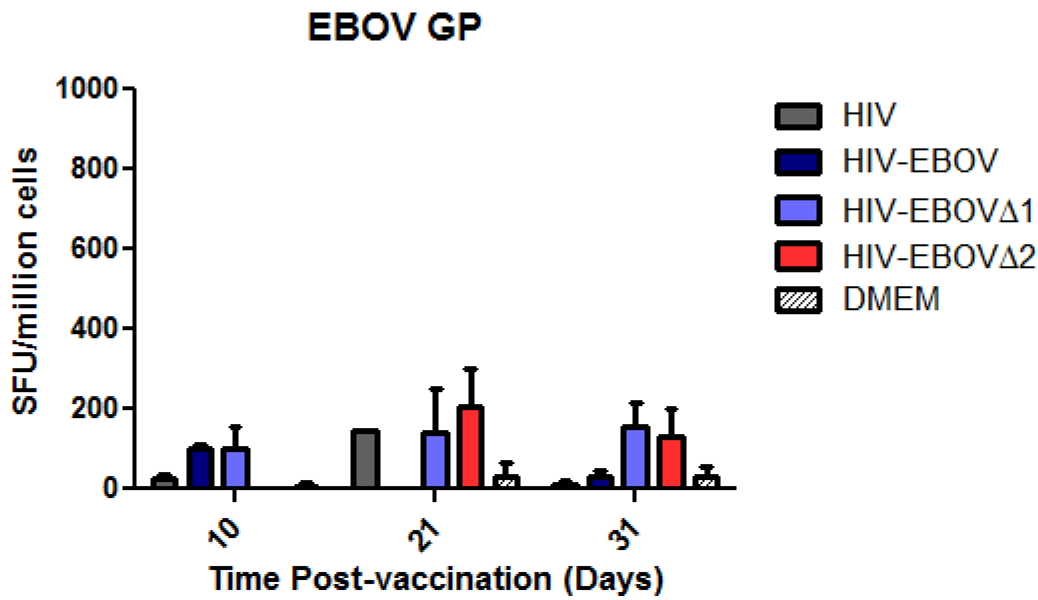

Figure 4.10. EBOV GP-specific interferon-γ T cell responses induced by the homologous prime-boost HIV-EBOV vaccine regimen in mice upon stimulation with EBOV GP peptides. BALB/c mice were prime immunized and boosted intraperitoneally with HIV-EBOV vaccines, HIV, or DMEM at day 0 and day 21, respectively. At days 10, 21, and 31 post-vaccination, 3 mice per group were sacrificed and ELISPOTs were performed on splenocytes stimulated with EBOV GP peptide pools in order to quantify spot-forming units (SFU) indicating IFN-γ secretion by T cells.

4.7. HIV-EBOV VACCINES INDUCED ANTI-HIV AND ANTI-EBOV HUMORAL IMMUNE RESPONSES IN MICE

4.7.1. HIV-EBOV and HIV-EBOVΔ1 homologous prime-boost vaccine regimens induced significant total anti-HIV p24 and anti-EBOV GP IgG titres in mice at 42 days post-vaccination

Total anti-HIV p24 and anti-EBOV GP IgG ELISAs using serum harvested from immunized mice at days 21 and 42 post-immunization was performed in order to quantify humoral immune responses induced by the homologous prime-boost HIV-EBOV vaccine regimens. Minimal anti-HIV p24 and anti-EBOV GP IgG responses were elicited by all interventions at day 21, but robust IgG responses were observed at day 42 as depicted in **Figure 4.11**. As shown in **Figure 4.11A**, total anti-HIV p24 IgG titers did not exceed baseline levels for HIV, HIV-EBOV, HIV-EBOVΔ1, and HIV-EBOVΔ2 at 21 days post-immunization. However, at 42 days post-immunization, the HIV-EBOVΔ1 and HIV-EBOV homologous prime-boost vaccine regimens demonstrated significant ($p<0.05$) total anti-HIV p24 IgG titers compared to HIV inoculation, with mean reciprocal endpoint dilutions of 8800.0 ± 4000.0 and 8533.3 ± 4266.7, respectively; the mean reciprocal end-point dilution of serum from HIV-inoculated mice was 66.7 ± 33.3. Mice receiving the HIV-EBOVΔ2 homologous prime-boost vaccine regimen demonstrated a mean reciprocal endpoint dilution of 4533.3 ± 4133.3, which was above those induced by wild-type HIV, but not statistically significant (**Figure 4.11A**).

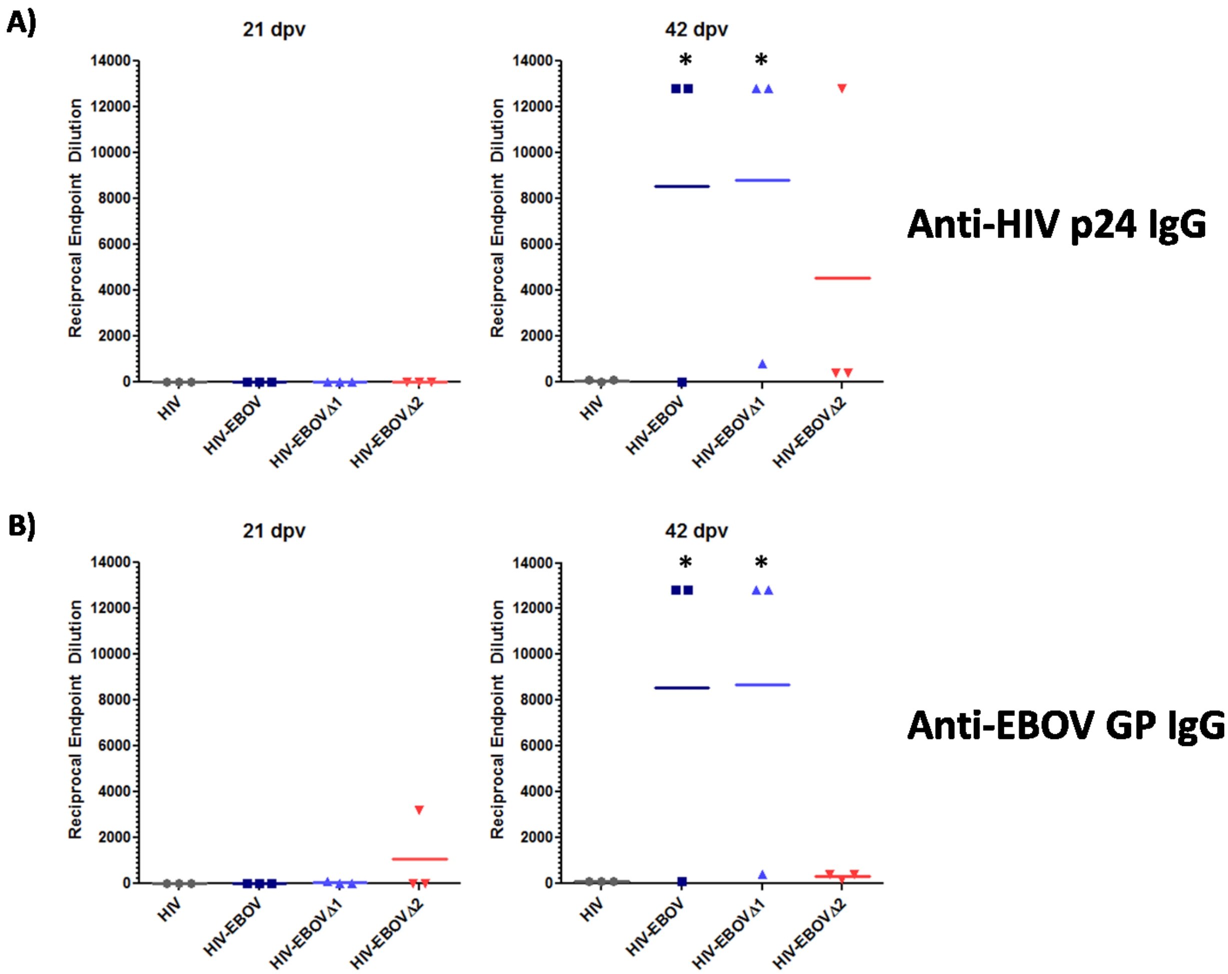

Figure 4.10. Total anti-HIV p24 IgG and total anti-EBOV GP IgG response induced by the homologous prime-boost HIV-EBOV vaccine regimen in mice. BALB/c mice were prime immunized and boosted intraperitoneally with HIV-EBOV vaccines, HIV, or DMEM at day 0 and day 21, respectively. At days 21 and 42 post-vaccination, 3 mice per group were sacrificed and titers for total anti-HIV p24 IgG (A), total anti-EBOV GP IgG (B) were obtained by ELISA.

As shown in **Figure 4.11B**, total anti-EBOV GP IgG titers did not exceed baseline levels for HIV and HIV-EBOV at 21 days post-immunization. Mice receiving the HIV-EBOVΔ1 and HIV-EBOVΔ2 homologous prime-boost regimens demonstrated mean reciprocal endpoint dilutions of 33.3 ± 33.3 and 1066.7 ± 1066.7 at 21 days post-immunization, respectively. In contrast, at 42 days post-immunization, the HIV-EBOVΔ1 and HIV-EBOV homologous prime-boost vaccine regimens demonstrated significant ($p<0.05$) total anti-HIV p24 IgG titers compared to HIV inoculation, with mean reciprocal endpoint dilutions of 8666.7 ± 4133.3 and 8566.7 ± 4233.3, respectively; the mean reciprocal endpoint dilution of serum from HIV-inoculated mice was 100. Mice receiving the HIV-EBOVΔ2 homologous prime-boost vaccine regimen demonstrated a mean reciprocal endpoint dilution of 333.3 ± 66.7, which was above those induced by wild-type HIV, but not statistically significant (**Figure 4.11B**).

4.7.2 All HIV-EBOV homologous prime-boost vaccine regimens were unable to generate significant EBOV neutralizing antibody titers in mice

In order to quantify the EBOV neutralizing antibody responses induced by the homologous prime-boost HIV-EBOV vaccine regimens, an EBOV-GFP neutralization assay was performed on serum harvested from immunized mice at days 21 and 42 post-immunization. The HIV-EBOV vaccine regimens did not elicit neutralizing antibodies at days 21 and 42 post-immunization as depicted in **Figure 4.12**. HIV-treated mice also demonstrated no EBOV neutralizing antibodies (**Figure 4.12**).

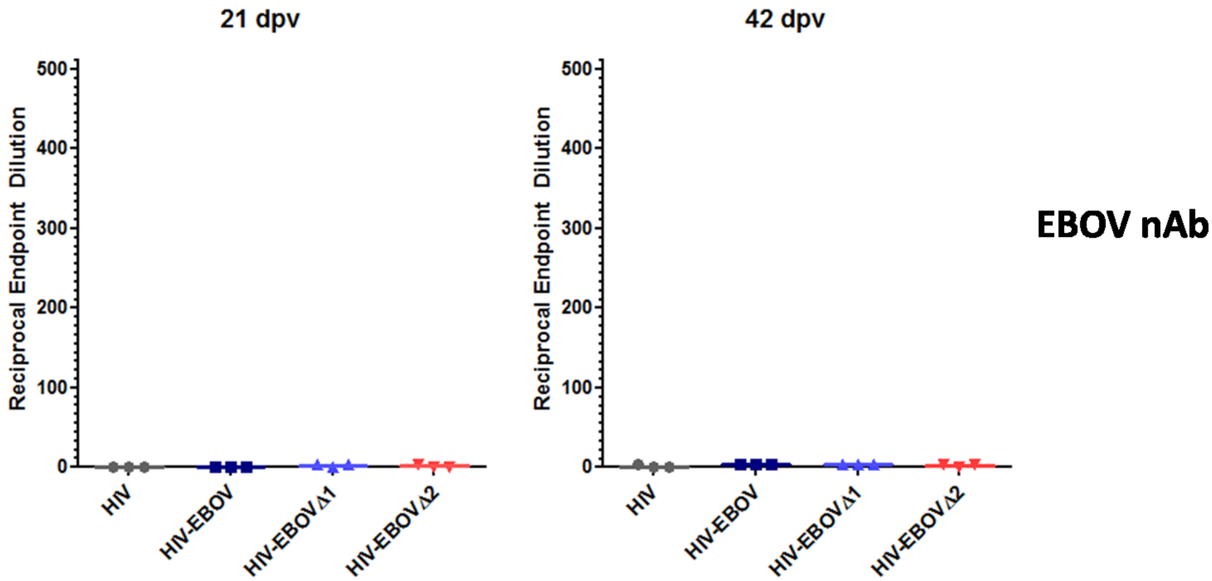

Figure 4.12. EBOV neutralizing antibody response induced by the homologous prime-boost HIV-EBOV vaccine regimen in mice. BALB/c mice were prime immunized and boosted intraperitoneally with HIV-EBOV vaccines, HIV, or DMEM at day 0 and day 21, respectively. At days 21 and 42 post-vaccination, 3 mice per group were sacrificed and EBOV neutralizing antibodies titers were obtained via an EBOV-GFP neutralization assay.

4.8. HIV-EBOV VACCINES WERE ABLE TO CONFER PROTECTION AGAINST A LETHAL EBOV CHALLENGE IN MICE

4.8.1. HIV-EBOVΔ1, HIV-EBOVΔ2, and HIV-EBOV demonstrated 83, 67, and 50% protective efficacy against lethal EBOV challenge in mice, respectively

To evaluate the protective efficacy of the homologous prime-boost HIV-EBOV vaccine regimens against lethal EBOV infection, mice were challenged 42 days post-immunization. All HIV-EBOV vaccines were able to elicit different levels of protection against EBOV as depicted in **Figure 4.13**. All mice primed and boosted with DMEM succumbed to mouse-adapted EBOV infection within 5-9 days of challenge, while all mice primed and boosted with wild-type HIV succumbed to infection within 5-7 days of challenge. The most efficacious homologous prime-boost vaccine regimen was HIV-EBOVΔ1, which demonstrated a protective efficacy of 83%, with five out of six animals surviving EBOV challenge ($p=0.0059$). The HIV-EBOVΔ1-immunized mouse that succumbed to illness died at day 7 post-challenge. The second most efficacious homologous prime-boost vaccine regimen was HIV-EBOV, which demonstrated a protective efficacy of 67%, with 4 out of six animals surviving EBOV challenge ($p=0.0098$). The HIV-EBOV-immunized mice that succumbed to illness died at day 7 post-challenge. Lastly, the HIV-EBOVΔ2 homologous prime-boost vaccine regimen demonstrated 50% protective efficacy, with three out of six animals surviving EBOV challenge ($p=0.0187$). The HIV-EBOVΔ2-immunized mice that succumbed to illness died at day 7 ($n=1$) and day 8 ($n=2$) post-challenge.

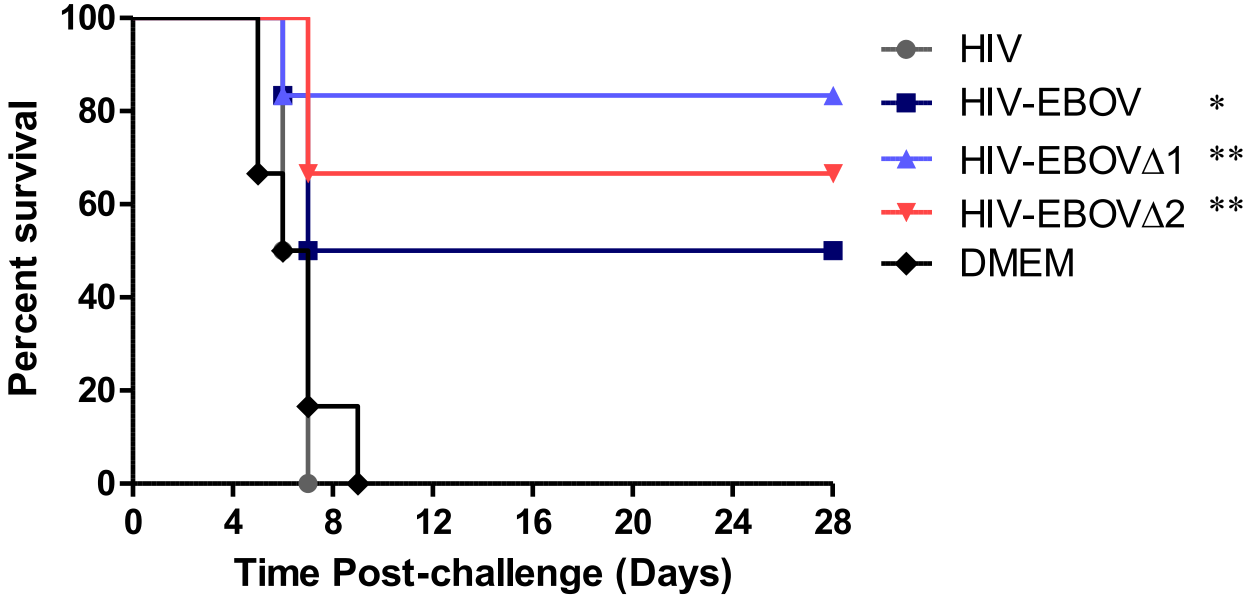

Figure 4.13. Protective efficacy of the homologous prime-boost HIV-EBOV vaccine regimens against lethal EBOV challenge in mice. BALB/c mice were prime immunized and boosted intraperitoneally with HIV-EBOV vaccines, HIV, or DMEM at day 0 and day 21, respectively. At day 42 post-immunization, mice were challenged intraperitoneally with 1000 LD_{50} of mouse-adapted EBOV. Mice were monitored for survival for 28 days. ** indicates significance of $p<0.01$, * indicates significance of $p<0.05$ on a log-rank Mantel-Cox test.

4.8.2. Mice immunized with the HIV-EBOVΔ1 homologous prime-boost regimen demonstrated minimal weight loss after lethal EBOV challenge

In order to monitor morbidity induced by EBOV infection in mice immunized with the HIV-EBOV vaccines, mice were weight daily after challenge. Both wild-type HIV and DMEM-treated controls experienced significant weight loss as depicted in **Figure 4.12**. Between 4-6 days post-EBOV challenge, the mean weights of HIV-treated mice decreased from 93.4- 89.4% of original. Between 4-8 days post-EBOV challenge, the mean weights of DMEM-treated mice decreased from 89.9- 83.1% of original weight. Between 4-9 days post-EBOV challenge, both HIV-EBOV and HIV-EBOVΔ2 immunized mice experienced decreases in mean weights, weighing 96.6- 95.2% and 97.4- 94.0% of original weights, respectively. However, both of these groups demonstrated an increase in weight 10 days post-EBOV challenge, weighing 113.8% and 111.8% of original weight by day 28. Mice immunized with the HIV-EBOVΔ1 homologous prime-boost vaccine regimen demonstrated minimal weight loss during the course of the challenge study. Between 4-9 days post-EBOV challenge, the mean weights of HIV-EBOVΔ1-immunized mice increased from their lowest 99.2% to 103.6% of their original weight. At day 28, HIV-EBOVΔ1-immunized mice were 111.8% of their original weight.

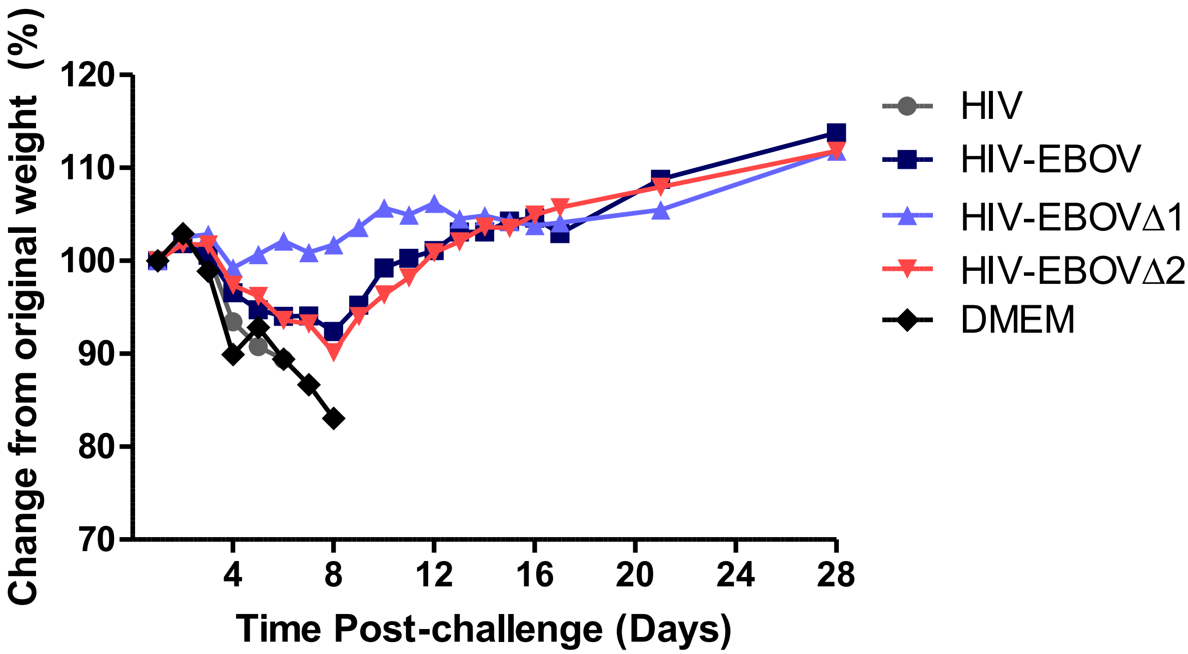

Figure 4.14. Percentage of weight change experienced by mice immunized with HIV-EBOV homologous prime-boost regimens after lethal EBOV challenge. BALB/c mice were prime immunized and boosted intraperitoneally with HIV-EBOV vaccines, HIV, or DMEM at day 0 and day 21, respectively. At day 42 post-immunization, mice were challenged intraperitoneally with 1000 LD_{50} of mouse-adapted EBOV. Mice were weighed as an indicator of disease morbidity for 28 days.

CHAPTER 5: DISCUSSION

5.1. MOLECULAR CLONES FOR THE RESCUE OF VACCINE CANDIDATES, HIV-EBOV, HIV-EBOVΔ1, AND HIV-EBOVΔ2

In the present study, three molecular clones were developed for the rescue of HIV recombinants expressing EBOV GP truncations. Generation of the HIV-EBOV molecular clones containing different truncations of the EBOV GP coding sequence was simplified by In-Fusion (HD) cloning. Previously, generation of molecular clones for the HIV-EBOV vaccines was attempted by ligating the coding sequence for EBOV GP directly into the SalI- and BamHI-digested pNL4-3 vector. However, as a result of restriction digestion, an additional deletion of 435 bp at the 5' end of the HIV envelope sequence, including nucleotides within the open reading frames of vpr, tat, and vpu, occurred in previously developed constructs. Due to the limited availability of unique restriction sites within the pNL4-3 vector, site-directed mutagenesis to create a unique XbaI restriction site at nucleotide position 6314-6319 within the vector. However, the engineered restriction sites formed mutations within the signal peptide sequence of HIV Env, which could have altered proper processing of the downstream EBOV GP sequence. To alleviate these issues, In-Fusion (HD) cloning was used to develop the HIV-EBOV constructs evaluated in this study. The 435 bp sequence deleted by restriction digestion were included within the DNA fragments 4-3A and 4-3AΔSP. Since In-Fusion (HD) cloning uses homologous end joining, rather than DNA ligation, the deleted sequence re-incorporated into the molecular clones without the need to engineer an additional unique restriction site. Instead, In-Fusion cloning incorporates inserts into restriction-digested vectors by using the 3′–5′ proofreading activity of poxvirus DNA polymerase to remove nucleotides from the homologous 3' ends, allowing them to anneal to homologous 5' ends through base pairing. Upon introduction into *E. coli*, single-stranded gaps generated during end-joining are repaired. Although full-length inserts were generated for cloning into the digested pNL4-3 vector, In-Fusion cloning could also have been used to insert over four DNA inserts in one reaction (Zhu, Cai, Hall, & Freeman, 2007). For example, chimeric PCR assembly of the IF-GP could have been omitted and the pNL4-3-ZGP construct could have been generated by cloning fragments 4-3A, 4-3B-GP, and 4-3C directly into the digested HIV vector.

The HIV-EBOV molecular clones incorporated the sequence for a stop codon at the end of each EBOV GP sequence in order to prevent the translation of a EBOV GP:HIV gp41 fusion protein. Subsequently, each vaccine construct lacked HIV gp41 expression. However, the preservation of HIV gp41 may have been useful for vaccine purposes. Since gp120 needed to be deleted in order to prevent $CD4^+$ T cell tropism, most broadly HIV-neutralizing antibodies could not be induced by all of the HIV-EBOV vaccines described in this study. However, preservation of HIV gp41 within the HIV-EBOV vaccines may have been able to induce the production of antibodies similar to the gp41 membrane proximal external region-specific antibody, 10E8, which was demonstrated to confer broad and potent HIV neutralization. An added benefit of including HIV gp41 as a vaccine antigen is that it is a highly conserved region of HIV, which may allow induced immune responses to protect against a vast array of HIV variants (Huang et al., 2012). Thus, further optimization of the HIV-EBOV molecular clones may consider incorporating the DNA sequence encoding a furin cleavage site (RRTRR) between the EBOV GP coding sequence and the gp41 coding sequence instead of a stop codon. Furin cleavage sites are utilized by the proprotein convertase furin to mediate cleavage of the polyprotein, pre-GP into functional subunits, GP1 and GP2 (Volchkov, Feldmann, Volchkova, & Klenk, 1998). Upon translation of an EBOV GP:HIV gp41 polypeptide, the additional furin cleavage site may allow appropriate processing of gp41 molecules for expression on the vaccine surface.

5.2. RESCUE OF THE HIV-EBOV, HIV-EBOVΔ1, AND HIV-EBOVΔ2 VACCINES

This study demonstrated the ability of the pNL4-3ZGP, pNL4-3ZGPΔ1, and pNL4-3ZGPΔ2 molecular clones to generate HIV recombinants upon transfection of HEK 293T cells. The pNL4-3ZGPΔ2 molecular clone was originally believed to be a defective construct due to the initial inability to detect EBOV GP in transfection supernatants with the anti-EBOV GP antibody, 7C9, developed by the Public Health Agency of Canada (data not shown) (Shahhosseini et al., 2007). However, the failure to detect EBOV GP in the HIV-EBOVΔ2 vaccine occurred since 7C9 binds epitopes within the mucin-like domain, which was deleted in EBOV GP expressed by this vaccine candidate (Qiu et al., 2011). Subsequently, the mouse IgG antibody ZGP42/3.7, which does not bind the mucin-like domain, was used to successfully detect the MLD-deleted EBOV GP of HIV-EBOVΔ2 by western blot analysis (**Figure 4.4**) (Takada et al., 2003). Thus, after confirming the expression of the appropriate EBOV GP truncation, HIV-EBOVΔ2 was confirmed as a vaccine candidate and used in subsequent analyses.

5.3. HIV-LIKE MORPHOLOGY OF HIV-EBOV AND HIV-EBOVΔ1, AND FILAMENTOUS MORPHOLOGY OF HIV-EBOVΔ2

The HIV-like morphology demonstrated by HIV-EBOV and HIV-EBOVΔ1 vaccines rescued from HEK 293T cells (**Figure 4.5**) was expected due to their similar structural protein expression as their parental wild-type virus. In particular, the expression of the Gag polyprotein precursor is independently capable of forming spherical HIV-1 virus-like particles in a manner dependent on the N-terminal capsid domain (Jalaguier, Turcotte, Danylo, Cantin, & Tremblay, 2011). The wild-type HIV, HIV-EBOV, and HIV-EBOVΔ1 virions shown budding from transfected HEK 293T cells after 48 hours demonstrated features consistent with electron micrographs of immature HIV virions, such as a dark, thick outer layer comprising unprocessed Gag polyprotein, as well as the absence of the distinctive conical core found in fully matured HIV particles (Sakuragi, 2011). For these vaccine candidates, as well as wild-type HIV, very few virions were observed budding from the transfected HEK 293T cell membrane. Future electron microscopic analysis after 48 hours of transfection may be required to observe a greater number of virus particles.

The aberrant filamentous particles observed by electron microscopy of HEK 293T cells producing HIV-EBOVΔ2 (**Figure 4.5D**) was unexpected. The filamentous morphology of EBOV is dependent on VP40, which is the major virion protein involved in EBOV assembly and budding. Independent expression of VP40 results in virus-like particles with filamentous morphology, whereas independent expression of EBOV GP induces the formation of pleiomorphic particles (Noda et al., 2002). Since the MLD-deleted HIV-EBOVΔ2 construct contained a 543 bp shorter EBOV GP coding sequence, it may be possible that higher levels of EBOV GP expression occurred for the HIV-EBOVΔ2 vaccine. High levels of EBOV GP expression has been demonstrated to impair EBOV virus-like particle production since low level GP expression is optimal for maximum virus production, trafficking, assembly, and release (Mohan et al., 2015)**.** It would be interesting to determine whether the filamentous structures observed from the rescue of HIV-EBOVΔ2 are truly functional virions with MLD-deleted EBOV GP stably expressed on the virion surface. Future studies could use immunogold labelling of EBOV GP and HIV p24 in order to determine whether the filamentous structures express EBOV GP on their surface and contain the HIV core (Yi et al., 2015).

5.4. INFECTIVITY OF THE HIV-EBOV VACCINES IN TZM-BL CELLS

The present study demonstrated the ability of the HIV-EBOV vaccines to infect TZM-bl cells. However, at a multiplicity of infection of 10 and 1, wild-type HIV caused a significant disruption of the TZM-bl monolayers by 24 and 48 hours, respectively (data not shown). As a result, less cells were able to be harvested for subsequent time points, causing the apparent decrease in infectivity at MOI 10 and 1 (**Figure 4.6A, B**). At these MOIs, HIV-EBOVΔ2 demonstrated reduced infectivity compared to HIV-EBOV and HIV-EBOVΔ1. This may have been a result of the aberrant filamentous HIV-EBOVΔ2 particles isolated from transfected HEK 293T cells , which likely lacked the viral genome required to express HIV Tat (**Figure 4.5D**). As hypothesized in **Section 5.3**, the possible increase of EBOV GP expression that may have contributed to aberrant particle formation could also be involved in decreasing the infectivity of HIV-EBOVΔ2. High levels of EBOV GP expression were shown to impair the infective capacity of EBOV GP-pseudotyped HIV and EBOV virus-like particles. Again, lower levels of EBOV GP expression was demonstrated to be optimal for maximum infectivity (Mohan et al., 2015). Thus, the aberrant-shaped HIV-EBOVΔ2 vaccine may actually comprise non-infectious virions similar to virus-like particles, while HIV-like viruses, HIV-EBOV and HIV-EBOVΔ1 remain better candidates for the live, bivalent vaccines proposed in this thesis.

At an MOI of 0.1, the HIV-EBOV vaccines demonstrated similar infectivity of TZM-bl cells as wild-type HIV. It is important to note that entry of HIV into TZM-bl HeLa cells differs from its mechanism of entry into $CD4^+$ T cells. While HIV enters $CD4^+$ T cells by CD4 and co-receptor-dependent attachment and fusion with target plasma membranes, HIV enters HeLa TZM-bl cells by fusing with endosomes. This endocytic pathway is initiated by the interaction of HIV Env with engineered CD4 receptors and CXCR4 or CCR5 co-receptors on the TZM-bl cell surface (de la Vega et al., 2011). Although the HIV-EBOV vaccines did not express HIV Env, they were likely able to enter TZM-bl cells through clathrin-mediated endocytosis, similar to the pathway utilized by vesicular stomatitis virus glycoprotein-pseudotyped HIV to enter TZM-bl cells (Miyauchi, Kim, Latinovic, Morozov, & Melikyan, 2009).

5.5. TROPISM AND REPLICATION OF THE HIV-EBOV VACCINES

5.5.1. Tropism of HIV-EBOV vaccines in THP-1 cells and SupT1 cells

As hypothesized, the HIV-EBOV vaccines demonstrated tropism for the monocytic cell line, THP-1, and diminished tropism for the $CD4^+$ T cell line, SupT1. Initially, the tropism of the HIV-EBOV vaccines was analyzed by infecting peripheral blood mononuclear cells (PBMCs) at an MOI of 1 and 10, followed by HIV p24 ELISA to quantify viral growth and flow cytometric analysis with a 14-colour panel adapted from a previously described panel to identify monocyte, T cell, and dendritic cell subsets (Autissier, Soulas, Burdo, & Williams, 2010). However, these experiments failed to show viral growth of the HIV-EBOV vaccines, as well as wild-type HIV (data not shown). The inability of wild-type HIV p24 to be detected in $CD4^+$ T cells by flow cytometry initially suggested the failure of the infection protocol. Subsequently, the same experiments were repeated using phytohemagglutinin (PHA)-activated PBMCs, but still demonstrated similar findings (data not shown). One explanation for the failure of wild-type HIV, as well as the HIV-EBOV vaccines, to infect PBMCs could be donor PBMC-specific variability in their ability to bind HIV, which could contribute to some donor PBMCs being less susceptible to HIV infection than others (Anzinger et al., 2008). In addition, cells may have been harvested too early after infection. Even after 6-7 days post-infection, only 1-3% of $CD4^+$ T cells expressed intracellular p24 after infection with HIV at a concentration of 100 ng p24 per million cells in a previous study (Sloan et al., 2015).

Subsequently, the tropism of the HIV-EBOV vaccines was evaluated in cell lines, which simplified the flow cytometric analysis to two markers for viability and HIV p24, instead of 14. In addition, the immortalized cell lines did not require cytokine stimulation for survival or HIV infection. The ability of the HIV-EBOV vaccines to infect THP-1 cells was expected because EBOV GP-mediated entry into these cells has been demonstrated by EBOV VLPs (O. Martinez et al., 2013). However, low levels of THP-1 cells infected with the HIV-EBOV vaccines were observed (**Figure 4.8A**). In a study by Martinez et al. (2013), THP-1 cells were infected at an MOI of 5 and 10 with EBOV VLPs and were able to achieve levels of infection above 20% (O. Martinez et al., 2013). Therefore, the infections at an MOI of 10 with the HIV-EBOV vaccines infected a smaller proportion of cells than expected. It is possible that the p24 ELISAs, which used p24 concentration to calculate virus titers may have provided an overestimation of the actual amount of infectious units in each virus stock. In order to calculate the titers in infectious units, the number of lentivirus particles obtained from HIV p24 concentration was divided by 1000 to account for defective particles, as suggested in the Lenti-X p24 RapidTiter Kit User Manual (Clontech, CA, USA). It could be possible that more defective particles were obtained from virus rescue, which may have contributed to an overestimation of infectious units calculated by this method. Therefore, the lower proportion of infected cells may have been the result of infecting at a lower actual MOI. The small proportion of infected THP-1 cells observed by flow cytometry could also be explained by the fact that undifferentiated THP-1 cells express only low levels of the NPC1 receptor required for EBOV GP-mediated entry. Martinez et al. (2013) demonstrated that phorbol myristate acetate (PMA)-stimulation to induce differentiation of THP-1 into macrophage-like cells enhanced permissiveness to EBOV GP-mediated infection by upregulating the NPC1 receptor. Therefore, THP-1 cells differentiated into macrophages by stimulation with PMA could be performed in future studies to determine the tropism of the HIV-EBOV vaccines for macrophages; these cells will likely demonstrate greater permissiveness to infection by the HIV-EBOV vaccines. Lastly, the tropism of wild-type HIV occurred as expected since THP-1 cells express low levels of CD4, CCR5, and CXCR4, which can interact with HIV Env. Even when undifferentiated, THP-1 are permissive to X4-tropic HIV infection (Cassol, Alfano, Biswas, & Poli, 2006).

In contrast to THP-1 cells, the HIV-EBOV vaccines demonstrated decreased tropism for the SupT1 $CD4^+$ T cell line, as hypothesized. However, wild-type HIV, which was used as a positive control for this experiment also demonstrated a decreased proportion of infected cells than expected. In other studies, the NL4-3 was able to infect approximately 6-20% of different T cell lines by 48 hours post-infection at an MOI of 0.25. These cell lines included C8166, H9, A 3.01, and Jurkat cell lines (Srivastava et al., 1991). Thus, even in the event that the infectious titers of the virus stocks were overestimated, the wild-type virus should have infected a higher proportion of cells by 2 dpi. Future studies could use a "spinfection" procedure, in which cells are centrifuged with the inoculum at 1200 ×g for 2 hours to improve infection (Sloan et al., 2015). In order to determine whether the EBOV GP expressed by the HIV-EBOV vaccines significantly decreased tropism of the virus away from $CD4^+$ T cells, such as the SupT1 cell line, and towards antigen presenting cells, such as the monocytic THP-1 cell line, these experiments will need to be performed in larger replicates in order to provide adequate data for statistical analysis.

5.5.2. Infectivity of HIV-EBOV vaccines in the monocyte cell line, THP-1

The HIV-EBOV vaccines demonstrated infectivity for the THP-1 cell line. This was expected since wild-type HIV is also able to replicate in THP-1 cells (Konopka, Pretzer, Plowman, & Düzgüneş, 1993). HIV-EBOVΔ1 and HIV-EBOV demonstrated higher levels of virus growth compared to wild type HIV and HIV-EBOVΔ2. Growth of the HIV-EBOVΔ2 vaccine was unexpected due to the aberrant morphology of the virus observed by electron microscopy (**Figure 4.6**). While the majority of particles released from HEK 293T cells were filamentous and believed to be defective particles, it may be possible that a few functional and infectious particles were rescued.

One major limitation of this study was that the growth of the HIV-EBOV vaccines was not evaluated in $CD4^+$ T cells. Based on the decreased tropism of the HIV-EBOV vaccines for SupT1 cells (**Figure 4.8A**), it is likely that the HIV-EBOV vaccines will demonstrate diminished replication in this cell line due to their apparent decreased ability to enter SupT1 cells. However, future studies will need to demonstrate that the HIV-EBOV vaccines lack or experience impaired replication in $CD4^+$ T cells, by infection of cell lines, such as SupT1s, or infection of primary $CD4^+$ T cells isolated from human PBMCs. This will be crucial to ensure that the HIV-EBOV vaccines will not be able to mediate the depletion of $CD4^+$ T cells, which is involved in the progression of HIV infection to AIDS.

5.5.3. Other cell lines to be considered in future vaccine tropism and replication studies

In order to achieve a more comprehensive analysis for tropism and replication, future studies will need to evaluate the ability of the HIV-EBOV vaccines to infect and replicate in other professional antigen presenting cells, such as macrophages, dendritic cells, and B cells. M1 macrophages can be generated from THP-1 cells by incubating the cell line with PMA at a concentration of 10 ng/ml for 24 hours and subsequently supplementing with lipopolysaccharide at a concentration of 15 ng/ml LPS or IFN-γ a concentration of 50 ng/ml for 48 hours (Smith, Young, Hurlstone, & Wellbrock, 2015). Mature dendritic cells can also be generated from THP-1 cells by incubating the cell line with recombinant human granulocyte-macrophage colony-stimulating factor (GM-CSF), TNF-α, ionomycin, and IL-4 at a concentration of 1500 IU/ml, 2000 IU/ml, 200 ng/ml, and 3000 IU/ml, respectively, for 24 hours (Berges et al., 2005). These cells can subsequently be infected and analyzed as described in **Section 3.6.2** and **Section 3.6.3**. In addition, tropism and replication in other T cell lines could also be performed in future studies, including C8166, H9, A 3.01, and Jurkat cells.

5.6. ANTI-HIV AND ANTI-EBOV CELL-MEDIATED IMMUNE RESPONSES INDUCED BY HIV-EBOV VACCINES IN MICE

5.6.1. HIV p24-specific IFN-γ-secreting T cell responses

The HIV-EBOVΔ1 homologous prime-boost regimen elicited the most robust IFN-γ-secreting T cell response against HIV p24 compared to the other vaccines and wild-type HIV at 21 days post-vaccination (**Figure 4.6**). The lower HIV p24-specific T cell responses induced by the HIV-EBOVΔ2 vaccine may be related to its decreased infectivity compared to the other vaccines. Since the $CD8^+$ T cell response is dependent on TCR engagement with antigen presented by MHC-I molecules, it may be possible that the inability of HIV-EBOVΔ2 to actively infect cells prevented the endogenous processing required for antigen presentation by MHC-I molecules (Murphy, 2012). In contrast, the increased infectious capacity of HIV-EBOV and HIV-EBOVΔ1 may have contributed to increased $CD8^+$ T cell activation due to their potential ability to be endogenously processed by antigen presenting cells.

Interestingly, the anti-HIV p24 T cell response induced by HIV-EBOVΔ1 and HIV-EBOV were more robust than those induced by wild-type HIV at each time point. Since titers in IFU for each virus were obtained using p24 concentration, all mice received the same quantity of HIV p24 for every intervention dose, eliminating the possibility that these effects were due to increased antigen concentration in the HIV-EBOVΔ1 and HIV-EBOV-immunized mice compared to HIV-inoculated mice. The decreased ability of HIV to induce HIV p24-specific IFN-γ-secreting T cells could be due to the fact that the transmembrane domain of HIV Env directly interacts with and inhibits the PRR, toll-like receptor 2 (TLR-2). This interaction results in decreased secretion of TNF-α, IL-6, and MCP-1 by macrophages (Reuven et al., 2014). Preventing the secretion of TNF-α may have inhibited the downstream signalling events in T cells that lead to IFN-γ, as well as IL-2, IL-4, and IL-5 production, in addition to cell division and T cell survival (Croft, 2009). Decreased MCP-1 production may have led to decreased migration of T cells towards antigen presenting cells, limiting their stimulation (Cambien et al., 2001). In contrast, EBOV GP interacts with TLR-4, resulting in the production of pro-inflammatory cytokines, such as SOCS1, IL-6, TNF-α, and IFN-β, in human monocyte cell lines as well as dendritic cells (Okumura, Pitha, Yoshimura, & Harty, 2010). IL-6 promotes survival and enhances proliferation of $CD8^+$ T cells upon TCR engagement *in vitro* and *in vivo*. Adjuvant-induced IL-6 has also been demonstrated to be crucial in cytotoxic $CD8^+$ T cell differentiation after vaccination. In the absence of IL-6, the generation of long-lived $CD8^+$ memory T cells is severely inhibited (Daudelin et al., 2013). Thus, the greater ability of EBOV GP of the HIV-EBOV vaccines to enhance IL-6 production may have been a factor contributing the enhanced HIV p24-specific IFN-γ-secreting T cell response upon homologous prime-boost vaccination compared to wild-type HIV inoculation in mice.

Even more interestingly, the same phenomenon could also explain the decreased anti-HIV p24 T cell responses induced by the HIV-EBOVΔ2 vaccine. The EBOV GP-induced NF-kB signalling in dendritic cells that leads to IL-6, IL-8, MIP-1a, and IP-10 production is dependent on the presence of the mucin-like domain. EBOV VLPs lacking the MLD within GP fail to stimulate IkB degradation in DC that leads to NF-kB signalling compared to VLPs comprised of MLD-containing GP (Osvaldo Martinez et al., 2007). Thus, the decreased IL-6 production induced by the MLD-deleted HIV-EBOVΔ2 vaccine may have contributed to decreased anti-HIV p24 T cell responses, as well as the decreased induction of other anti-HIV and anti-EBOV immune responses evaluated subsequently.

5.6.2. EBOV GP-specific IFN-γ-secreting T cell responses

Although the HIV-EBOV vaccine regimens were able to induce EBOV GP-specific IFN-γ-secreting T cell responses (**Figure 4.7**), these were less robust compared to the HIV p24-specific T cell responses. Since the EBOV GP gene was inserted in place of the gp120 sequence, it is likely that the HIV-like viruses, HIV-EBOV and HIV-EBOVΔ1, express EBOV GP in similar quantities as HIV Env. Each HIV virion contains approximately 7–14 glycoprotein trimers of HIV Env (Sundquist & Kräusslich, 2012). In contrast, approximately 2,000 molecules of p24 are expressed per HIV virion (Liu et al., 1995). Thus, the higher abundance of HIV p24 compared to

EBOV GP per HIV-EBOV vaccine particle may have contributed to the larger number of HIV p24-specific IFN-γ-secreting T cells compared to EBOV GP-specific IFN-γ-secreting T cells induced upon vaccination.

5.6.3. Other cell-mediated immune responses to be considered during future vaccine immunogenicity studies

In this study, IFN-γ-secreting T cell responses were the only cell-mediated responses analyzed in mice upon vaccination with the HIV-EBOV homologous prime-boost regimens. However, other T cell responses are increasing in importance in the context of HIV protection. For example, HIV progressors demonstrate some levels of HIV-specific IFN-γ T cell responses, as well as CD107a and MIP-1β production. Thus, IFN-γ secretion of T cells alone may not provide sufficient estimation about the ability of the HIV-EBOV vaccines to induce responses associated with protection against HIV. In contrast, HIV non-progressors elicit $CD8^+$ T cells with increased TNF-α and IL-2 secretion, in addition to IFN-γ secretion (Betts et al., 2006). Therefore, future readouts to characterize the immunogenicity of the HIV-EBOV vaccines could include HIV-specific TNF-α and IL-2-secreting T cell responses, as indicators of protective capacity, and HIV-specific CD107a and MIP-1β-secreting T cell responses as indicators of less desirable responses to vaccination.

5.7. ANTI-HIV AND ANTI-EBOV HUMORAL IMMUNE RESPONSES INDUCED BY HIV-EBOV VACCINES IN MICE

5.7.1. HIV p24-specific IgG responses

HIV-EBOV and HIV-EBOVΔ1 homologous prime-boost regimens elicited increased total HIV p24-specific IgG levels compared to HIV-EBOVΔ2 (**Figure 4.8A**). Since HIV-EBOVΔ2 demonstrated decreased ability to infect TZM-bl cells compared to the other two vaccines and likely comprises non-live particles, decreased danger signals to trigger sufficient innate activation could have inhibited B cell differentiation into antibody-secreting plasma cells, which may have led to decreased IgG induction against the same antigen. In addition, the potentially live HIV-EBOVΔ1 and HIV-EBOV vaccines may have induced prolonged antigen persistence compared to HIV-EBOVΔ2, which generally translates into higher antibody responses elicited by live vaccines (Pashine, Valiante, & Ulmer, 2005).

Similar to the HIV p24-specific IFN-γ-secreting T cell responses, the total anti-p24 IgG responses elicited by HIV-EBOVΔ1 and HIV-EBOV were more robust than those elicited by wild-type HIV inoculation, which administered the same dose of HIV p24. As hypothesized in **Section 5.6**, the contrasting abilities of HIV Env and EBOV GP to induce specific innate immune responses may also be involved in the differing abilities of wild-type HIV and HIV-EBOV vaccines to elicit antibody responses against the same antigen. The ability of EBOV GP to promote IL-6 production in monocytes and dendritic cells may have contributed to enhanced anti-HIV p24 IgG responses in the HIV-EBOV and HIV-EBOVΔ1-immunized mice since IL-6 is involved in inducing the differentiation of naïve B cells into Ig-secreting plasma cells (Jego et al., 2003; Okumura et al., 2010). In contrast, the ability of HIV Env to inhibit IL-6 production by cell subsets, such as macrophages, may have contributed to decreased HIV p24-specific IgG-secreting plasma cells (Reuven et al., 2014).

5.7.2. EBOV GP-specific IgG responses

HIV-EBOV and HIV-EBOVΔ1 homologous prime-boost regimens elicited increased total EBOV-specific IgG levels compared to HIV-EBOVΔ2 (**Figure 4.8B**). This is likely due to the same factors that resulted in the differences in anti-HIV p24 IgG responses between the vaccines. Explicitly, the greater anti-EBOV GP antibody production elicited by HIV-EBOV and HIV-EBOVΔ1 vaccination compared to HIV-EBOVΔ2 may be due to the fact that they resemble live vaccines, whereas HIV-EBOVΔ2 resembles a non-infectious, virus-like particle vaccine. As mentioned previously, live vaccines induce more robust antibody-secreting responses by B cells (Baxter, 2007).

5.8. EBOV-NEUTRALIZING ANTIBODY RESPONSE INDUCED BY HIV-EBOV VACCINES IN MICE

All of the HIV-EBOV homologous prime-boost vaccine regimens were unable to generate significant EBOV-neutralizing antibody titers in mice (**Figure 4.9**). However, some level of EBOV neutralizing antibody production was expected from the HIV-EBOV and HIV-EBOVΔ1 vaccines due to the high titers of total anti-EBOV GP IgG elicited by these vaccines in mice. However, regardless of their inability to induce significant EBOV neutralizing antibodies in mice, HIV-EBOV and HIV-EBOVΔ1 may still be useful for protection against EBOV, since neutralizing antibodies do not correlate significantly with protection in NHP models of EBOV (Wong et al., 2012).

5.8.1. Other antibody-mediated immune responses to be considered during future vaccine immunogenicity studies

Other mechanisms of antibody-mediated protection may be analyzed in future studies in order to further understand how the antibodies induced by HIV-EBOV vaccination mediate protection. For example, non-neutralizing anti-EBOV antibodies, such as 6D8, conferred protection against EBOV upon passive transfer in mice (Wilson et al., 2000). One alternate mechanism includes antibody-dependent cell cytotoxicity (ADCC), in which, virus-specific antibodies bind the surface of infected cells to promote killing by other cytolytic cells, such as NK cells. Another potential mechanism of antibody-mediated protection is complement-dependent cytotoxicity (CDC), in which, antibodies that recognize antigen expressed on infected cells are bound by complement, initiating activation of the complement cascade that results in the killing of virus-infected cells. Antibodies induced in NHPs vaccinated with EBOV VLPs were capable of mediating both ADCC and CDC against EBOV GP-expressing cells. ADCC can be analyzed by incubating antigen-expressing cells with plasma containing antibodies from immunized mice and measuring lysis upon addition of effector cells. CDC can be analyzed by incubating antigen-expressing cells with plasma containing antibodies from immunized mice and measuring spontaneous lysis upon addition of complement (Kelly L. Warfield et al., 2007) .

5.9. PROTECTIVE EFFICACY OF HIV-EBOV VACCINES AGAINST A LETHAL EBOV CHALLENGE IN MICE

As hypothesized, the HIV-EBOV vaccines were able to induce levels of protection against a lethal EBOV challenge in mice when used in a homologous prime-boost regimen. The highest protective efficacy of 83% elicited by the HIV-EBOVΔ1 homologous prime-boost regimen against lethal EBOV challenge in mice appeared to correlate with the ability of HIV-EBOVΔ1 to induce the highest average total anti-EBOV GP titers at day 42 compared to the other two vaccines (**Figure 4.10**). This is consistent with a study that demonstrated that increased vaccine-induced anti-EBOV GP IgG strongly correlates with protection against EBOV in mice (Wong et al., 2012). The better survival of mice induced by HIV-EBOVΔ1 was also associated with minimal weight loss occurring upon EBOV challenge compared with the other regimens, perhaps suggesting its ability to prevent EBOV-induced morbidity in mice. It is possible that increasing the dose of HIV-EBOVΔ1 for future protective efficacy studies could increase the protective efficacy of the vaccine to approach 100%.

In contrast, the protective efficacy of 67% induced by HIV-EBOVΔ2 was unexpected due to the decreased average total anti-EBOV GP IgG induced compared to HIV-EBOV, which demonstrated only 50% protective efficacy against EBOV despite robust titers. In contrast to HIV-EBOVΔ1, HIV-EBOVΔ2 and HIV-EBOV-immunized mice demonstrated some weight loss, suggesting that the EBOV challenge may have been able to establish infection of target cells, but may have been cleared by vaccine-induced immune cells. It will be necessary to repeat these experiments in order to establish statistical significance of these results.

5.9.1. Other mouse models to be considered during future vaccine evaluation

One of the greatest limitations of both the EBOV protective efficacy studies and the immunological characterization of the HIV-EBOV vaccines was the mouse model used for analysis. While BALB/c mice are an excellent option for modelling EBOV infection due to the availability of a mouse-adapted EBOV challenge virus, BALB/c mice are unable to model HIV infection for multiple reasons (Bray et al., 1998; Denton & García, 2011). The strict species tropism of HIV for humans and chimpanzees has severely hinder the replication of HIV in mice at various stages during the replication cycle, such as the lack of human CD4 receptors on mouse T cells required for entry (Browning et al., 1997). In addition, rodent cells are incapable of HIV Tat-mediated transactivation due to their lack of the human Tat co-factor, CycT1 (Bieniasz & Cullen, 2000). Productive HIV assembly is also blocked in murine cells due to the limited ability of Gag to target to the cell membrane (Mariani et al., 2000). Impaired HIV replication in the BALB/c mouse model used in this study prevented evaluation of the HIV-EBOV vaccines as live, replication-competent vaccine candidates. Therefore, the results obtained from immunogenicity studies and protective efficacy studies are more representative of baseline level immunogenicity and survival induced by non-replicating versions of the HIV-EBOV vaccines. However, the baseline immunogenicity and protective efficacy yielded from these experiments, especially by HIV-EBOVΔ1, demonstrate potential that the vaccines will be even more robust in a model in which the HIV-EBOV vaccines can act as live, replicating vaccines. The inability of BALB/c mice to facilitate HIV infection and recapitulate clinical symptoms of human AIDS, also prevented the evaluation the protective efficacy of the HIV-EBOV vaccines against wild-type HIV challenge.

Humanized mice, which are immunodeficient mice reconstituted with human $CD34^+$ hematopoietic progenitor cells, have gained popularity for the evaluation of HIV biology and pathogenesis in recent years. Reconstitution with human immune cells gives the ability of humanized mice to mediate HIV replication, allowing for the quantification of HIV viral load levels and $CD4^+$ T cell depletion (Denton & García, 2011). Thus, humanized mice would provide a better model to analyze the immunogenicity and protective efficacy of HIV-EBOV candidates as live, replicating vaccines. Humanized NOD SCID gamma (hu-NSG) mice have a severe combined immune deficiency mutation (SCID) and IL-2 receptor gamma chain deficiency, depleting them of mouse hematopoietic cells. This allows them to be reconstituted with human immune cells, which can be harvested to monitor HIV-EBOV vaccine replication and tropism *in vivo* (Kumar et al., 2008). However, since hu-NSG mice lack human organs required for immune cell maturity, such as the liver and thymus, these mice would be unable to recapitulate immunogenicity and protective efficacy mediated by human immune cells induced upon vaccination.

A more advanced humanized mouse model to overcome these obstacles is bone marrow liver thymus (BLT) mice, which are NOD/SCID mice depleted of mouse hematopoietic stem cells and reconstituted with human autologous $CD34^+$ hematopoietic stem cells, as well as human liver and thymus tissues. This would allow for the evaluation of human-like immune responses generated upon immunization with the HIV-EBOV vaccine candidates (Wege, Melkus, Denton, Estes, & Garcia, 2008). Since functional immune responses can be generated with this model, protective efficacy of the HIV-EBOV vaccines as live, replicating vectors against lethal EBOV can be evaluated. Furthermore, the ability of BLT mice to host HIV replication would allow for subsequent infection with a fluorescently-tagged wild-type HIV. Thus, the ability the HIV-EBOV vaccines to induce immune responses that prevent or decrease wild-type HIV replication could also be evaluated in the BLT mouse model.

CHAPTER 6: CONCLUSIONS

Molecular clones, pNL4-3ZGP, pNL4-3ZGPd1, and pNL4-3ZGPd2 were designed and used to rescue three HIV-EBOV vaccine candidates, HIV-EBOV, HIV-EBOVΔ1, and HIV-EBOVΔ2, respectively. These vaccines expressed full-length, signal peptide-deleted, and MLD-deleted EBOV GP as a replacement for HIV Env. HIV-EBOV AND HIV-EBOVΔ1 demonstrated HIV-like morphology, while HIV-EBOVΔ2 demonstrated filamentous morphology under transmission electron microscopy. As hypothesized, the HIV-EBOV vaccines demonstrated decreased tropism for the $CD4^+$ T cell line, SupT1, compared to wild-type HIV and greater tropism for the monocytic cell line, THP-1. While the HIV-EBOV vaccines were capable of replicating in THP-1 cells, their ability to replicate in SupT1 cells remains to be determined. Future studies to evaluate the tropism and replication of the virus in other $CD4^+$ T cell lines and antigen presenting cells lines will be necessary to ensure that the HIV-EBOV vaccines will not be able to mediate the depletion of $CD4^+$ T cells, but instead enhance adaptive immune responses to the virus by targeting APCs.

Cell-mediated and humoral immune responses against HIV and EBOV were evaluated in mice upon receiving a homologous prime-boost HIV-EBOV vaccine regimen. Also as hypothesized, the HIV-EBOV vaccines were able to induce both IFN-γ-secreting T cell responses against HIV p24 and EBOV GP at 21 days post-vaccination. However, IFN-γ-secreting T cell responses directed against HIV p24 were significantly greater than those directed against EBOV GP. The HIV-EBOV and HIV-EBOVΔ1 vaccines elicited significant total anti-HIV p24 and anti-EBOV GP IgG titers in mice at 42 days post-vaccination. Interestingly, both the IFN-γ-secreting T cell and total IgG responses elicited by these vaccines were higher than those induced by wild-type HIV, despite providing mice with the same amount of HIV p24 per intervention. Future evaluation of innate cytokine responses induced by the HIV-EBOV vaccines could provide insight on whether the differences in the production of mediators, such as IL-6, by infected APCs contributed to the differences in adaptive immune responses elicited against the same antigen by HIV-EBOV and HIV-EBOVΔ1 compared to wild type HIV.

Lastly, the protective efficacy of the homologous prime-boost HIV-EBOV vaccine regimens against lethal MA-EBOV challenge in a mouse model was evaluated. As hypothesized, the HIV-EBOV vaccines were able to confer protection in BALB/c mice against a lethal EBOV challenge. The homologous prime-boost HIV-EBOVΔ1 regimen demonstrated the highest efficacy inducing 83% protection against a lethal EBOV challenge in mice, with minimal weight loss occurring upon EBOV infection. These results correlated with the increased total anti-EBOV GP IgG elicited by HIV-EBOVΔ1 compared to the other vaccines in the immunogenicity studies. However, minimal anti-EBOV neutralizing antibodies were elicited by the HIV-EBOVΔ1, suggesting other mechanisms of antibody-mediated protection could play a role in its efficacy against EBOV challenge and will need to be evaluated in future studies. In addition, due to the inability of BALB/c mice to host productive replication of HIV, the results from the immunogenicity and protective efficacy induced by the HIV-EBOV vaccines reflect those of a non-replicating vaccine. Future studies evaluating the HIV-EBOV vaccines in a humanized mouse model, such as BLT mice, will be necessary to demonstrate immunogenicity and protective efficacy of these candidates as live, replicating vaccines. In addition, humanized mice would also allow for the evaluation of their protective efficacy against a wild type HIV challenge.

REFERENCES

Agnandji, S. T., Huttner, A., Zinser, M. E., Njuguna, P., Dahlke, C., Fernandes, J. F., … Siegrist, C.-A. (2015). Phase 1 Trials of rVSV Ebola Vaccine in Africa and Europe — Preliminary Report. *New England Journal of Medicine*, 150401140035006. http://doi.org/10.1056/NEJMoa1502924

Alimonti, J. B., Koesters, S. a, Kimani, J., Matu, L., Wachihi, C., Plummer, F. a, & Fowke, K. R. (2005). CD4+ T cell responses in HIV-exposed seronegative women are qualitatively distinct from those in HIV-infected women. *The Journal of Infectious Diseases*, *191*(1), 20–24. http://doi.org/10.1086/425998

Anzinger, J. J., Olinger, G. G., Spear, G. T., Cloyd, M., Moore, B., Williams, L., … Spear, G. (2008). Donor variability in HIV binding to peripheral blood mononuclear cells. *Virology Journal*, *5*(1), 95. http://doi.org/10.1186/1743-422X-5-95

Arts, E. J., & Hazuda, D. J. (2012). HIV-1 Antiretroviral Drug Therapy. *Cold Spring Harbor Perspectives in Medicine*, *2*(4), a007161–a007161. http://doi.org/10.1101/cshperspect.a007161

Autissier, P., Soulas, C., Burdo, T. H., & Williams, K. C. (2010). Evaluation of a 12-color flow cytometry panel to study lymphocyte, monocyte, and dendritic cell subsets in humans. *Cytometry Part A*, *77*(5), 410–419. http://doi.org/10.1002/cyto.a.20859

Baxter, D. (2007). Active and passive immunity, vaccine types, excipients and licensing. *Occupational Medicine*, *57*(8), 552–556. http://doi.org/10.1093/occmed/kqm110

Bell, S. K. (2007). Pathogenesis. In H. J. Libman, H., Makadon (Ed.), *HIV* (3rd ed., pp. 17–24). Philadelphia, PA, USA: College of Physicians Press.

Berges, C., Naujokat, C., Tinapp, S., Wieczorek, H., Höh, A., Sadeghi, M., … Daniel, V. (2005). A cell line model for the differentiation of human dendritic cells. *Biochemical and Biophysical Research Communications*, *333*(3), 896–907. http://doi.org/10.1016/j.bbrc.2005.05.171

Berkowitz, R. D., Alexander, S., Bare, C., Linquist-Stepps, V., Bogan, M., Moreno, M. E., … McCune, J. M. (1998). CCR5- and CXCR4-utilizing strains of human immunodeficiency virus type 1 exhibit differential tropism and pathogenesis in vivo. *Journal of Virology*, *72*(12), 10108–17. Retrieved from http://www.pubmedcentral.nih.gov/articlerender.fcgi?artid=110545&tool=pmcentrez&rendertype=abstract

Berzofsky, J. A., Bensussan, A., Cease, K. B., Bourge, J. F., Cheynier, R., Lurhuma, Z., … Zagury, D. (1988). Antigenic peptides recognized by T lymphocytes from AIDS viral envelope-immune humans. *Nature*, *334*(6184), 706–8. http://doi.org/10.1038/334706a0

Betts, M. R., Nason, M. C., West, S. M., De Rosa, S. C., Migueles, S. A., Abraham, J., … Koup, R. A. (2006). HIV nonprogressors preferentially maintain highly functional HIV-specific CD8 Ƨ T cells, *107*, 4781–4789. http://doi.org/10.1182/blood-2005-12-4818

Bieniasz, P. D., & Cullen, B. R. (2000). Multiple blocks to human immunodeficiency virus type 1 replication in rodent cells. *Journal of Virology*, *74*(21), 9868–77. Retrieved from http://www.ncbi.nlm.nih.gov/pubmed/11024113

Boberg, A., Bråve, A., Johansson, S., Wahren, B., Hinkula, J., & Rollman, E. (2008). Murine models for HIV vaccination and challenge. *Expert Review of Vaccines*, *7*(1), 117–30. http://doi.org/10.1586/14760584.7.1.117

Booth, C., Geretti, A. M. (2011). Pathogenesis of HIV infection. In M. A. Rodger, A.J., Mahungu, T.W., Johnson (Ed.), *HIV/AIDS: Atlas of investigation and management* (1st ed., pp. 13–30). Oxford: Atlas Medical Publishing Ltd.

Bray, M., Davis, K., Geisbert, T., Schmaljohn, C., & Huggins, J. (1998). A mouse model for evaluation of prophylaxis and therapy of Ebola hemorrhagic fever. *The Journal of Infectious Diseases*, *178*(3), 651–61. Retrieved from http://www.ncbi.nlm.nih.gov/pubmed/9728532

Browning, J., Horner, J. W., Pettoello-Mantovani, M., Raker, C., Yurasov, S., DePinho, R. A., & Goldstein, H. (1997). Mice transgenic for human CD4 and CCR5 are susceptible to HIV infection. *Proceedings of the National Academy of Sciences of the United States of America*, *94*(26), 14637–41. Retrieved from http://www.ncbi.nlm.nih.gov/pubmed/9405665

Bruce, C. B., Akrigg, A., Sharpe, S. A., Hanke, T., Wilkinson, G. W., & Cranage, M. P. (1999). Replication-deficient recombinant adenoviruses expressing the human immunodeficiency virus Env antigen can induce both humoral and CTL immune responses in mice. *The Journal of General Virology*, *80 (Pt 10*, 2621–8. http://doi.org/10.1099/0022-1317-80-10-2621

Bukh, I., Calcedo, R., Roy, S., Carnathan, D. G., Grant, R., Qin, Q., … Wilson, J. M. (2014a). Increased mucosal CD4+ T cell activation in rhesus macaques following vaccination with an adenoviral vector. *Journal of Virology*, *88*(15), 8468–78. http://doi.org/10.1128/JVI.03850-13

Bukh, I., Calcedo, R., Roy, S., Carnathan, D. G., Grant, R., Qin, Q., … Wilson, J. M. (2014b). Increased mucosal CD4+ T cell activation in rhesus macaques following vaccination with an adenoviral vector. *Journal of Virology*, *88*(15), 8468–78. http://doi.org/10.1128/JVI.03850-13

Butler, D. (2014). Ebola drug trials set to begin amid crisis. *Nature*, *513*(7516), 13–14. http://doi.org/10.1038/509015a

Cambien, B., Pomeranz, M., Millet, M. A., Rossi, B., Schmid-Alliana, A., Baggiolini, M., … Rees, R. (2001). Signal transduction involved in MCP-1-mediated monocytic transendothelial migration. *Blood*, *97*(2), 359–66. http://doi.org/10.1182/blood.v97.2.359

Cao, J., Jin, Y., Li, W., Zhang, B., He, Y., Liu, H., … Yan, J. (2013). DNA vaccines targeting the encoded antigens to dendritic cells induce potent antitumor immunity in mice. *BMC Immunology*, *14*, 39. http://doi.org/10.1186/1471-2172-14-39

Cassol, E., Alfano, M., Biswas, P., & Poli, G. (2006). Monocyte-derived macrophages and myeloid cell lines as targets of HIV-1 replication and persistence. *Journal of Leukocyte Biology*, *80*(5), 1018–1030. http://doi.org/10.1189/jlb.0306150

Chan, S. Y., Speck, R. F., Ma, M. C., & Goldsmith, M. A. (2000). Distinct mechanisms of entry by envelope glycoproteins of Marburg and Ebola (Zaire) viruses. *Journal of Virology*, *74*(10), 4933–7. Retrieved from http://www.pubmedcentral.nih.gov/articlerender.fcgi?artid=112022&tool=pmcentrez&rendertype=abstract

Choi, Y., & Chang, J. (2013). Viral vectors for vaccine applications. *Clinical and Experimental Vaccine Research*, *2*(2), 97–105. http://doi.org/10.7774/cevr.2013.2.2.97

Chowell, G., & Nishiura, H. (2014). Transmission dynamics and control of Ebola virus disease (EVD): a review. *BMC Medicine*, *12*(1), 196. http://doi.org/10.1186/s12916-014-0196-0

Ciavarra, R. P., Greene, A. R., Horeth, D. R., Buhrer, K., van Rooijen, N., & Tedeschi, B. (2000). Antigen processing of vesicular stomatitis virus in situ. Interdigitating dendritic cells present viral antigens independent of marginal dendritic cells but fail to prime CD4(+) and CD8(+) T cells. *Immunology*, *101*(4), 512–20. Retrieved from http://www.pubmedcentral.nih.gov/articlerender.fcgi?artid=2327105&tool=pmcentrez&rendertype=abstract

Clem, A. S. (2011). Fundamentals of vaccine immunology. *Journal of Global Infectious Diseases*, *3*(1), 73–8. http://doi.org/10.4103/0974-777X.77299

ClinicalTrials.gov. (2014a). Clinical Study to Assess Efficacy and Safety of Amiodarone in Treating Patients With Ebola. Virus Disease (EVD) in Sierra Leone. EASE (EMERGENCY Amiodarone Study Against Ebola). Retrieved from https://clinicaltrials.gov/ct2/show/NCT02307591

ClinicalTrials.gov. (2014b). Phase III, Open-labeled, Multicenter Study of the Safety and Efficacy of Brincidofovir (CMX001) in the Treatment of Early Versus Late Adenovirus Infection (CMX001 Adv). Retrieved from https://clinicaltrials.gov/ct2/show/NCT02087306

ClinicalTrials.gov. (2014c). Safety, Tolerability and Pharmacokinetic First in Human (FIH) Study for Intravenous (IV) TKM-100802. Retrieved from https://clinicaltrials.gov/ct2/show/NCT02041715

ClinicalTrials.gov. (2015a). Emergency Evaluation of Convalescent Plasma for Ebola Viral Disease (EVD) in Guinea (Ebola-Tx). Retrieved from https://clinicaltrials.gov/ct2/show/NCT02342171

ClinicalTrials.gov. (2015b). Partnership for Research on Ebola Vaccines in Liberia (PREVAIL) (NCT02344407). Retrieved March 28, 2016, from https://clinicaltrials.gov/ct2/show/NCT02344407?term=ebola+vaccine&rank=3

ClinicalTrials.gov. (2015c). Phase 3 Efficacy and Safety Study of Favipiravir for Treatment of Uncomplicated Influenza in Adults. Retrieved from https://www.clinicaltrials.gov/ct2/show/record/NCT02008344

ClinicalTrials.gov. (2015d). Putative Investigational Therapeutics in the Treatment of Patients With Known Ebola Infection. Retrieved from https://clinicaltrials.gov/ct2/show/NCT02363322

ClinicalTrials.gov. (2015e). Safety and Pharmacokinetics of a Single ZMappTM Administration in Healthy Adult Volunteers. Retrieved from https://clinicaltrials.gov/ct2/show/NCT02389192

ClinicalTrials.gov. (2015f). STRIVE (Sierra Leone Trial to Introduce a Vaccine Against Ebola) (NCT02378753). Retrieved March 30, 2016, from https://clinicaltrials.gov/ct2/show/NCT02378753?term=ebola+vaccine&rank=39

Corey, L., Gilbert, P. B., Tomaras, G. D., Haynes, B. F., Pantaleo, G., & Fauci, A. S. (2015). Immune correlates of vaccine protection against HIV-1 acquisition. *Science Translational Medicine*, *7*(310), 310rv7. http://doi.org/10.1126/scitranslmed.aac7732

Croft, M. (2009). The role of TNF superfamily members in T-cell function and diseases. *Nature Reviews Immunology*, *9*(4), 271–285. http://doi.org/10.1038/nri2526

Daudelin, J.-F., Mathieu, M., Boulet, S., Labrecque, N., Boulet, S., Labrecque, N., … Labrecque, N. (2013). IL-6 Production by Dendritic Cells Is Dispensable for CD8 $^{+}$ Memory T-Cell Generation. *BioMed Research International*, *2013*, 1–12. http://doi.org/10.1155/2013/126189

Davidson, E., Bryan, C., Fong, R. H., Barnes, T., Pfaff, J., Mabila, M., … Doranz, B. J. (2015). Mechanism of Binding to Ebola Virus Glycoprotein by the ZMapp, ZMAb, and MB-003 Cocktail Antibodies. *Journal of Virology*. http://doi.org/10.1128/JVI.01490-15

De la Vega, M., Marin, M., Kondo, N., Miyauchi, K., Kim, Y., Epand, R. F., … Melikyan, G. B. (2011). Inhibition of HIV-1 endocytosis allows lipid mixing at the plasma membrane, but not complete fusion. *Retrovirology*, *8*, 99. http://doi.org/10.1186/1742-4690-8-99

De Santis, O., Audran, R., Pothin, E., Warpelin-Decrausaz, L., Vallotton, L., Wuerzner, G., … Genton, B. (2016). Safety and immunogenicity of a chimpanzee adenovirus-vectored Ebola vaccine in healthy adults: a randomised, double-blind, placebo-controlled, dose-finding, phase 1/2a study. *The Lancet. Infectious Diseases*, *16*(3), 311–20. http://doi.org/10.1016/S1473-3099(15)00486-7

Denton, P. W., & García, J. V. (2011). Humanized mouse models of HIV infection. *AIDS Reviews*, *13*(3), 135–48. Retrieved from http://www.ncbi.nlm.nih.gov/pubmed/21799532

Ellis, R. W. (1996). The new generation of recombinant viral subunit vaccines. *Current Opinion in Biotechnology*, *7*(6), 646–52. Retrieved from http://www.ncbi.nlm.nih.gov/pubmed/8939634

Engelman, A., & Cherepanov, P. (2012). The structural biology of HIV-1: mechanistic and therapeutic insights. *Nature Reviews. Microbiology*, *10*(4), 279–90. http://doi.org/10.1038/nrmicro2747

Excler, J.-L., Tomaras, G. D., & Russell, N. D. (2013). Novel directions in HIV-1 vaccines revealed from clinical trials. *Current Opinion in HIV and AIDS*, *8*(5), 421–31. http://doi.org/10.1097/COH.0b013e3283632c26

Falasca, L., Agrati, C., Petrosillo, N., Di Caro, A., Capobianchi, M. R., Ippolito, G., & Piacentini, M. (2015). Molecular mechanisms of Ebola virus pathogenesis: focus on cell death. *Cell Death and Differentiation*, *22*(8), 1250–9. http://doi.org/10.1038/cdd.2015.67

Feldmann, H., Sanchez, A., & Gesibert, T. W. (2013). Filoviridae: Marburg and Ebola viruses. In G. Knipe DM, Howley PM, Cohen JI & R. B. DE, Lamb RA, Martin MA, Racaniello VR (Eds.), *Fields virology* (pp. 1410–1448). Philadelphia, PA, USA: Lippincott Williams & Wilkins.

Fonteneau, J. F., Kavanagh, D. G., Lirvall, M., Sanders, C., Cover, T. L., Bhardwaj, N., & Larsson, M. (2003). Characterization of the MHC class I cross-presentation pathway for cell-associated antigens by human dendritic cells. *Blood*, *102*(13), 4448–55. http://doi.org/10.1182/blood-2003-06-1801

Francica, J. R., Matukonis, M. K., & Bates, P. (2009). Requirements for cell rounding and surface protein down-regulation by Ebola virus glycoprotein. *Virology*, *383*(2), 237–247. http://doi.org/10.1016/j.virol.2008.10.029

Freed, E. O. (2001). HIV-1 Replication. *Somatic Cell and Molecular Genetics*, *26*(1-6), 13–33. http://doi.org/10.1023/A:1021070512287

Fukazawa, Y., Park, H., Cameron, M. J., Lefebvre, F., Lum, R., Coombes, N., … Picker, L. J. (2012). Lymph node T cell responses predict the efficacy of live attenuated SIV vaccines. *Nature Medicine*, *18*(11), 1673–81. http://doi.org/10.1038/nm.2934

Gallo, R. C. (2012). The AIDS virus. In S. A. Editors (Ed.), *HIV and AIDS: A Global Health Pandemic* (pp. 1–130). London, England: Macmillan.

Gamvrellis, A., Leong, D., Hanley, J. C., Xiang, S. D., Mottram, P., & Plebanski, M. (2004). Vaccines that facilitate antigen entry into dendritic cells. *Immunology and Cell Biology*, *82*(5), 506–516. http://doi.org/10.1111/j.0818-9641.2004.01271.x

Garg, H., Mohl, J., & Joshi, A. (2012). HIV-1 induced bystander apoptosis. *Viruses*, *4*(11), 3020–3043. http://doi.org/10.3390/v4113020

Geisbert, T. W., & Jahrling, P. B. (1995). Differentiation of filoviruses by electron microscopy. *Virus Research*, *39*(2-3), 129–150. http://doi.org/10.1016/0168-1702(95)00080-1

Guimard, Y., Bwaka, M. A., Colebunders, R., Calain, P., Massamba, M., De Roo, A., … Kipasa, M. A. (1999). Organization of patient care during the Ebola hemorrhagic fever epidemic in Kikwit, Democratic Republic of the Congo, 1995. *The Journal of Infectious Diseases*, *179 Suppl* , S268–73. http://doi.org/10.1086/514315

Henao-Restrepo, A. M., Longini, I. M., Egger, M., Dean, N. E., Edmunds, W. J., Camacho, A., … Røttingen, J.-A. (2015). Efficacy and effectiveness of an rVSV-vectored vaccine expressing Ebola surface glycoprotein: interim results from the Guinea ring vaccination cluster-randomised trial. *The Lancet*, *6736*(15), 1–10. http://doi.org/10.1016/S0140-6736(15)61117-5

Heymann, D. L., Weisfeld, J. S., Webb, P. A., Johnson, K. M., Cairns, T., & Berquist, H. (1980). Ebola hemorrhagic fever: Tandala, Zaire, 1977-1978. *The Journal of Infectious Diseases*, *142*(3), 372–6. Retrieved from http://www.ncbi.nlm.nih.gov/pubmed/7441008

Huang, J., Ofek, G., Laub, L., Louder, M. K., Doria-Rose, N. A., Longo, N. S., … Connors, M. (2012). Broad and potent neutralization of HIV-1 by a gp41-specific human antibody. *Nature*, *491*(7424), 406–12. http://doi.org/10.1038/nature11544

Huttner, A., Dayer, J.-A., Yerly, S., Combescure, C., Auderset, F., Desmeules, J., … Siegrist, C.-A. (2015). The effect of dose on the safety and immunogenicity of the VSV Ebola candidate vaccine: a randomised double-blind, placebo-controlled phase 1/2 trial. *The Lancet Infectious Diseases*, *3099*(15), 1–11. http://doi.org/10.1016/S1473-3099(15)00154-1

Ilinykh, P. A., Lubaki, N. M., Widen, S. G., Renn, L. A., Theisen, T. C., Rabin, R. L., … Bukreyev, A. (2015). Different Temporal Effects of Ebola Virus VP35 and VP24 Proteins on Global Gene Expression in Human Dendritic Cells. *Journal of Virology*, *89*(15), 7567–83. http://doi.org/10.1128/JVI.00924-15

ISRCTN.com. (2015). Convalescent plasma for early Ebola virus disease in Sierra Leone. Retrieved from http://www.isrctn.com/ISRCTN13990511

Jalaguier, P., Turcotte, K., Danylo, A., Cantin, R., & Tremblay, M. J. (2011). Efficient production of HIV-1 virus-like particles from a mammalian expression vector requires the N-terminal capsid domain. *PloS One*, *6*(11), e28314. http://doi.org/10.1371/journal.pone.0028314

Janeway Jr, C. A., Travers, P., Walport, M., & Shlomchik, M. J. (2001). Immunological memory. Garland Science. Retrieved from http://www.ncbi.nlm.nih.gov/books/NBK27158/

Jego, G., Palucka, A. K., Blanck, J.-P., Chalouni, C., Pascual, V., & Banchereau, J. (2003). Plasmacytoid dendritic cells induce plasma cell differentiation through type I interferon and interleukin 6. *Immunity*, *19*(2), 225–34. Retrieved from http://www.ncbi.nlm.nih.gov/pubmed/12932356

Jin, X., Bauer, D. E., Tuttleton, S. E., Lewin, S., Gettie, A., Blanchard, J., … Ho, D. D. (1999). Dramatic rise in plasma viremia after CD8(+) T cell depletion in simian immunodeficiency virus-infected macaques. *The Journal of Experimental Medicine*, *189*(6), 991–8. Retrieved from http://www.pubmedcentral.nih.gov/articlerender.fcgi?artid=2193038&tool=pmcentrez&rendertype=abstract

Johnson, K. M., Lange, J. V, Webb, P. A., & Murphy, F. A. (1977). Isolation and partial characterisation of a new virus causing acute haemorrhagic fever in Zaire. *Lancet (London, England)*, *1*(8011), 569–71. Retrieved from http://www.ncbi.nlm.nih.gov/pubmed/65661

Keating, R. (2012). Introduction: A Modern Pandemic. In S. A. Editors (Ed.), *HIV and AIDS: A Global Health Pandemic* (pp. 1–130). London: Macmillan.

Khan, K. H. (2013). DNA vaccines: roles against diseases. *Germs*, *3*(1), 26–35. http://doi.org/10.11599/germs.2013.1034

Klein, F., Mouquet, H., Dosenovic, P., Scheid, J. F., Scharf, L., & Nussenzweig, M. C. (2013). Antibodies in HIV-1 vaccine development and therapy. *Science (New York, N.Y.)*, *341*(6151), 1199–204. http://doi.org/10.1126/science.1241144

Konopka, K., Pretzer, E., Plowman, B., & Düzgüneş, N. (1993). Long-term noncytopathic productive infection of the human monocytic leukemia cell line THP-1 by human immunodeficiency virus type 1 (HIV-1IIIB). *Virology*, *193*(2), 877–87. Retrieved from http://www.ncbi.nlm.nih.gov/pubmed/8460491

Kuhn, J. H., Becker, S., Ebihara, H., Geisbert, T. W., Johnson, K. M., Kawaoka, Y., … Jahrling, P. B. (2010). Proposal for a revised taxonomy of the family Filoviridae: classification, names of taxa and viruses, and virus abbreviations. *Archives of Virology*, *155*(12), 2083–103. http://doi.org/10.1007/s00705-010-0814-x

Kumar, P., Ban, H.-S., Kim, S.-S., Wu, H., Pearson, T., Greiner, D. L., … Shankar, P. (2008). T cell-specific siRNA delivery suppresses HIV-1 infection in humanized mice. *Cell*, *134*(4), 577–86. http://doi.org/10.1016/j.cell.2008.06.034

Kuroda, M., Fujikura, D., Nanbo, A., Marzi, A., Noyori, O., Kajihara, M., … Takada, A. (2015). Interaction between TIM-1 and NPC1 Is Important for Cellular Entry of Ebola Virus. *Journal of Virology*, *89*(12), 6481–93. http://doi.org/10.1128/JVI.03156-14

Ledgerwood, J. E., Costner, P., Desai, N., Holman, L., Enama, M. E., Yamshchikov, G., … Graham, B. S. (2010). A replication defective recombinant Ad5 vaccine expressing Ebola virus GP is safe and immunogenic in healthy adults. *Vaccine*, *29*(2), 304–13. http://doi.org/10.1016/j.vaccine.2010.10.037

Lee, J. E., & Saphire, E. O. (2009). Ebolavirus glycoprotein structure and mechanism of entry. *Future Virology*, *4*(6), 621–635. http://doi.org/10.2217/fvl.09.56

Levy, J. A. (2007a). Antiviral Therapies. In J. A. Levy (Ed.), *HIV and the Pathogenesis of AIDS* (3rd ed., pp. 363–396). Washington: American Society for Microbiology (ASM).

Levy, J. A. (2007b). Discovery, Structure, Heterogeneity, and Origins of HIV. In J. A. Levy (Ed.), *HIV and the Pathogenesis of AIDS* (3rd ed., pp. 1–26). Washington: American Society for Microbiology (ASM).

Li, Y., Bergeron, J. J., Luo, L., Ou, W. J., Thomas, D. Y., & Kang, C. Y. (1996). Effects of inefficient cleavage of the signal sequence of HIV-1 gp 120 on its association with calnexin, folding, and intracellular transport. *Proceedings of the National Academy of Sciences of the United States of America*, *93*(18), 9606–11. Retrieved from http://www.pubmedcentral.nih.gov/articlerender.fcgi?artid=38475&tool=pmcentrez&rendertype=abstract

Liu, H., Wu, X., Newman, M., Shaw, G. M., Hahn, B. H., & Kappes, J. C. (1995). The Vif Protein of Human and Simian Immunodeficiency Viruses Is Packaged into Virions and Associates with Viral Core Structures. *JOURNAL OF VIROLOGY*, *69*(12), 7630–7638.

Luo, M., Sainsbury, J., Tuff, J., Lacap, P. A., Yuan, X.-Y., Hirbod, T., … Plummer, F. A. (2012). A Genetic Polymorphism of FREM1 Is Associated with Resistance against HIV Infection in the Pumwani Sex Worker Cohort. *Journal of Virology*, *86*(21), 11899.

Ma, Y., Li, X., & Kuang, E. (2016). Viral Evasion of Natural Killer Cell Activation. *Viruses*, *8*(4). http://doi.org/10.3390/v8040095

Maartens, G., Celum, C., & Lewin, S. R. (2014). HIV infection: epidemiology, pathogenesis, treatment, and prevention. *Lancet*, *384*(9939), 258–71. http://doi.org/10.1016/S0140-6736(14)60164-1

Mahdavi, M., Ebtekar, M., Mahboudi, F., Khorram Khorshid, H., Rahbarizadeh, F., Azadmanesh, K., … Hassan, Z. M. (2009). Immunogenicity of a new HIV-1 DNA construct in a BALB/c mouse model. *Iranian Journal of Immunology : IJI*, *6*(4), 163–73. http://doi.org/IJIv6i4A1

Mahungu, T. W. (2011). Introduction. In M. A. Rodger, A.J., Mahungu, T.W., Johnson (Ed.), *HIV/AIDS: Atlas of investigation and management* (1st ed., pp. 1–12). Oxford: Atlas Medical Publishing Ltd.

Malbec, M., Porrot, F., Rua, R., Horwitz, J., Klein, F., Halper-Stromberg, A., … Schwartz, O. (2013). Broadly neutralizing antibodies that inhibit HIV-1 cell to cell transmission. *The Journal of Experimental Medicine*, *210*(13), 2813–21. http://doi.org/10.1084/jem.20131244

Mansky, L. M., & Temin, H. M. (1995). Lower in vivo mutation rate of human immunodeficiency virus type 1 than that predicted from the fidelity of purified reverse transcriptase. *Journal of Virology*, *69*(8), 5087–94. Retrieved from http://www.pubmedcentral.nih.gov/articlerender.fcgi?artid=189326&tool=pmcentrez&rendertype=abstract

Mariani, R., Rutter, G., Harris, M. E., Hope, T. J., Kräusslich, H. G., & Landau, N. R. (2000). A block to human immunodeficiency virus type 1 assembly in murine cells. *Journal of Virology*, *74*(8), 3859–70. Retrieved from http://www.ncbi.nlm.nih.gov/pubmed/10729160

Martin, J. E., Sullivan, N. J., Enama, M. E., Gordon, I. J., Roederer, M., Koup, R. A., … Graham, B. S. (2006). A DNA vaccine for Ebola virus is safe and immunogenic in a phase I clinical trial. *Clinical and Vaccine Immunology : CVI*, *13*(11), 1267–77. http://doi.org/10.1128/CVI.00162-06

Martinez, O., Johnson, J. C., Honko, A., Yen, B., Shabman, R. S., Hensley, L. E., … Basler, C. F. (2013). Ebola Virus Exploits a Monocyte Differentiation Program To Promote Its Entry. *Journal of Virology*, *87*(7), 3801–3814. http://doi.org/10.1128/JVI.02695-12

Martinez, O., Tantral, L., Mulherkar, N., Chandran, K., & Basler, C. F. (2011). Impact of Ebola mucin-like domain on antiglycoprotein antibody responses induced by Ebola virus-like particles. *The Journal of Infectious Diseases*, S825–32. http://doi.org/10.1093/infdis/jir295

Martinez, O., Valmas, C., & Basler, C. F. (2007). Ebola virus-like particle-induced activation of NF-kappaB and Erk signaling in human dendritic cells requires the glycoprotein mucin domain. *Virology*, *364*(2), 342–54. http://doi.org/10.1016/j.virol.2007.03.020

Marx, J. L. (1985). A virus by any other name . . . *Science (New York, N.Y.)*, *227*(4693), 1449–51. Retrieved from http://www.ncbi.nlm.nih.gov/pubmed/2983427

Marzi, A., Akhavan, A., Simmons, G., Gramberg, T., Hofmann, H., Bates, P., … Pöhlmann, S. (2006). The signal peptide of the ebolavirus glycoprotein influences interaction with the cellular lectins DC-SIGN and DC-SIGNR. *Journal of Virology*, *80*(13), 6305–17. http://doi.org/10.1128/JVI.02545-05

Marzi, A., Engelmann, F., Feldmann, F., Haberthur, K., Shupert, W. L., Brining, D., … Messaoudi, I. (2013). Antibodies are necessary for rVSV/ZEBOV-GP-mediated protection against lethal Ebola virus challenge in nonhuman primates. *Proceedings of the National Academy of Sciences of the United States of America*, *110*(5), 1893–8. http://doi.org/10.1073/pnas.1209591110

Marzi, A., & Feldmann, H. (2014). Ebola virus vaccines: an overview of current approaches. *Expert Review of Vaccines*, *13*(4), 521–31. http://doi.org/10.1586/14760584.2014.885841

Masemola, A., Mashishi, T., Khoury, G., Mohube, P., Mokgotho, P., Vardas, E., … Gray, C. M. (2004). Hierarchical targeting of subtype C human immunodeficiency virus type 1 proteins by CD8+ T cells: correlation with viral load. *Journal of Virology*, *78*(7), 3233–43. Retrieved from http://www.pubmedcentral.nih.gov/articlerender.fcgi?artid=371059&tool=pmcentrez&rendertype=abstract

Masopust, D. (2009). Developing an HIV cytotoxic T-lymphocyte vaccine: issues of CD8 T-cell quantity, quality and location. *Journal of Internal Medicine*, *265*(1), 125–37. http://doi.org/10.1111/j.1365-2796.2008.02054.x

Matano, T., Shibata, R., Siemon, C., Connors, M., Lane, H. C., & Martin, M. A. (1998). Administration of an anti-CD8 monoclonal antibody interferes with the clearance of chimeric simian/human immunodeficiency virus during primary infections of rhesus macaques. *Journal of Virology*, *72*(1), 164–9. Retrieved from http://www.pubmedcentral.nih.gov/articlerender.fcgi?artid=109361&tool=pmcentrez&rendertype=abstract

Mate, S. E., Kugelman, J. R., Nyenswah, T. G., Ladner, J. T., Wiley, M. R., Cordier-Lassalle, T., … Palacios, G. (2015). Molecular Evidence of Sexual Transmission of Ebola Virus. *The New England Journal of Medicine*, *373*(25), 2448–54. http://doi.org/10.1056/NEJMoa1509773

McDermott, A. B., & Koup, R. A. (2012). CD8(+) T cells in preventing HIV infection and disease. *AIDS (London, England)*, *26*(10), 1281–92. http://doi.org/10.1097/QAD.0b013e328353bcaf

Mendoza, E. J., Qiu, X., & Kobinger, G. P. (2016). Progression of Ebola Therapeutics During the 2014-2015 Outbreak. *Trends in Molecular Medicine*, *22*(2), 164–173. http://doi.org/10.1016/j.molmed.2015.12.005

Messaoudi, I., Amarasinghe, G. K., & Basler, C. F. (2015). Filovirus pathogenesis and immune evasion: insights from Ebola virus and Marburg virus. *Nature Reviews. Microbiology*, *13*(11), 663–76. http://doi.org/10.1038/nrmicro3524

Meyers, L., Frawley, T., Goss, S., & Kang, C. (2015). Ebola Virus Outbreak 2014: Clinical Review for Emergency Physicians. *Annals of Emergency Medicine*, *65*(1), 101–108. http://doi.org/10.1016/j.annemergmed.2014.10.009

Minor, P. D. (2015). Live attenuated vaccines: Historical successes and current challenges. *Virology*, *479-480*, 379–92. http://doi.org/10.1016/j.virol.2015.03.032

Miyauchi, K., Kim, Y., Latinovic, O., Morozov, V., & Melikyan, G. B. (2009). HIV enters cells via endocytosis and dynamin-dependent fusion with endosomes. *Cell*, *137*(3), 433–44. http://doi.org/10.1016/j.cell.2009.02.046

Mohamadzadeh, M., Chen, L., & Schmaljohn, A. L. (2007). How Ebola and Marburg viruses battle the immune system. *Nature Reviews. Immunology*, *7*(7), 556–67. http://doi.org/10.1038/nri2098

Mohan, G. S., Ye, L., Li, W., Monteiro, A., Lin, X., Sapkota, B., … Yang, C. (2015). Less is more: Ebola virus surface glycoprotein expression levels regulate virus production and infectivity. *Journal of Virology*, *89*(2), 1205–17. http://doi.org/10.1128/JVI.01810-14

Montefiori, D. C. (2009). Measuring HIV neutralization in a luciferase reporter gene assay. *Methods in Molecular Biology (Clifton, N.J.)*, *485*, 395–405. http://doi.org/10.1007/978-1-59745-170-3_26

Mühlberger, E. (2007). Filovirus replication and transcription. *Future Virology*, *2*(2), 205–215. http://doi.org/10.2217/17460794.2.2.205

Murphy, K. (2012). *Janeway's Immunobiology* (8th ed.). New York, NY: Garland Science, Taylor & Francis Group.

Muyembe-Tamfum, J. J., Kipasa, M., Kiyungu, C., & Colebunders, R. (1999). Ebola outbreak in Kikwit, Democratic Republic of the Congo: discovery and control measures. *The Journal of Infectious Diseases*, *179 Suppl* (Supplement 1), S259–62. http://doi.org/10.1086/514302

Nabel, G. J. (2013). Designing tomorrow's vaccines. *The New England Journal of Medicine*, *368*(6), 551–60. http://doi.org/10.1056/NEJMra1204186

Ndawinz, J. D. A., Cissé, M., Diallo, M. S. K., Sidibé, C. T., & D'Ortenzio, E. (2015). Prevention of HIV spread during the Ebola outbreak in Guinea. *Lancet (London, England)*, *385*(9976), 1393. http://doi.org/10.1016/S0140-6736(15)60713-9

Ndung'u, T., & Weiss, R. A. (2012). On HIV diversity. *AIDS (London, England)*, *26*(10), 1255–60. http://doi.org/10.1097/QAD.0b013e32835461b5

Nguyen, V. K., Binder, S. C., Boianelli, A., Meyer-Hermann, M., & Hernandez-Vargas, E. A. (2015). Ebola virus infection modeling and identifiability problems. *Frontiers in Microbiology*, *6*, 257. http://doi.org/10.3389/fmicb.2015.00257

Nkoghe, D., Leroy, E. M., Toung-Mve, M., & Gonzalez, J. P. (2012). Cutaneous manifestations of filovirus infections. *International Journal of Dermatology*, *51*(9), 1037–1043. http://doi.org/10.1111/j.1365-4632.2011.05379.x

Noda, T., Sagara, H., Suzuki, E., Takada, A., Kida, H., & Kawaoka, Y. (2002). Ebola virus VP40 drives the formation of virus-like filamentous particles along with GP. *Journal of Virology*, *76*(10), 4855–65. Retrieved from http://www.ncbi.nlm.nih.gov/pubmed/11967302

Nqoko, B., Day, C. L., Mansoor, N., De Kock, M., Hughes, E. J., Hawkridge, T., … Hanekom, W. A. (2011). HIV-specific gag responses in early infancy correlate with clinical outcome and inversely with viral load. *AIDS Research and Human Retroviruses*, *27*(12), 1311–6. http://doi.org/10.1089/AID.2011.0081

Ogunbodede, E. O. (2004). HIV/AIDS situation in Africa. *International Dental Journal*, *54*(6 Suppl 1), 352–60. Retrieved from http://www.ncbi.nlm.nih.gov/pubmed/15631096

Okoye, A. A., & Picker, L. J. (2013). CD4(+) T-cell depletion in HIV infection: mechanisms of immunological failure. *Immunological Reviews*, *254*(1), 54–64. http://doi.org/10.1111/imr.12066

Okulicz, J. F., Marconi, V. C., Landrum, M. L., Wegner, S., Weintrob, A., Ganesan, A., … Dolan, M. J. (2009). Clinical outcomes of elite controllers, viremic controllers, and long-term nonprogressors in the US Department of Defense HIV natural history study. *The Journal of Infectious Diseases*, *200*(11), 1714–23. http://doi.org/10.1086/646609

Okumura, A., Pitha, P. M., Yoshimura, A., & Harty, R. N. (2010). Interaction between Ebola virus glycoprotein and host toll-like receptor 4 leads to induction of proinflammatory cytokines and SOCS1. *Journal of Virology*, *84*(1), 27–33. http://doi.org/10.1128/JVI.01462-09

Okware, S. I., Omaswa, F. G., Zaramba, S., Opio, A., Lutwama, J. J., Kamugisha, J., … Lamunu, M. (2002). An outbreak of Ebola in Uganda. *Tropical Medicine & International Health : TM & IH*, *7*(12), 1068–75. Retrieved from http://www.ncbi.nlm.nih.gov/pubmed/12460399

Olinger, G. G., Bailey, M. A., Dye, J. M., Bakken, R., Kuehne, A., Kondig, J., … Hart, M. K. (2005). Protective cytotoxic T-cell responses induced by venezuelan equine encephalitis virus replicons expressing Ebola virus proteins. *Journal of Virology*, *79*(22), 14189–96. http://doi.org/10.1128/JVI.79.22.14189-14196.2005

PACTR.org. (2015). Rapid Assessment of Potential Interventions & Drugs for Ebola (RAPIDE). Retrieved from http://www.pactr.org/ATMWeb/appmanager/atm/atmregistry?dar=true&tNo=PACTR201501000997429

Pan African Clinical Trials Registry. (2015). Ebola Vaccine Ring Vaccination Trial in Guinea (PACTR201503001057193). Retrieved April 17, 2016, from http://www.pactr.org/ATMWeb/appmanager/atm/atmregistry?dar=true&tNo=PACTR201503001057193

Parks, C. L., Picker, L. J., & King, C. R. (2013). Development of replication-competent viral vectors for HIV vaccine delivery. *Current Opinion in HIV and AIDS*, *8*(5), 402–11. http://doi.org/10.1097/COH.0b013e328363d389

Parpia, A. S., Ndeffo-Mbah, M. L., Wenzel, N. S., & Galvani, A. P. (2016). Effects of Response to 2014-2015 Ebola Outbreak on Deaths from Malaria, HIV/AIDS, and Tuberculosis, West Africa. *Emerging Infectious Diseases*, *22*(3), 433–441. http://doi.org/10.3201/eid2203.150977

Pashine, A., Valiante, N. M., & Ulmer, J. B. (2005). Targeting the innate immune response with improved vaccine adjuvants. *Nature Medicine*, *11*(4 Suppl), S63–8. http://doi.org/10.1038/nm1210

Permanyer, M., Ballana, E., & Esté, J. A. (2010). Endocytosis of HIV: anything goes. *Trends in Microbiology*, *18*(12), 543–51. http://doi.org/10.1016/j.tim.2010.09.003

Pettitt, J., Zeitlin, L., Kim, D. H., Working, C., Johnson, J. C., Bohorov, O., … Olinger, G. G. (2013). Therapeutic intervention of Ebola virus infection in rhesus macaques with the MB-003 monoclonal antibody cocktail. *Science Translational Medicine*, *5*(199), 199ra113. http://doi.org/10.1126/scitranslmed.3006608

Pollara, G., Kwan, A., Newton, P. J., Handley, M. E., Chain, B. M., & Katz, D. R. (2005). Dendritic cells in viral pathogenesis: protective or defective? *International Journal of Experimental Pathology*, *86*(4), 187–204. http://doi.org/10.1111/j.0959-9673.2005.00440.x

Poon, B., Hsu, J. F., Gudeman, V., Chen, I. S. Y., & Grovit-Ferbas, K. (2005). Formaldehyde-treated, heat-inactivated virions with increased human immunodeficiency virus type 1 env can be used to induce high-titer neutralizing antibody responses. *Journal of Virology*, *79*(16), 10210–7. http://doi.org/10.1128/JVI.79.16.10210-10217.2005

Poudrier, J., Thibodeau, V., & Roger, M. (2012). Natural Immunity to HIV: a delicate balance between strength and control. *Clinical & Developmental Immunology*, *2012*, 875821. http://doi.org/10.1155/2012/875821

Qiu, X., Alimonti, J. B., Melito, P. L., Fernando, L., Ströher, U., & Jones, S. M. (2011). Characterization of Zaire ebolavirus glycoprotein-specific monoclonal antibodies. *Clinical Immunology (Orlando, Fla.)*, *141*(2), 218–27. http://doi.org/10.1016/j.clim.2011.08.008

Qiu, X., Audet, J., Wong, G., Pillet, S., Bello, A., Cabral, T., … Kobinger, G. P. (2012). Successful treatment of ebola virus-infected cynomolgus macaques with monoclonal antibodies. *Science Translational Medicine*, *4*(138), 138ra81. http://doi.org/10.1126/scitranslmed.3003876

Qiu, X., Wong, G., Audet, J., Bello, A., Fernando, L., Alimonti, J. B., … Kobinger, G. P. (2014). Reversion of advanced Ebola virus disease in nonhuman primates with ZMapp. *Nature*, *advance on*. http://doi.org/10.1038/nature13777

Radebe, M., Gounder, K., Mokgoro, M., Ndhlovu, Z. M., Mncube, Z., Mkhize, L., … Ndung'u, T. (2015). Broad and persistent Gag-specific CD8+ T-cell responses are associated with viral control but rarely drive viral escape during primary HIV-1 infection. *AIDS (London, England)*, *29*(1), 23–33. http://doi.org/10.1097/QAD.0000000000000508

Rappuoli, R., Pizza, M., Del Giudice, G., & De Gregorio, E. (2014). Vaccines, new opportunities for a new society. *Proceedings of the National Academy of Sciences of the United States of America*, *111*(34), 12288–93. http://doi.org/10.1073/pnas.1402981111

Regules, J. A., Beigel, J. H., Paolino, K. M., Voell, J., Castellano, A. R., Muñoz, P., … Thomas, S. J. (2015). A Recombinant Vesicular Stomatitis Virus Ebola Vaccine - Preliminary Report. *New England Journal of Medicine*. http://doi.org/10.1056/NEJMoa1414216

Rerks-Ngarm, S., Pitisuttithum, P., Nitayaphan, S., Kaewkungwal, J., Chiu, J., Paris, R., … Kim, J. H. (2009). Vaccination with ALVAC and AIDSVAX to prevent HIV-1 infection in Thailand. *The New England Journal of Medicine*, *361*(23), 2209–20. http://doi.org/10.1056/NEJMoa0908492

Reuven, E. M., Ali, M., Rotem, E., Schwarzer, R., Schwarzter, R., Gramatica, A., … Shai, Y. (2014). The HIV-1 envelope transmembrane domain binds TLR2 through a distinct dimerization motif and inhibits TLR2-mediated responses. *PLoS Pathogens*, *10*(8), e1004248. http://doi.org/10.1371/journal.ppat.1004248

Riedel, S. (2005). Edward Jenner and the history of smallpox and vaccination. *Proceedings (Baylor University. Medical Center)*, *18*(1), 21–5. Retrieved from http://www.pubmedcentral.nih.gov/articlerender.fcgi?artid=1200696&tool=pmcentrez&rendertype=abstract

Rodger, A.J., Marshall, N., Geretti, A.M., Booth, C. (2011). Treatment of HIV infection. In M. A. Rodger, A.J., Mahungu, T.W., Johnson (Ed.), *HIV/AIDS: Atlas of investigation and management* (1st ed., pp. 31–60). Oxford: Atlas Medical Publishing Ltd.

Rowe, A. K., Bertolli, J., Khan, A. S., Mukunu, R., Muyembe-Tamfum, J. J., Bressler, D., … Ksiazek, T. G. (1999). Clinical, virologic, and immunologic follow-up of convalescent Ebola hemorrhagic fever patients and their household contacts, Kikwit, Democratic Republic of the Congo. Commission de Lutte contre les Epidémies à Kikwit. *The Journal of Infectious Diseases*, *179 Suppl* , S28–35. http://doi.org/10.1086/514318

Sakuragi, J.-I. (2011). Morphogenesis of the Infectious HIV-1 Virion. *Frontiers in Microbiology*, *2*, 242. http://doi.org/10.3389/fmicb.2011.00242

Sarma, J. V., & Ward, P. A. (2011). The complement system. *Cell and Tissue Research*, *343*(1), 227–35. http://doi.org/10.1007/s00441-010-1034-0

Sarwar, U. N., Costner, P., Enama, M. E., Berkowitz, N., Hu, Z., Hendel, C. S., … Ledgerwood, J. E. (2015). Safety and immunogenicity of DNA vaccines encoding Ebolavirus and

Marburgvirus wild-type glycoproteins in a phase I clinical trial. *The Journal of Infectious Diseases*, *211*(4), 549–57. http://doi.org/10.1093/infdis/jiu511

Saunders, K. O., Rudicell, R. S., & Nabel, G. J. (2012). The design and evaluation of HIV-1 vaccines. *AIDS (London, England)*, *26*(10), 1293–302. http://doi.org/10.1097/QAD.0b013e32835474d2

Schmitz, J. E., Kuroda, M. J., Santra, S., Sasseville, V. G., Simon, M. A., Lifton, M. A., … Reimann, K. A. (1999). Control of viremia in simian immunodeficiency virus infection by CD8+ lymphocytes. *Science (New York, N.Y.)*, *283*(5403), 857–60. Retrieved from http://www.ncbi.nlm.nih.gov/pubmed/9933172

Sekaly, R.-P. (2008). The failed HIV Merck vaccine study: a step back or a launching point for future vaccine development? *The Journal of Experimental Medicine*, *205*(1), 7–12. http://doi.org/10.1084/jem.20072681

Shahhosseini, S., Das, D., Qiu, X., Feldmann, H., Jones, S. M., & Suresh, M. R. (2007). Production and characterization of monoclonal antibodies against different epitopes of Ebola virus antigens. *Journal of Virological Methods*, *143*(1), 29–37. http://doi.org/10.1016/j.jviromet.2007.02.004

Sharp, P. M., & Hahn, B. H. (2011). Origins of HIV and the AIDS pandemic. *Cold Spring Harbor Perspectives in Medicine*, *1*(1), a006841. http://doi.org/10.1101/cshperspect.a006841

Sheets, R. L., Zhou, T., & Knezevic, I. (2016). Review of efficacy trials of HIV-1/AIDS vaccines and regulatory lessons learned: A review from a regulatory perspective. *Biologicals : Journal of the International Association of Biological Standardization*, *44*(2), 73–89. http://doi.org/10.1016/j.biologicals.2015.10.004

Sloan, D. D., Lam, C.-Y. K., Irrinki, A., Liu, L., Tsai, A., Pace, C. S., … Koenig, S. (2015). Targeting HIV Reservoir in Infected CD4 T Cells by Dual-Affinity Re-targeting Molecules (DARTs) that Bind HIV Envelope and Recruit Cytotoxic T Cells. *PLoS Pathogens*, *11*(11), e1005233. http://doi.org/10.1371/journal.ppat.1005233

Smith, M. P., Young, H., Hurlstone, A., & Wellbrock, C. (2015). Differentiation of THP1 Cells into Macrophages for Transwell Co-culture Assay with Melanoma Cells. *Bio-Protocol*, *5*(21). Retrieved from http://www.pubmedcentral.nih.gov/articlerender.fcgi?artid=4811304&tool=pmcentrez&rendertype=abstract

Sperandio, B., Fischer, N., & Sansonetti, P. J. (2015). Mucosal physical and chemical innate barriers: Lessons from microbial evasion strategies. *Seminars in Immunology*, *27*(2), 111–8. http://doi.org/10.1016/j.smim.2015.03.011

Srivastava, K. K., Fernandez-Larsson, R., Zinkus, D. M., & Robinson, H. L. (1991). Human immunodeficiency virus type 1 NL4-3 replication in four T-cell lines: rate and efficiency of entry, a major determinant of permissiveness. *Journal of Virology*, *65*(7), 3900–2. Retrieved from http://www.pubmedcentral.nih.gov/articlerender.fcgi?artid=241424&tool=pmcentrez&rendertype=abstract

Stern, A. M., & Markel, H. (2005). The history of vaccines and immunization: familiar patterns, new challenges. *Health Affairs (Project Hope)*, *24*(3), 611–21. http://doi.org/10.1377/hlthaff.24.3.611

Streeck, H., Frahm, N., & Walker, B. D. (2009). The role of IFN-gamma Elispot assay in HIV vaccine research. *Nature Protocols*, *4*(4), 461–9. http://doi.org/10.1038/nprot.2009.7

Sullivan, N. J., Geisbert, T. W., Geisbert, J. B., Shedlock, D. J., Xu, L., Lamoreaux, L., … Nabel, G. J. (2006). Immune protection of nonhuman primates against Ebola virus with single low-dose adenovirus vectors encoding modified GPs. *PLoS Medicine*, *3*(6), e177. http://doi.org/10.1371/journal.pmed.0030177

Sullivan, N. J., Hensley, L., Asiedu, C., Geisbert, T. W., Stanley, D., Johnson, J., … Nabel, G. J. (2011). CD8+ cellular immunity mediates rAd5 vaccine protection against Ebola virus infection of nonhuman primates. *Nature Medicine*, *17*(9), 1128–31. http://doi.org/10.1038/nm.2447

Sullivan, N., Yang, Z.-Y., & Nabel, G. J. (2003). Ebola Virus Pathogenesis: Implications for Vaccines and Therapies. *Journal of Virology*, *77*(18), 9733–9737. http://doi.org/10.1128/JVI.77.18.9733-9737.2003

Sundquist, W. I., & Kräusslich, H.-G. (2012). HIV-1 assembly, budding, and maturation. *Cold Spring Harbor Perspectives in Medicine*, *2*(7), a006924. http://doi.org/10.1101/cshperspect.a006924

Takada, A. (2012). Filovirus tropism: Cellular molecules for viral entry. *Frontiers in Microbiology*, *3*(FEB), 1–9. http://doi.org/10.3389/fmicb.2012.00034

Takada, A., Feldmann, H., Stroeher, U., Bray, M., Watanabe, S., Ito, H., … Kawaoka, Y. (2003). Identification of protective epitopes on ebola virus glycoprotein at the single amino acid level by using recombinant vesicular stomatitis viruses. *Journal of Virology*, *77*(2), 1069–74. Retrieved from http://www.ncbi.nlm.nih.gov/pubmed/12502822

Tapia, M. D., Sow, S. O., Lyke, K. E., Haidara, F. C., Diallo, F., Doumbia, M., … Levine, M. M. (2016). Use of ChAd3-EBO-Z Ebola virus vaccine in Malian and US adults, and boosting of Malian adults with MVA-BN-Filo: a phase 1, single-blind, randomised trial, a phase 1b, open-label and double-blind, dose-escalation trial, and a nested, randomised, double-bli. *The Lancet. Infectious Diseases*, *16*(1), 31–42. http://doi.org/10.1016/S1473-3099(15)00362-X

Tattevin, P., Baysah, M. K., Raguin, G., Toomey, J., Chapplain, J.-M., Taylor, M. E., … Yazdanpanah, Y. (2015). Retention in care for HIV-infected patients in the eye of the Ebola storm: lessons from Monrovia, Liberia. *AIDS (London, England)*, *29*(6), N1–2. http://doi.org/10.1097/QAD.0000000000000614

Towner, J. S., Rollin, P. E., Bausch, D. G., Sanchez, A., Crary, S. M., Vincent, M., … Nichol, S. T. (2004). Rapid diagnosis of Ebola hemorrhagic fever by reverse transcription-PCR in an outbreak setting and assessment of patient viral load as a predictor of outcome. *Journal of Virology*, *78*(8), 4330–41. Retrieved from http://www.pubmedcentral.nih.gov/articlerender.fcgi?artid=374287&tool=pmcentrez&rendertype=abstract

UNAIDS. (2015). UNAIDS Global Statistics. Retrieved May 24, 2016, from http://www.unaids.org/en/resources/campaigns/HowAIDSchangedeverything/factsheet

Ura, T., Okuda, K., & Shimada, M. (2014). Developments in Viral Vector-Based Vaccines. *Vaccines*, *2*(3), 624–41. http://doi.org/10.3390/vaccines2030624

Volchkov, V. E., Feldmann, H., Volchkova, V. A., & Klenk, H. D. (1998). Processing of the Ebola virus glycoprotein by the proprotein convertase furin. *Proceedings of the National Academy of Sciences of the United States of America*, *95*(10), 5762–7. Retrieved from http://www.ncbi.nlm.nih.gov/pubmed/9576958

Wahl-Jensen, V., Kurz, S., Feldmann, F., Buehler, L. K., Kindrachuk, J., DeFilippis, V., … Feldmann, H. (2011). Ebola virion attachment and entry into human macrophages profoundly effects early cellular gene expression. *PLoS Neglected Tropical Diseases*, *5*(10), e1359. http://doi.org/10.1371/journal.pntd.0001359

Wainberg, M. A., & Lever, A. M. L. (2014). How will the ebola crisis impact the HIV epidemic? *Retrovirology*, *11*, 110. http://doi.org/10.1186/s12977-014-0110-z

Warfield, K. L., & Olinger, G. G. (2011). Protective role of cytotoxic T lymphocytes in filovirus hemorrhagic fever. *Journal of Biomedicine & Biotechnology*, *2011*, 984241. http://doi.org/10.1155/2011/984241

Warfield, K. L., Swenson, D. L., Olinger, G. G., Kalina, W. V., Aman, M. J., & Bavari, S. (2007). Ebola Virus- Like Particle–Based Vaccine Protects Nonhuman Primates against Lethal Ebola Virus Challenge. *The Journal of Infectious Diseases*, *196*(s2), S430–S437. http://doi.org/10.1086/520583

Wege, A. K., Melkus, M. W., Denton, P. W., Estes, J. D., & Garcia, J. V. (2008). Functional and phenotypic characterization of the humanized BLT mouse model. *Current Topics in Microbiology and Immunology*, *324*, 149–65. Retrieved from http://www.ncbi.nlm.nih.gov/pubmed/18481459

Wei, X., Decker, J. M., Liu, H., Zhang, Z., Arani, R. B., Kilby, J. M., … Kappes, J. C. (2002). Emergence of resistant human immunodeficiency virus type 1 in patients receiving fusion inhibitor (T-20) monotherapy. *Antimicrobial Agents and Chemotherapy*, *46*(6), 1896–905. Retrieved from http://www.ncbi.nlm.nih.gov/pubmed/12019106

WHO. (2014). Ethical considerations for use of unregistered interventions for Ebola virus disease. Retrieved March 25, 2016, from http://www.who.int/csr/resources/publications/ebola/ethical-considerations/en/

WHO. (2016). Ebola Situation Report - 16 March 2016. Retrieved from http://apps.who.int/ebola/current-situation/ebola-situation-report-9-december-2015

Williams, K. J. N., Qiu, X., Fernando, L., Jones, S. M., & Alimonti, J. B. (2015). VSVΔG/EBOV GP-induced innate protection enhances natural killer cell activity to increase survival in a lethal mouse adapted Ebola virus infection. *Viral Immunology*, *28*(1), 51–61. http://doi.org/10.1089/vim.2014.0069

Wilson, J. A., Hevey, M., Bakken, R., Guest, S., Bray, M., Schmaljohn, A. L., & Hart, M. K. (2000). Epitopes involved in antibody-mediated protection from Ebola virus. *Science (New York, N.Y.)*, *287*(5458), 1664–6. Retrieved from http://www.ncbi.nlm.nih.gov/pubmed/10698744

Wong, G., Richardson, J. S., Pillet, S., Patel, A., Qiu, X., Alimonti, J., … Kobinger, G. P. (2012). Immune parameters correlate with protection against ebola virus infection in rodents and nonhuman primates. *Science Translational Medicine*, *4*(158), 158ra146. http://doi.org/10.1126/scitranslmed.3004582

Yi, H., Strauss, J. D., Ke, Z., Alonas, E., Dillard, R. S., Hampton, C. M., … Wright, E. R. (2015). Native immunogold labeling of cell surface proteins and viral glycoproteins for cryo-electron microscopy and cryo-electron tomography applications. *The Journal of Histochemistry and Cytochemistry : Official Journal of the Histochemistry Society*, *63*(10), 780–92. http://doi.org/10.1369/0022155415593323

Yonezawa, A., Cavrois, M., & Greene, W. C. (2005). Studies of ebola virus glycoprotein-mediated entry and fusion by using pseudotyped human immunodeficiency virus type 1 virions: involvement of cytoskeletal proteins and enhancement by tumor necrosis factor alpha. *Journal of Virology*, *79*(2), 918–26. http://doi.org/10.1128/JVI.79.2.918-926.2005

Yuan, T., Li, J., & Zhang, M.-Y. (2013). HIV-1 envelope glycoprotein variable loops are indispensable for envelope structural integrity and virus entry. *PloS One*, *8*(8), e69789. http://doi.org/10.1371/journal.pone.0069789

Zhou, L., Chong, M. M. W., & Littman, D. R. (2009). Plasticity of CD4+ T Cell Lineage Differentiation. *Immunity*, *30*(5), 646–655. http://doi.org/10.1016/j.immuni.2009.05.001

Zhu, B., Cai, G., Hall, E. O., & Freeman, G. J. (2007). In-fusion assembly: seamless engineering of multidomain fusion proteins, modular vectors, and mutations. *BioTechniques*, *43*(3), 354–9. Retrieved from http://www.ncbi.nlm.nih.gov/pubmed/17907578

APPENDIX

Table A1. Primer sequences for the DNA sequencing of HIV-EBOV molecular clones.

Primer	Primer Sequence	Primer location
pNL4-3-1F	tggaagggctaatttggtcccaa	1..23
pNL4-3-2F	cttcagacaggatcagaagaacttagatca	991..1020
pNL4-3-3F	agcaggaactactagtacccttcagga	1497..1523
pNL4-3-4F	ctgttggaaatgtggaaaggaaggac	2025..2050
pNL4-3-5F	gtcaacataattggaagaaatctgttga	2496..2523
pNL4-3-6F	ggatggaaaggatcaccagcaatatt	3003..3028
pNL4-3-7F	gtgtattatgacccatcaaaagacttaatag	3498..3528
pNL4-3-8F	gctttgcaggattcgggattagaagta	4002..4028
pNL4-3-9F	cagagacagggcaagaaacagcatac	4501..4526
pNL4-3-10F	agtagtgccaagaagaaaagcaaagatca	5003..5031
pNL4-3-11F	ataaaaccaaaacagataaagccaccttt	5500..5528
pNL4-3-12F	gctcatcagaacagtcagactcatca	6001..6026
pNL4-3-13F	acatgtggaaaaatgacatggtagaacaga	6501..6530
pNL4-3-14F	gcagtctagcagaagaagatgtagtaattag	7002..7032
pNL4-3-15F	gcaatgtatgcccctcccatca	7511..7532
pNL4-3-16F	gttgctctggaaaactcatttgca	8004..8027
pNL4-3-17F	cctcttcagctaccaccgcttga	8506..8528
pNL4-3-18F	caggtacctttaagaccaatgacttacaa	9003..9031
pNL4-3-19F	gcagctgctttttgcctgtactg	9507..9529
pNL4-3-20F	taaacacccaagacataaacacccaa	10239..10264
pNL4-3-21F	gacaaccggggccagtcact	10971..10990
pNL4-3-22F	cagttcggtgtaggtcgttcgctc	11736..11759
pNL4-3-23F	tccgcctccatccagtctattaattg	12505..12530
pNL4-3-24F	taggggttccgcgcacatttc	13232..13252
pNL4-3-1R	ctaggaggctgtcaaacttccacact	254..279
pNL4-3-2R	ctccgctagtcaaaatttttggcgt	750..774
pNL4-3-3R	aagccttctcttctactacttttaccca	1252..1279
pNL4-3-4R	tgggttcgcattttggaccaa	1753..1773
pNL4-3-5R	gctgccaaagagtgatctgaggga	2251..2274
pNL4-3-6R	aatctactaattttctccatttagtactgtc	2748..2778
pNL4-3-7R	tactgtccatttatcaggatggagttc	3246..3272
pNL4-3-8R	caccatgcttcccatgtttcctt	3732..3754
pNL4-3-9R	ttcttgggccttatctattccatct	4235..4259
pNL4-3-10R	ccatttgtactgctgtcttaagatgttc	4737..4764
pNL4-3-11R	ccagtctctttctcctgtatgcagac	5252..5277
pNL4-3-12R	gttgcagaattcttattatggcttcc	5729..5754
pNL4-3-13R	tctccacaagtgctgatacttctcct	6231..6256
pNL4-3-14R	aagaatgcatattctttctgcaccttatctc	6717..6747
pNL4-3-15R	caaattgttctcttaatttgctagctatctg	7244..7274
pNL4-3-16R	gaacaaagctcctattcccactgctct	7745..7771
pNL4-3-17R	ataccacagccaatttgttatgttaaac	8230..8257

pNL4-3-18R	cttctaggtatgtggcgaatagctct	8726..8751
pNL4-3-19R	ctcttctaccttatctggctcaactgg	9225..9251
pNL4-3-20R	cgatcttggctcactgcaacct	9722..9743
pNL4-3-21R	gctggatcacttgagcccagga	10928..10949
pNL4-3-22R	ggagtcaggcaactatggatgaac	12329..12352
pNL4-3-23R	aagtaaaagatgctgaagatcagttgg	13025..13051
pNL4-3-24R	cacagtagagactaaaaaaattgtgaatca	14428..14457
pNL4-3-25R	gcctttcctggtgtaagtagaactgg	14800..14825
ZGP-1F	atgggcgttacaggaatattgcag	1..24
ZGP-2F	aggaacgactttcgctgaaggtg	516..538
ZGP-3F	cacaaaatcatggcttcagaaaattc	1014..1039
ZGP-4F	aatgctcaacccaaatgcaacc	1515..1536
ZGP-1R	ctaaaagacaaatttgcatatacagaataaag	1999..2030
ZGP-2R	ggtccaggaagtcagtgctcttg	1313..1335
ZGP-3R	actagacgggtcctccgttgcat	611..633

pNL4-3 sequencing primers span the pNL4-3 vector sequence. ZGP sequencing primers are located within the pCAGGS-EBOV GP vector sequence. All the primers were designed based on the HIV-1 vector pNL4-3 (GenBank Accession: AF324493) and EBOV (Mayinga) GP gene, complete coding sequence (GenBank Accession: U23187.1). “F” stands for forward and “R” stands for reverse indicating the direction of primer extension.